University of Alberta

Understanding the Role of Rhomboid Proteases and Their Substrates in Parkinson's Disease

by

Melissa Morrison

A thesis submitted to the Faculty of Graduate Studies and Research

in partial fulfillment of the requirements for the degree of

Master of Science

Department of Biochemistry

Fall 2013

Edmonton, Alberta

Abstract

PINK1 (Phosphatase Tensin homologue (PTEN)-Induced Kinase) is a neuroprotective kinase involved in mitochondrial dynamics. It is composed of an N-terminal mitochondrial targeting sequence, transmembrane domain and C-terminal kinase domain. PINK1 is imported into mitochondria and anchored into the IMM, where it is rapidly cleaved by intramembrane rhomboid protease, PARL (Presenilin-Associated Rhomboid-Like). Mutations that prevent cleavage or signaling events of the kinase domain result in Parkinson's disease.

This thesis aims to assess the structure of the PINK1 membrane domain to further understand its interactions with PARL. We predict that Parkinson's disease mutations found in the transmembrane domain may alter the secondary structure to prevent cleavage of PINK1 by PARL. The PINK1 TM domain was expressed and purified in *E. coli* and been analyzed by nuclear magnetic resonance (NMR). An expression and screening system has been developed in *Pichia pastoris,* which has been used to design a preliminary expression regimen for PARL.

Acknowledgments

Firstly, I am truly indebted and thankful to Dr. Joanne Lemieux. Joanne, you has been a great role model, mentor, leader and friend over the past three years. You have really facilitated a journey and phase of my life that I would have never anticipated, but would not trade for anything. You are truly passionate about science in a way that is contagious, and it is from you I caught my momentum and motivation to complete this degree. As I am concluding this chapter of my life, I can't express enough thanks for the many ways you've supported me, encouraged me, pushed and challenged me to grow as a person, student and scientist.

I also want to extend thanks to the fantastic members of the Lemieux lab: Dr. Cory Brooks, Dr. Elena Arutyunova, Dr. Pankaj Panwar, Christelle Lazareno-Saez, Michelle Mak and Chris Lukowski. I would like to thank each and every one of you for all your support, time and help over the last three years. A special thanks goes to Dr. Cory Brooks; you are an incredible teacher and coach. I can't thank you enough for patiently working with me and teaching me almost everything I know on the bench, starting when I was just an undergraduate student. You have really taught me what practical science is, and were undoubtedly the most entertaining part of being in the lab every day. Sincere thanks to Elena and Michelle, for the endless advice on more than just science. It's been such a privilege to have such genuine and caring people like you to work with every day.

I would like to thank my committee members Dr. Joe Casey and Dr. Larry Fliegel. It has been such an honor to have such passionate scientists on my committee. I can't express how much your support, advice, and approval has meant throughout this degree. I would like to also thank Dr. Bernie Lemire for all the helpful conversation and encouragement. I would like to extend a thank you to Dr. Simonetta Sipione for participating in my thesis defense.

I would like to extend a final thank you to all the friends and family who supported me through this process. I want to thank David Kramer. Thank you for your unwavering friendship through two degrees. A very special thanks goes to Mike Burkat; thank you for being the best cheerleader a girl could ask for. Thank you for your endless encouragement and support; I know I couldn't have gotten through this thesis without you. You really are the best.

Table of Contents

List of Figures

List of Tables

List of Abbreviations

°C	Degree Celsius
aa	Amino acid
AO	Alcohol oxidase
APS	Ammonium persulfate
ATP	Adenosine Triphosphate
bp	Base pair
βME	Beta mercaptoethanol
COSY	Correlation spectroscopy
CyPET	Cyan fluorescent protein for energy transfer
ddH_2O	Double distilled water
DDM	n-Dodecyl-β-D-maltoside
DMSO	Dimethyl sulfoxide
dNTP	Deoxyribonucleotide triphosphate
DPC	n-dodecylphosphocholine
DTT	dithiothreitol
E. coli	*Escherichia coli*
ER	Endoplasmic reticulum
EDTA	Ethylene diamine tetra acetic acid
FRET	Förster resonance energy transfer
FSEC	Fluorescence size exclusion chromatography
GFP	Green fluorescent protein
h	Hour
IMM	Inner mitochondrial membrane
IPTG	Isopropyl β-D thiogalactoside
kb	kilobase
kDa	kilo Dalton
L	Litre

M	Molar
MBP	Maltose binding protein
min	Minute
mg	Milligram
mL	Millilitre
mM	Millimolar
MMP	Mitochondrial membrane potential
MPP	Mitochondrial processing protein
MTS	Mitochondrial targeting sequence
MW	Molecular weight
Ni-NTA	Nickel nitrilotriacetic acid
NMR	Nuclear magnetic resonance
NOESY	Nuclear overhauser effect spectroscopy
OD	Optical Density
OMM	Outer mitochondrial membrane
PARL	Presenilin-associated rhomboid like
PBS	Phosphate buffered saline
PCR	Polymerase chain reaction
PD	Parkinson's disease
PEMT	Phosphatidylethanolamine-N-methyl transferase
PINK1	Phosphatase tensin homologue induced kinase 1
PMSF	Phenylmethyl sulfonyl fluoride
ppm	Parts per million
PSE	Phosphate salt EDTA buffer
ROS	Reactive oxygen species
s	Second(s)
SDS	Sodium dodecyl sulphate
SDS-PAGE	Sodium docecyl sulphate polyacrylamide gel electrophoresis

TEMED	Tetramethylenediamine
TEV	Tobacco etch virus
TIM	Translocase of the inner membrane
TOM	Translocase of the outer membrane
TOCSY	Total correlation spectroscopy
TM	Transmembrane
TMD	Transmembrane domain
Tris	Tris(hydroxylmethyl)aminomethane
U	Units
YNB	Yeast nitrogen base
YPET	Yellow fluorescent protein for energy transfer
µl	Microlitre
1D	One dimensional
2D	Two dimensional

Chapter 1

Introduction

1.1 Parkinson's Disease

Parkinson's disease (PD) is a debilitating movement and neurodegenerative disorder. It is recognized as the most prevalent movement disorder, and second most prevalent neurodegenerative disorder to Alzheimer's disease[1]. According to the Parkinson's Disease Foundation, it affects 7-10 million worldwide. PD progression can vary from patient to patient. Currently there is no cure for Parkinson's disease, and treatments ranging from physical, occupational and speech therapy are used to manage symptoms. Furthermore, we are just beginning to understand the mechanism for neurodegeneration associated with different forms of PD.

Patients clinically present with resting tremors, slow movement (bradykinesia), rigidity and postural instability[2,3]. Neurologically, PD is characterized by dopaminergic neurodegeneration in the substantia nigra pars compacta and its depigmentation in color[1,4], as well as neurodegeneration of the ventral tegmental area and locus coeruleus[5]. Degeneration is not limited to dopaminergic neurons, but also noradrenergic, serotonergic and cholinergic systems in the brain[1,3]. Another typical characteristic of PD is the formation of Lewy bodies[3] which are intra-cytoplasmic proteinaceous deposits, containing aggregated α-synuclein species[1]. PD had originally been presumed to be a sporadic disease, potentially caused by environmental factors. For example, a mitochondrial complex I inhibitor has been discovered where chronic parkinsonism was a side effect in patients[6].

There has been a gap in understanding the etiology of PD despite the good characterization of its pathology and physiology[5,7]. Over the last 16 years, a large shift in causal understanding has occurred due to genetic developments and the discovery of specific protein mutations. Though PD was originally perceived to be a sporadic illness, the evidence for genetic susceptibility is mounting[8]. This was brought about by the first genetic analysis of a large American-Italian family with autosomal dominant presentation of PD symptoms. It was later discovered that the family had an A53T missense mutation in α-synuclein, a presynaptic protein involved in neuronal plasticity and a major component of Lewy bodies[7]. This protein was the first of several proteins suggested to play a role in PD pathology, where compromising mutations and gene deletions contributed to a parkinsonism phenotype in patients. Other proteins uncovered in the last 16 years have been Parkin, PTEN-induced kinase1 (PINK1), DJ1, Leucine-rich repeat kinase2 (LRRK2), ATPase type 13A2, phospholipase A2, F-box protein 7, vacuolar sorting protein 35 and pantothenate kinase 2[1,5,7,9](Table 1.1).

It is important to keep in mind that to date, it is predicted ~10% of PD patients have the condition due to genetic reasons[5] and that a well understood pathology can have many different causes. Within the genetic variations of Parkinson's alone, there are variations in symptom severity, psychological issues (such as dementia or schizophrenia), levodopamine responsiveness, age of onset, dystonia, and presence of multiple system atrophy (MSA), Lewy bodies and glial cytoplasmic exclusions[7,10]. It is also

worth noting that certain mutations, such as in the PINK1 kinase, result in parkinsonism that has a neuropathology indistinguishable from idiopathic PD, which makes it very difficult to assess the cause without genetic analysis[11].

1.2 Mutations in PINK1

As the cause of Parkinson's disease has become better characterized, two forms of the disease are recognized. Sporadic Parkinson's disease refers to the true idiopathic form, where familial Parkinson's disease refers to the disease which results from genetic mutations. A focus of research has been identifying the genes linked to different familial forms of PD. PARK6 is a recessive form of Parkinson's due to mutations in PINK1 that result in a PD phenotype. This is the second most common form of recessive PD, second to PARK2, which affects the function of Parkin, an E3 ubiquitin ligase in the PINK1/Parkin mitophagy pathway[12] (Table 1.1).

Clinically, PINK1 heterozygous mutations result in early onset (characterized as onset before the age of 50[13]) and presents as a slowly progressive levodopa-responsive disease. Other symptoms include pronounced dystonia and pyramidal signs[7]. In 2010, a neuropathological report was released about a large Spanish family with five generations of genetic analysis. Family members with a PINK1 exon 7 deletion had 50% loss of neurons in the lateral and medial tiers of the substantia nigra pars compacta with a few neurons containing Lewy bodies[13].

Locus	Gene Symbol	Gene Product	Inheritance	Age of Onset (years)	Ref
PARK1/ PARK4	*SNCA*	α-synuclein	AD	30-60	[14,15]
PARK2	*PARK2*	Parkin	AR	10-50	[16]
PARK6	*PINK1*	PTEN-induced kinase1	AR	30-50	[17]
PARK7	*PAKR7*	DJ1	AR	20-40	[18]
PARK8	*LRRK2*	Leucine-rich repeat kinase2	AD	30-50	[19,20]
PARK9	*ATP13A2*	ATPase type 13A2	AR	10-22	[21]
PARK14	*PLA2G6*	Phospholipid A2	AR	10	[22]
PARK15	*FBXO7*	F-box protein7	AR	20s	[23]
PARK17	*VPS35*	Vacuolar protein sorting 35 homologue	AD	40-50	[24,25]
	PANK2	Pantothenate kinase 2	AR	15-20	[26,27]

Table 1.1: Genetic forms of Parkinsons Disease. A compiled list of all forms of PARK resulting in Parkinson's Disease[7]. Adapted from Houlden, H., and Singleton, A. B. (2012) The genetics and neuropathology of Parkinson's disease. *Acta Neuropathologica 124*, 325–338.

This neurological study is evidence towards how complex and unique to each individual the presentation of the disease is. PINK1 mutations contribute to a multisystem cellular failure in cases of PD, and give reason to characterize how this protein causes this disease.

1.3 Mitochondrial Biogenesis

The mitochondrion is a double-membrane bound organelle essential for many cellular and metabolic processes such as oxidative phosphorylation, lipid metabolism, calcium homeostasis and cell death pathways [1,28]. It consists of an outer mitochondrial membrane (OMM), intermembrane space (IMS), inner mitochondrial membrane (IMM) and the mitochondrial matrix. It represents a very dynamic organelle in the cell, continuously undergoing rapid transitions of fission and fusion as a response to changes in metabolism. These transitions are mediated by guanosine triphosphatases (GTPases) from the dynamin family[28]. The dynamic balance of the mitochondrial membrane is essentially controlled by dynamin proteins, such as Drp1, Mfn1, Mfn2 and OPA1[29].

Fission is a process that generates new mitochondria as a means of division (Figure 1.1). Fission segregates damaged mitochondria and represents an essential part of cell division. This process is mediated by Drp1 (dynamin related protein 1), a cytosolic dynamin that polymerizes and constricts around mitochondria to separate both IMM and OMM[28,29]. This process is heavily regulated by post-translational modifications. Sites of

fission are marked by mitochondrial fission 1 protein (Fis1) and mitochondrial fission factor 1 (Mff1) works as an adaptor for Drp1 to promote polymerization[29] (Figure1.1).

Fusion is an essential process that joins membranes through gradual membrane mixing. This is an important means of ensuring mitochondrial homogeneity, as well as a means of compensating for high metabolic activity. Membrane anchored dynamin proteins, mitofusion 1 and 2 (Mfn1 and Mfn2), are responsible for joining the OMM. IMM fusion is mediated by a separate dynamin, optic atrophy type 1 protein (OPA1), which is located in the inner mitochondrial space[28,29](Figure 1.1).

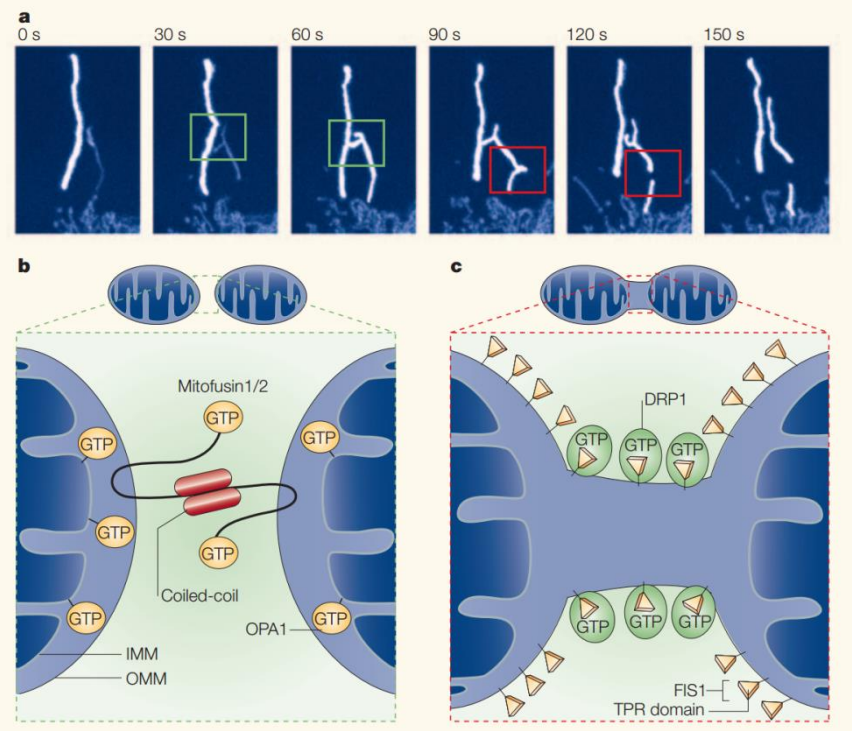

Figure 1.1: Dynamics of the mitochondrial network in mammalian cells.

A) Confocal time-lapse images of fluorescently labeled mitochondria. Mitochondrial fusion is shown in green and fission is shown in red B) Schematic demonstrating mitochondrial fusion where mitochondria fuse via interactions between OMM anchored mitofusins. OPA1 (optic atrophy 1), which is anchored partially on the IMM, participates in the membrane fusion process. C) Fis1 encircles the OMM and recruits the dynamin GTPase Drp1 which subsequently joins mitochondrial scission sites[28]. Adapted from Youle, R. J., and Narendra, D. P. (2011) Mechanisms of mitophagy. *Nature reviews. Molecular Cell Biology 12*, 9–14.

1.4 PINK1/Parkin Mediated Mitophagy

Mitophagy is an essential process to maintain the quality of mitochondria and ultimately the viability of the cell. Since oxidative phosphorylation produces reactive oxygen species (ROS), which are extremely damaging to the cell, there must be mechanisms in place to isolate and remove damaged organelles to maintain mitochondrial integrity.

Several layers of quality control mechanisms exist in mitochondria (Figure 1.2). In the instance of unfolded or misfolded proteins, mitochondria has its own proteasome, the ATP-dependent AAA-proteases which degrade proteins within the matrix and IMS[30,31]. It has also been suggested that mitochondria have their own lysosomal pathway in which mitochondria under oxidative stress can bud off vesicles targeted to the lysosome[30,32]. Ultimately, if there is no compensation for mitochondrial damage, damaged parts of the organelle are segregated and separated through a polarized fission event[28]. Upon the loss of the mitochondrial membrane potential, mitochondria are selectively degraded and engulfed by autophagosomes[33,34]. Selective autophagy was first observed though confocal microscopy[33], a process now understood to be mitophagy. Mitophagy is defined as the selective engulfment of mitochondria by autophagosomes and their catabolism by lysosomes[35].

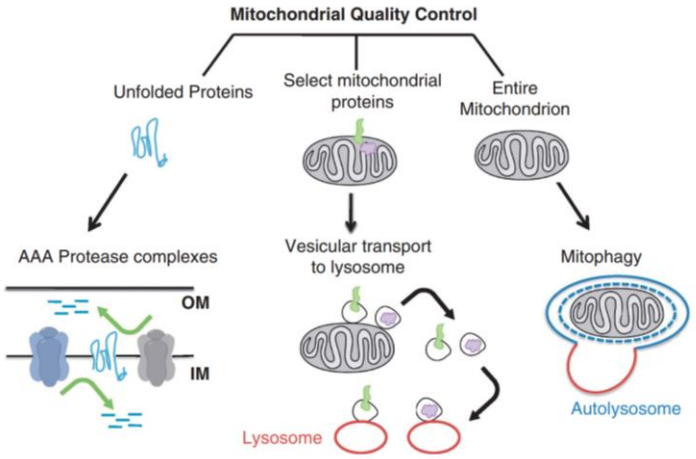

Figure 1.2: Pathways of mitochondrial quality control. Misfolded mitochondrial membrane proteins can be degraded in three pathways. Firstly, AAA protease complexes located in the inner membrane can degrade proteins from either the matrix or inner mitochondrial space faces. Secondly, mitochondrial proteins can be transferred to lysosomes for degradation. This is accomplished by budding mitochondrial vesicles with accumulated proteins for degradation, which are targeted to the lysosome for degradation. The third pathway, mitophagy, involves degradation of entire mitochondria, contained within the double-membrane autophagosomes which ultimately fuses with a lysosome[30]. Taken from Ashrafi, G., and Schwarz, T. L. (2013) The pathways of mitophagy for quality control and clearance of mitochondria. *Cell Death and Differentiation 20*, 31–42.

Proteins PINK1 and Parkin trigger an irreversible pathway for the removal of damaged mitochondria[36](Figure 1.3). Parkin is an E3 ubiquitin ligase responsible for adding ubiquitin chains on proteins, targeting them for both proteosomal and autophagy degradation respectively. It is presumed that phosphorylation of Parkin activates the protein, resulting in its translocation into the OMM[30,36]. The role of PINK1 and Parkin as the essential proteins to kick start mitophagy was validated when PINK1, overexpressed and targeted to the peroxisome, resulted in Parkin-induced peroxisomal autophagy[37]. In attempts to find direct targets of Parkin ubiquitination, studies were carried out in depolarized mitochondria, which results in compromised mitochondrial integrity and should initiate mitophagy. The degradation of a protein Miro was observed. Miro is a Rho GTPase on the OMM responsible for mitochondrial motility. This interaction was linked to PINK1/Parkin mitophagy when they observed a PINK1/Parkin/Miro protein complex in depolarized HEK293T, HeLa and neural cells[36]. The PINK1/Parkin mitophagy pathway also results in Parkin ubiquitination of Mfn1 and Mfn2. This prevents further fusion events of damaged fragments before degradation[30,38]. Other targets of Parkin, Fis1 and TOM70, were determined by a proteomic study in HeLa cells[39]. Accumulation of PINK1 is prevented by degradation via proteases which include PARL, an intramembrane serine protease residing in the IMM, where its proteolytic role thereby prevents mitophagy. PARL will be discussed in more detail in Chapter 5.

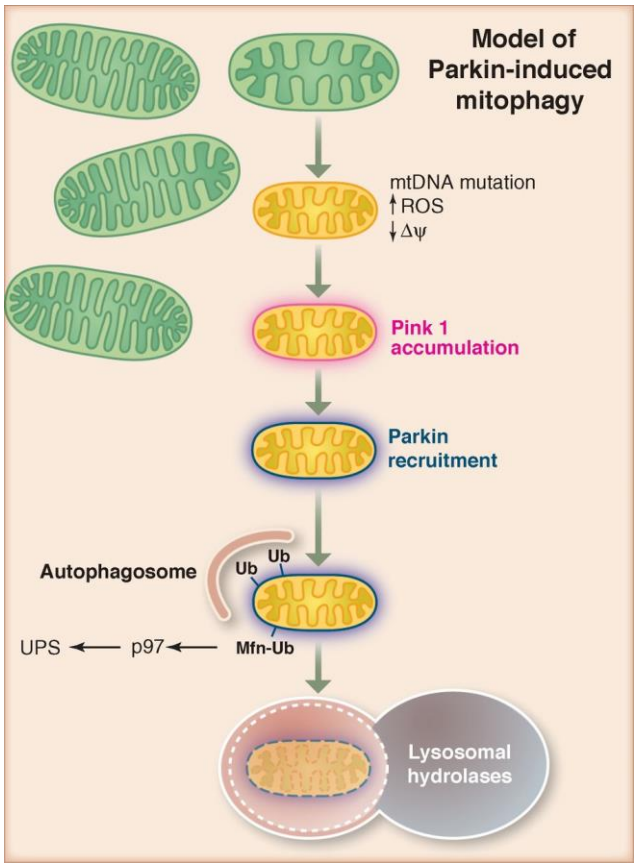

Figure 1.3: Model of mitophagy. PINK1, when localized to the IMM is processed through a membrane cleavage event by rhomboid protease PARL. When damage accumulates in mitochondria resulting in loss of membrane potential across the IMM, the import of PINK1 is restricted to the OMM. This prevents interaction with PARL. This results in recruitment of the E3 ligase Parkin from the cytosol, where it is phosphorylated by the PINK1 kinase. Parkin ubiquitinates (Ub) several outer membrane proteins. Parkin triggers autophagic elimination by lysosomal fusion. UPS - ubiquitin proteasome system[145]. Adapted from Youle, R. J., van der Bliek, A. M. (2012) Mitochondrial fission, fusion and stress. *Science 337,* 1062-1065.

1.5 Phosphatase Tensin Homologue (PTEN) Induced Kinase 1 (PINK1)

PINK1 is a neuroprotective serine/threonine kinase located in mitochondria, which plays major roles in mitochondrial trafficking, dynamics and structure and function[40]. Its neuroprotective roles centre on its ability to prevent apoptotic cell death and mitochondrial dysfunction[41]. PINK1 is a 581 amino acid protein with a canonical N-terminal mitochondrial targeting sequence (MTS), putative single pass transmembrane domain, and C-terminal serine/threonine kinase domain[42](Figure 1.4).

PINK1 transcripts have been found ubiquitously in the body, with higher expression in the heart, skeletal muscle, testes and brain, specifically the substantia nigra, hippocampus and cerebellar Purkinje cells[10]. Loss of function studies have been performed in mice and fly models. *Pink1*$^{-/-}$ mice had intact but enlarged mitochondria, which follows with the evidence to suggest that PINK1 enhances mitochondrial fission. Mitochondrial respiration was also impaired with reduction in respiratory complex I, complex II and aconitase, all enzymes sensitive to oxidation by ROS due to their iron sulfur clusters[43]. In *Drosophila melanogaster*, PINK1 loss of function flies had wing muscle degeneration, slow climbing ability, shorter lifespan, and a decrease in dopaminergic neurons over time as well as male sterility due to impaired sperm production[44].

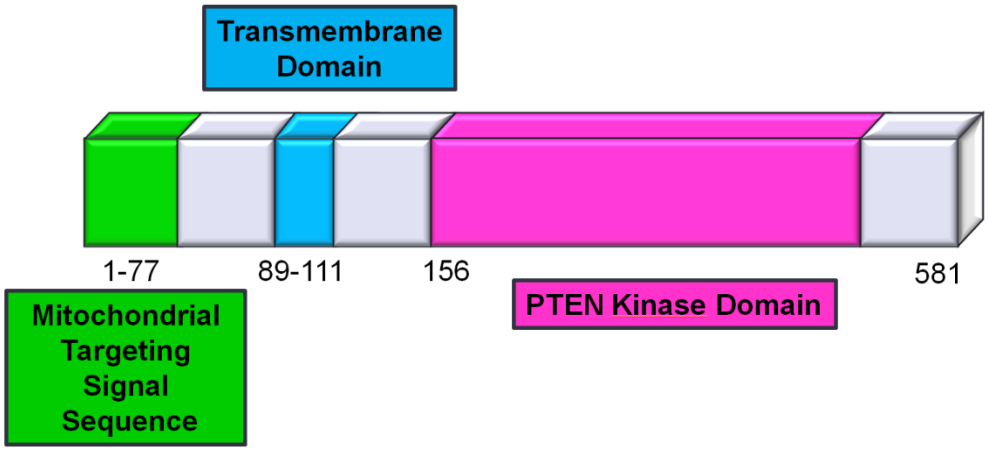

Figure 1.4: Putative domains of PINK1. A domain map of PINK1, showing an N-terminal mitochondrial targeting signal sequence presumed from residues 1-77, a putative transmembrane domain from 89-111, and a C-terminal PTEN (Phosphatase tensin homologue)-induced kinase domain[146]. Adapted from Kawajiir, S., Saiki, S., Sato S., and Hattori, N. (2010) Genetic mutations and functions of PINK1. *Trends in Pharmcological Sciences 32*, 573-580.

1.5.1 Localization of PINK1 in Mitochondria

One of the most controversial questions associated with PINK1 is regarding its localization within mitochondria. PINK1 is a nuclear encoded protein, which is synthesized in the cytosol and targeted to mitochondrial by an N-terminal targeting sequence[42,45]. PINK1 was originally suggested to be found in the outer membrane (OM) of mitochondria[28,46]. This was counterintuitive to the fact that PINK1 has an alpha helical N-terminal mitochondrial targeting sequence, which is typically responsible for directing proteins to the inner mitochondrial regions. Targeting sequences are generally 20-60 amino acids and are capable of folding into an amphipathic alpha helix with both hydrophobic and positively charged sides[42]. Targeting studies *in vivo* in HeLa cells with the MTS constructs of 1-33 aa, 1-77 aa, 1-156 aa attached to GFP were all found to localize to mitochondria[47]. The TM domain of PINK1 acts as a stop-transfer to prevent further import of the protein into the matrix, and that localization was dependent on the presence of the kinase domain and its interaction with Hsp90[47].

Import of PINK1 into mitochondria has been suggested to be facilitated by the TOM complex. PINK1 associates with the import complex to form a 700 kDa complex containing TOM40, TOM22, TOM20 and TOM70[37]. TOM70, which is known as the receptor for internal signals in hydrophobic proteins, is an important component of the TOM complex for mitochondrial import. In a cell free import assay, the knockdown of TOM70 alone resulted in significant reduction of PINK1 import[45]. TOM40, a protein required for the

import of MTS precursor proteins, was not essential for import of PINK1. This supports a hypothesis in the field that PINK1 may only be recognized by TOM70, but is integrated into the membrane by an unknown pathway[45,48]. Although PINK1 and TOM show clear association, Parkin has never been present in the complex, suggesting TOM association with the E3 ubiquitin ligase requires PINK1 to be inserted into the membrane[37,45].

PINK1 has been proposed to exist in both mitochondrial membranes. This has been seen in rat brain subcellular localization studies of PINK1[11,47] and many *in vivo* studies, using immunofluorescence, immunogold assays, western blotting, and subcellular fractionation[12,49-51]. This raises many questions about the role of the protein and produced many controversial hypotheses. A colocalization study with only the predicted MTS and TMD found PINK1 in both membranes[47].

To summarize, it has been proposed that PINK1 may be fully translocated into the IMM where it can be proteolytically processed by PARL, an IMM rhomboid protease, to release a soluble kinase domain into the IMS[34]. Alternatively, the protein may exist stretched through both OMM and IMM, leaving the kinase domain outside the OMM in the cytosol[52] (Figure 1.5). Interestingly, PINK1 and yeast fumarase are the only two proteins identified with MTS sequences that localize constitutively to mitochondria and cytosol[47]. The behavioral patterns of PINK1 highlights the complexity of

mitochondria and how there is much left to understand when it comes to protein import pathways and localization.

1.5.2 PINK1 Degradation

Upon arrival to the IMM, presumably facilitated by TIM23 of the TIM complex, the MTS was suggested to be cleaved by metallopeptidase mitochondrial processing protease (MPP)[42]. Recent studies have suggested otherwise. Cell-free radiolabelled expression of PINK1 was shown to not be processed by MPP in a cell free import assay with HeLa cell purified mitochondria[45]. Therefore this MTS cleavage enzyme remains undetermined.

One well characterized aspect of PINK1 localization is its behavior dependent on the mitochondrial membrane potential (MMP). PINK1 import into the IMM is dependent on an intact membrane potential[12,34,37,42,53,54]. The reason why import is prevented without a MMP still seems unclear. One hypothesis is that the presence of an MMP allows for a unidirectional "pulling" of the highly positively charged MTS into the TIM complex to form the contiguous TOM/TIM23 channel[42]. The loss of MMP prevents this type of import mechanism. Based on current understanding, this potential-dependent localization has led researchers to believe that PINK1 acts as a molecular checkpoint in mitochondrial quality control[55]. In healthy or stable mitochondria with a MMP, PINK1 localizes to the IMM, and is processed to undergo signaling events that maintain mitochondria and prevent apoptosis[42,56-58].

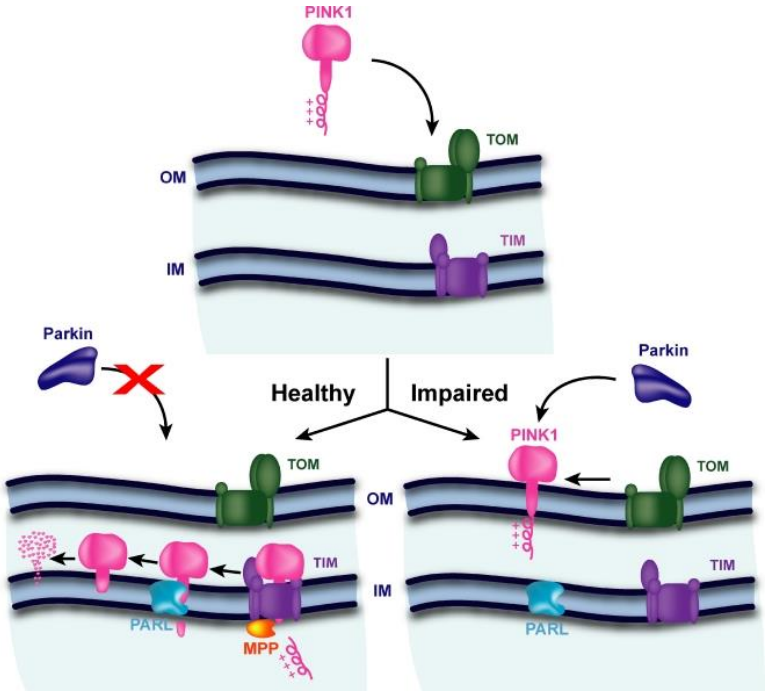

Figure 1.5: Model for PINK1 import and processing. The localization of PINK1 to the outer membrane (OM) or inner membrane (IM) and its IM proteolytic processing by PARL is dependent on an intact mitochondrial membrane potential. Localization of PINK1 to the IMM requires a polarized inner membrane where the positively charged mitochondrial targeting sequence is pulled based on its charge into the TIM complex. PINK1 then encounters PARL, an intramembrane protease located in the IMM, which cleaves the PINK1 release a soluble kinase domain into the IMS, where it is rapidly degraded. If the membrane potential is dissipated, mitochondrial targeting sequence cannot be pulled into the TIM complex, leaving PINK1 in the OMM where it can interact with Parkin and thereby induce mitophagy[34]. Adapted from Jin, S. M., Lazarou, M., Wang, C., Kane, L. A., Narendra, D. P., and Youle, R. J. (2010) *The Journal of Cell Biology 191*, 933–942.

In depolarized mitochondria, PINK1 is left trapped on the OMM, where it signals damage and actives PINK1/Parkin mitophagy pathway[12,34,40,42,54] (Figure 1.5).

1.5.3 PINK1 Interactions with PARL

Despite the various hypotheses about localization, a well characterized protein that interacts with PINK1 is PARL (presenilin-associated rhomboid like protein). PARL is an intermembrane protease responsible for cleaving single pass transmembrane segments, and *in vivo* has been determined to cleave PINK1 in the putative transmembrane domain at residue A103[59] (Figures 5.1 and 5.2). PARL was determined to be the primary protease responsible for generating the predominant PINK1 cleavage product of 53 kDa (Figure 1.5). When mitochondrial proteases Afg3L2, ClpP, Oma1, HtrA2/Omi, Paraplegin, Yme1 and PARL were knocked down using siRNA, PARL was observed to have the greatest effect on PINK1 behavior and cleavage. With polarized membranes, knockdown of PARL resulted in full length PINK1 accumulation. When the membranes were depolarized, PARL knockdown had no effect on normal PINK1 behaviour[34]. PARL also appears to play a role in PINK1 localization, since cleavage of PINK1 by PARL prevents insertion of full length PINK1 into the OMM and instead releases it to the cytosol[48]. The released 53 kDa cleavage PINK1 has a half-life of 30 min *in vivo*[12]. The cleavage of PINK1 by PARL has not been demonstrated *in vitro*.

1.5.4 Parkinsonism-linked PINK1 Mutations Associated with its Kinase Domain and Transmembrane Domain

The PINK1 serine/threonine kinase is one of two kinases causative in genetic forms of PD; the second kinases is the leucine-rich repeat kinase 2 (LRRK2) (Table 1.1). One of the effects of PARK6 mutations causing Parkinsonism comes from mutations in the kinase domain region. Eukaryotic protein kinases require essential conserved structural features to be intact. PINK1 kinase domain is homologous to the calcium/calmodulin family of kinases[60]. It has a two-lobed structure containing an the ATP-binding loop, the salt bridge formed by a lysine in β-strand 3 and glutamate on the helix c, the catalytic loop involved in phosphate transfer and the activation loop required for regulation[4,42] (Figure 1.6). Mutations that disrupt critical interactions in these regions can disable the ability of the kinase domain of PINK1 to phosphorylate targets. Examples of this are five mutations (A168P, A217D, E240K, G386A, E417G), which all affect conserved residues critical for kinase activity. A secondary perspective on kinase domain mutations is that they may result in aggregation, inactivation or deregulation[4].

The catalytic loop contains a conserved HRD motif (360-367) (Figure 1.6) with the catalytic aspartate 362 which acts as a catalytic base. In a well-coordinated active site, the D362 accepts a proton from the hydroxyl group of the target site, which facilitates a nucleophilic attack on the γ-phosphate of ATP (Figure 1.6). Noteworthy are the mutations N367S and L369P PD mutations, which are presumed to disrupt the catalytic D362 and disable it

from phosphorylating downstream targets[42]. ATP positioning is critical for coordinating the γ-phosphate in the active site, and this is determinant on the ATP binding domain corresponding to residues 163-170 with a GXGXXGXV β-hairpin motif. This coordination is aided by K219 on strand 3 (Figure 1.6), which orders both α and β phosphates of ATP. An assisting Mg^{2+} is also stabilized by a highly conserved DFG motif (384-386). The K219, DFG and GXGXXGXV motifs all act to stabilize and prime the ATP for catalysis. PD mutations A168P (affecting the β-hairpin motif), A217D (affecting the K219), A383T, A385L, G383A, C388R (affecting the DFG motif) are presumed to play a role in drastically reducing the kinase function[4,42,61].

The activation loop of the kinase domain is found in residues 384-417, flanked by the conserved DFG (384-386) and APE (415-417) regions on either end. There are eight known mutations that exist in this subdomain of the kinase. PINK1 is proposed to be activated by an autophosphorylation event on serine residue(s) in the activation loop, predicted to be on the highly conserved S402[4,42,49]. A subsequent study found that upon depolarization of the mitochondrial membrane, where PINK1 is predicted to be at the OMM, PINK1 undergoes two autophosphorylation events at S228 and S402, observed *in vivo* in HeLa cells in the presence of CCCP, a mitochondrial uncoupler[62]. Mutations that perturb kinase activity abolished the phosphorylation of these sites. Double mutations of S228A and S402A prevented autophosphorylation and Parkin recruitment to the OMM[62].

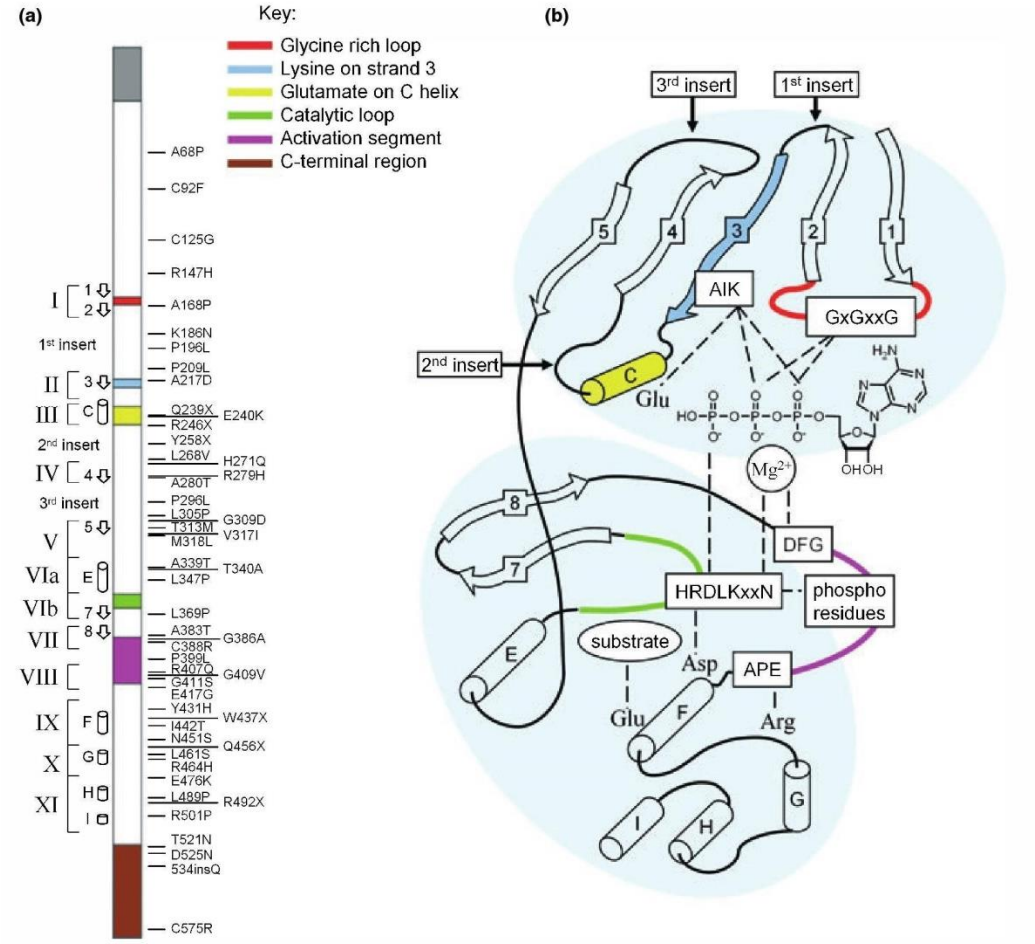

Figure 1.6: Kinase domain and Parkinson's disease associated mutations of PINK1. A) PINK1 linear sequence marked with Parkinson's disease associated mutations and color matched to kinase subdomains, predicted β-strands (shown as arrows) and α-helices (shown as cylinders). A predicted mitochondrial targeting sequence (residues 1-34) is shown in gray. B) A schematic of the PTEN serine-threonine kinase domain. Conserved motifs are shown in boxes. Dotted lines mark predicted interactions between within the protein between residues, ATP, and cofactor Mg^4. Adapted from Mills, R. D., Sim, C. H., Mok, S. S., Mulhern, T. D., Culvenor, J. G., and Cheng, H. (2008). *Journal of Neurochemistry 105*, 18–33.

P-3	P-2	P-1	P	P+1	P+2	P+3
F/L/I	A/G/V/L/I/F/Y/C/R	X	S/T	N/S/D/E	L/I/M/F	A/V/L/I/M/P/F/T/S/E/H/Q

Table 1.2: The optimal phosphorylation sequence of PINK1 predicted by PREDIKIN. PREDIKIN is based on analysis of 1) crystal structures of serine/threonine kinases in complex with peptide substrates, 2) kinase sequences, and 3) phosphorylation site sequences of kinases. P - phosphorylation site (serine/threonine). Residues N-terminal to P are referred to as P-1, P-2, P-3, and residues C-terminal to P are referred to as P+1, P+2, P+3. Residues are in order of preference. X - any residue[42]. Adapted from Sim, C. H., Gabriel, K., Mills, R. D., Culvenor, J. G., and Cheng, H. (2012) Analysis of the regulatory and catalytic domains of PTEN-induced kinase-1 (PINK1). *Human mutation 33*, 1408–1422.

1.5.5 Phosphorylation Targets of PINK1 Kinase

The phosphorylation targets of the PINK1 kinase domain have only begun to be uncovered, with only a handful of targets identified to date. Some of these proteins are Miro, Parkin, TRAP1 (Tumor necrosis factor-receptor associated protein 1 or Hsp75) and Omi (also known as HtrA2)[60](Figure 1.7). PINK1 has also been suggested to regulate Na^{+}/Ca^{2+} exchanger activity, which prevents calcium accumulation within the mitochondrial matrix, and ultimately prevents ROS accumulation[42,60]. It is accepted that the adaptor protein Miro, a Rho GTPase, is phosphorylated by PINK1 in conjunction to an interaction with Parkin on the OMM. The phosphorylation of Miro by PINK1 enables Parkin to ubiquinate and target the protein to the proteasome[36]. Miro is a protein regulated by cytosolic Ca^{2+} and acts to control mitochondrial mobility[36].

Another phosphorylation target is TRAP1, a poorly characterized protein also known as heat shock protein 75. TRAP1 localizes to the inner mitochondrial space. This was determined through affinity purification in PC12 cells and further verified *in vivo* and *in vitro*[56]. Phosphorylation of TRAP1 is abolished in the presence of PINK1 kinase inactivating mutations (G309D, L347P), which suggests that PINK1 is responsible for phorsphorylation[56]. An experiment which knocked down expression of TRAP1 found that its absence was correlated with an increase in oxidative stress in mitochondria. This knockdown also resulted in cytochrome c release into the cytosol which activated apoptosis[56]. It is presumed that

PINK1 phosphorylation of TRAP1 is part of an anti-apoptotic mechanism to prevent cell death from oxidative stress due to ROS build up (Figure 1.7). This is important for dopaminergic neurons where the production of dopamine increases ROS production[63]. In another link to PD, TRAP1 also appears to be the first protein linking PINK1 dysfunction in mitochondria to the build-up of α-synuclein toxicity, linking this pathways with PD symptoms of neuronal apoptosis and α-synuclein accumulation, better known as Lewy bodies[58].

In *Drosophila melanogaster* PINK1 null mutants, expression of Sir2 rescued flight muscle defects caused by PINK1 deficiency[64]. Sir2, silent information regulator 2, is hypothesized to mediate cellular stress. It is unknown how PINK1 interacts with Sir2. It may be directly regulated by PINK1 phosphorylation when the protein is found in the cytosol, or indirectly through other protein interactions[65]. Further genetic analysis found that the Sir2's ability to rescue PINK1 loss of function phenotype was abrogated by FOXO deletion, suggesting that Sir2 and FOXO act in a pathway downstream of PINK1[65]. FOXO or Forkhead box, is a protein recognized to protect cells against oxidative stress and glucose deprivation by regulation of SOD2[65] (Figure 1.7).

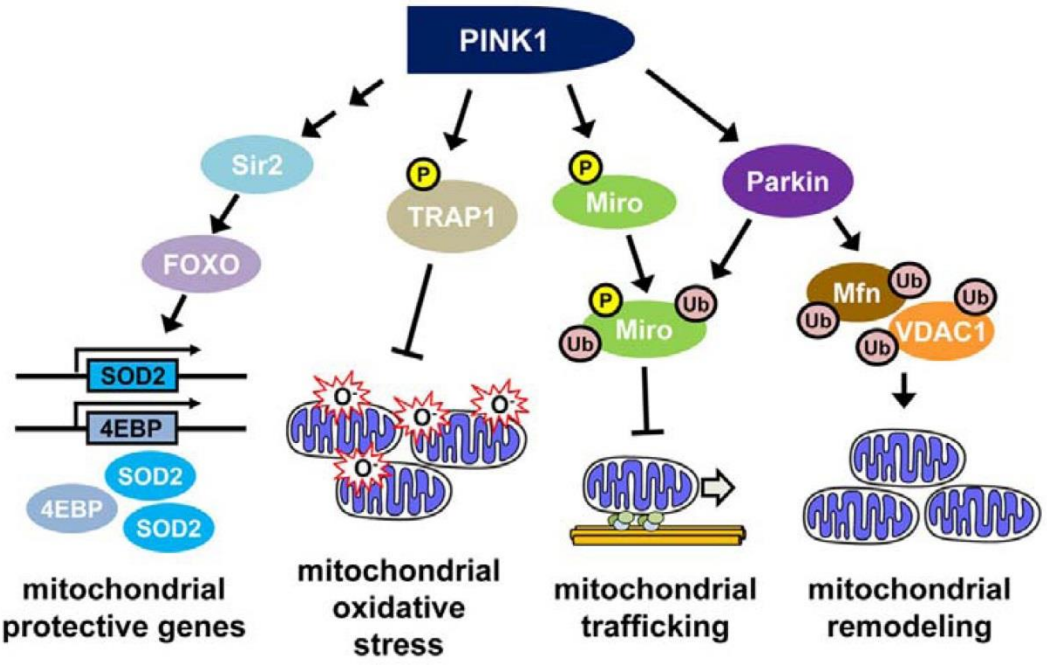

Figure 1.7: Phosphorylation targets of PINK1. PINK1 regulates mitophagy through the phosphorylation of Parkin, which ubiquitinates a variety of mitochondrial proteins. PINK1 also phosphorylates Miro which is involved in mitochondrial trafficking and inner mitochondrial space protein TRAP which protects against oxidative damage. PINK1 can also activate expression of genes SOD2 and 4EBP which are suggested to play a role in mitochondrial protection through the Sir2-FOXO pathway[65]. Adapted from H. Koh, J. Chung. Molecules and Cells. 34(2012): p. 7-13.

An important phosphorylation target of PINK1 is Parkin. PINK1 and Parkin are an intensely studied pair of proteins known to interact, but Parkin phosphorylation by PINK1 has been disputed. The arguments for phosphorylation were weak as there was no concrete phosphorylation site identified. A hypothesis existed that PINK1 and Parkin interactions were linked by mutual interactions with proteins like Miro, where PINK1 would phosphorylate Miro, then facilitating Parkin ubiquitination of the same target[36]. It was only recently that a Parkin-activation phosphorylation site was identified - a highly conserved Ser65. Parkin was phosphorylated in a PINK1-dependent manner when mitochondria are depolarized, and Parkin translocation into the OMM is dependent on this phosphorylation[66] (Figure 1.5). Phosphorylation of Parkin by PINK1 was also proposed to relieve autoinhibition, which would explain how only loss of membrane potential activates the Parkin mitophagy pathway[53,66].

PINK1 activates basal and starvation induced autophagy by interacting with Beclin-1, a pro-autophagic protein involved in other neurodegenerative diseases, such as Huntington's disease and Alzheimer's disease[10]. In the presence of a depolarized membrane, PINK1 phosphorylates Bcl-xL (an anti-apoptotic protein)[41].

In addition to PD mutations in the kinase domain, several mutations are located within or surrounding the predicted transmembrane domain (TMD). No study has been carried out to examine why these mutations lead

to PD. At the cellular level it is not known whether these mutations disrupt secondary structure, the localization of PINK1 or its cleavage by PARL, the intramembrane protease found in the inner mitochondrial membrane (Figure 1.5). Further study is needed to address these questions, which is the focus of this thesis. This topic will be discussed in detail in Chapter 3.

1.6 Membrane Protein Expression

One of the greatest bottlenecks in the study of membrane proteins structure and function is obtaining adequate quantities of protein[67,68]. In most cases, natural abundance of membrane proteins is low and insufficient for structural studies[69]. Early successes of membrane protein crystallography required protein sources with a rich native protein requiring no modification, such as the case of with Rhodopsin, a protein naturally abundant in the retina[70]. In contrast, the study of proteins that are low in abundance or eukaryotic targets that have complex folding patterns often requires recombinant expression with gene modifications to enhance stability, and enable detection and purification[69]. This has led to many different strategies and expression hosts that have been used to for heterologous membrane protein production.

Membrane proteins are extremely sensitive to the lipid environment, protein processing, folding and post-translational modifications. This makes finding an ideal and compatible expression system extremely valuable when producing quality membrane proteins. The *in vitro* study of eukaryotic

membrane proteins has been especially problematic, with the frequent requirement for a eukaryotic heterologous hosts for overexpression, including Sf9 insect cells, HEK cells, CHO cells, and yeasts such as *Pichia pastoris* and *Saccharomyces cerevisiae*[68,71].

1.7 *Pichia pastoris*

Pichia pastoris is a methylotrophic yeast expression system, which has recently become popular for its ability to express heterologous proteins. It uses methanol as a source for carbon and energy. Large scale expression requires an inexpensive medium and *P. pastoris* can grow to high cell densities[72], thereby resulting in high yields. Vectors for expression in *P. pastoris* have a strong promotor, the AOX1, which is powerful and tightly regulated, making it advantageous over *Saccharomyes cerevisiae*[67,73]. As post-translational modifications can be essential for proper folding and function[69], *P. pastoris* is capable of generating post-translational modifications such as N and O-linked glycosylations, which resemble those of higher eukaryotic organisms[74]. They are also capable of generating more authentic glycosylations than *S. cerevisiae,* with mannose additions of 8-14 residues in comparison to the 40-150 residue additions observed in *S. cerevisiae*[75].

The yeast expression system *P. pastoris* has been successfully used to produce many eukaryotic membrane proteins for structural studies including; G-protein coupled receptors[76,77], ion channels[78,79], aquaporins[80,81] and ABC transporters[76,77,82].

1.7.1 Basic Features of *P. pastoris* Expression System

In an analysis of criteria that make up a suitable expression system, *P. pastoris* meets many of the basic requirements. *P. pastoris* allows for simple genetic manipulation by linear gene integration into the host genome. It is a low cost production system made up of relatively inexpensive medium components, containing yeast extract, tryptone, peptone, salt, glycerol and methanol[76,77]. Yeast are also notorious for generation of very high cell densities relative to other microbial expression systems. They also meet safety requirements being non-pathogenic[83].

1.7.2 Promotor

One reason *Pichia pastoris* makes a strong system for heterologous overexpression is its strong inducible promotor, alcohol oxidase 1 (AOX1). Since methanol metabolism is capable of solely generating a source of carbon, *P. pastoris* is considered methylotropic yeast. The primary enzyme responsible for this metabolism is alcohol oxidase (AO), encoded exclusively by two genes, AOX1 and AOX2[84]. AOX1 is responsible for production of most AO within the cell. Alcohol oxidase catalyzes the conversion of methanol to formaldehyde and hydrogen peroxide. The production of alcohol oxidase is highly regulated by transcriptional factors[84], which is why it is utilized as such a strong promotor for expression of heterologous proteins. In the presence of methanol, expression of AO can make up 35% of all cellular proteins in *P. pastoris.* Under the conditions when yeast are grown with

glucose or any other carbon source, alcohol oxidase is not necessary for metabolism and is not present[85].

1.7.3 Gene Integration

P. pastoris requires gene integration into the host genome. Stable integration of genes into the host genome allows a predictable and consistent protein production[86]. One way of accomplishing this is digesting expression vectors in a way that they are flanked by 5' and 3' AOX1 sequences. The linearized gene undergoes a gene replacement event where the gene replaces the AOX1 gene while still remaining flanked with the 942 bp region of 5' AOX1 promotor and 3' region. This is accomplished with chemical transformation or electroporation. Gene integration occurs directly into the 5' AOX1 promotor so that intended expression of AO in the presence of methanol directly translates into expression of the desired protein[87]. Cells are then forced to generate AO from the weaker AOX2 gene, resulting in a Mut^{s} phenotype, meaning methanol utilizing slow. The Mut^{S} phenotype can be identified by slow growth of *P. pastoris* on medium containing methanol, and can be advantageous in protein expression as less methanol utilization is marked by slower growth and often, more foreign protein production. Transformation and gene integration is not limited to manipulation of the AOX1 promotor, but is also possible for genes to be incorporated at AOX2 or at the HIS4 loci of *P. pastoris*[87]. Since transformation involves a linear gene, multi-copy integration is probable and has produced questions regarding gene-dosage.

1.7.4 Multicopy Integration

Due to the method of recombinant integration of a desired gene into *Pichia pastoris*, multi-copy strains can be generated and it is often ideal to isolate these strains. Multi-copies in an expression cassette typically have higher protein yields than single-copy inserts. However, having increased gene dosage is not always the solution to obtaining the most protein. In the case of GPCR human μ-opioid expression in *Pichia pastoris*, a higher gene dosage does not equate to higher expression[88]. This can be due to spatial limitations of the membrane, as there is limited area to contain overexpressed membrane proteins in comparison to overexpressed soluble proteins in the cytosol.

For each protein, however, it is accepted that one must test an expression system as it is difficult to predict which system will generate a properly folded protein. This is particularly the case for eukaryotic membrane proteins and in particular those with more than one transmembrane domain, i.e. polytopic. This step however is essential for *in vitro* analysis of protein for both function and structure.

1.8 Thesis Objective:

The objective of this thesis centers on the study of membrane proteins and membrane domains. In order to analyze membrane proteins, well defined and optimized expression conditions and purification regimens must be developed. This is often very difficult as membrane proteins or the hydrophobic counterparts must be overexpressed, stabilized outside their native environment and purified homogenously.

There are two converging goals of this thesis. First is the optimization using the overexpression system, *Pichia pastoris,* for the purposes of screening for high expressing membrane proteins. Chapter 3 details the overexpression and purification of the transmembrane domain of PINK1, ending with a structural investigation, using solution NMR spectroscopy. Development of a rapid screening system to identify yeast colonies overexpressing the polytopic membrane protein, PARL, is outlined in Chapter 4. This system was used to find a stable overexpressing clone for PARL, a mitochondrial intramembrane rhomboid protease. The expression and purification of this protein is outlined in Chapter 5. This converges with the structural analysis of the transmembrane domain of PINK1, and mitochondrial kinase found to contain mutations resulting in Parkinson's disease. The transmembrane domain of PINK1 is cleaved by PARL, and this thesis outlines the developing story to analyze how these proteins interact and contribute to our understanding of why mutations in the TMD of PINK1 lead to Parkinson's disease.

This thesis discusses the strategies used for different kinds of membrane protein expression leading to the investigation of *in vitro* interactions between PINK1 and PARL.

Chapter 2

Materials and Methods

2.1 Materials

Reagents:

Standard lab reagents were purchased from Sigma-Aldrich (ON, Canada), Fisher Scientific (ON, Canada). Other reagents are listed below.

Kits:

- QuikChange Lightning Mutagenesis Kit (Stratagene)
- QIAquick Gel Extraction Kit (Qiagen)
- QIAspin Spin Miniprep Kit (Qiagen)
- QIAGEN Plasmid Maxi Kit (Qiagen)
- *Pichia* EasySelect™ Expression Kit (Invitrogen, USA)
- Clontech In-Fusion HD Cloning Kit (Clontech)

Enzymes:

- Restriction enzymes with appropriate buffers (Fermentas, USA)
- T4 DNA ligase (Invitrogen, USA)
- TopTaq DNA Polymerase (Qiagen)

Primers:

Synthesized by Integrated DNA Technolgies, USA

Culture medium:

- LB (Luria Bertani) liquid medium from Fisher Scientific
- LB Agar: LB liquid with 1.5% w/v Agar

Solutions:

Phosphate buffer solution (PBS)	137 mM NaCl, 10 mM phosphate buffer, 2.7 mM KCl, pH 7.4
Tris buffered saline	50 mM Tris, 150 mM NaCl, pH 7.5
SDS-PAGE gel-loading buffer	50 mM Tris-Cl pH 6.8, 100 mM dithiothreitol, 2% SDS, 0.1% bromophenol blue, 10 % glycerol
Agarose gel-loading (6 X)	0.02% bromophenol blue, 0.02% xylenecyanol, 30% glycerol in H_2O
Tris/Acetate/EDTA (TAE)	0.04 M Tris-acetate, 0.001 M EDTA, pH 8

Bacterial strains:

Strains	**Genotype**
Top 10	F– mcrA Δ(mrr-hsdRMS-mcrBC) Φ80lacZΔM15 ΔlacX74 recA1 araD139 Δ(ara leu) 7697 galU galK rpsL (StrR) endA1 nupG
DH5α	F– Φ80***lac***ZΔM15 Δ(***lac***ZYA-***arg***F) U169 ***rec***A1 ***end***A1 ***hsd***R17 (rK–, mK+) ***pho***A ***sup***E44 λ– ***thi***-1 ***gyr***A96 ***rel***A1

2.2 Methods:

2.2.1 Transformation

Competent cells (DH5α or Top10, Invitrogen) from -80 °C were thawed on ice for 15 min. 1 µL of plasmid, or 5 µL of ligation product were added to the competent cells, mixed and incubated on ice for 20 min. Cells were then heat shocked for 30 s and incubated on ice for 2 min. 1 mL of LB was added to the competent cells and incubated at 37 °C for 1 h with shaking. Cells were spread on an appropriate agar plate using sterile techniques and the plate was incubated at 37 °C

2.2.2 Standard Polymerase Chain Reaction

TopTaq Kit (Qiagen) was used standard lab PCR reactions. 50 µL PCR reactions were carried out with 5 µL 10X TopTaq buffer, 1 µL of 10 mM of both forward and reverse primers, 1 µL of 10 mM dNTPs, 1 µg of template plasmid, 0.25 µL TopTaq, with ddH_2O to 50 µL final volume. PCR cycling was carried out with the Eppendorf Thermocycler starting with a 3 min denaturation cycle (94 °C) and 30 cycles of denaturation (30 s, 94 °C), annealing (30 s, 60 °C) and extension (1 min/kb, 72 °C), with a final extension of 10 min (72 °C).

2.2.3 PCR Screening Protocol:

To ensure that transformed colonies from ligation reactions contained a desired gene insert, PCR screening was used on a collection of colonies from a plate. Each colony was selected off of the plate under sterile

conditions and mixed in a PCR tube containing 15 µL ddH_2O. The pipette tip containing the remainder of the colony was transferred to a sterile culture tube with LB and antibiotics. To the PCR tubes the following was added: 0.5 µL 10 mM dNTPs, 0.5 µL of 10 mM forward and reverse screening primers, 2.5 µL of 10X TopTaq buffer and 0.125 µL of TopTaq (Qiagen). The samples were cycled in Eppendorf Thermocycler with an initial denaturation (95 °C, 3 min), 25 cycles of denaturation (94 °C, 30 s), annealing (58 °C, 1 min), and extension (72 °C, 1 min), with a final extension (72 °C, 5 min).

2.2.4 1% Agarose Gel Protocol

An agarose gel (1%) was prepared by melting 1 g of agarose into 100 mL 1X TAE buffer in a microwave. After cooling, 7.5 µL of 10 mg/mL stock ethidium bromide was added, thoroughly mixed, and poured into the gel apparatus. Gels were loaded with samples in 6X loading dye (Thermo Scientific), and a base pair ladder (100 bp or 1 kbp) for reference (GeneRuler DNA ladder, Thermo Scientific), and electrophoresed at 85 V. Gels were visualized with UV light in the ImageQuant LAS4000 (GE healthcare, USA).

2.3 Expression and Purification of PINK1 Transmembrane Domain

2.3.1 Cloning of PINK1 into pMAL

New England Biolab vector pMAL-c2 which contains an N-terminal Maltose Binding Protein (MBP) followed by a tobacco etch virus (TEV) cleavage site was obtained from the laboratory of Dr. Howard Young (University of Alberta). This vector comes with the signal sequence removed

for cytoplasmic expression. The PINK1 transmembrane (TM) sequence from amino acids 89-111 was codon optimized for *E. coli* expression. Long primers; forward 5' GAT CCG CCT GGG GCT GCG CGG GCC CGT GCG GCC GCG CGG TGT TTC TGG CGT TTG GCC TGG GCC TGG GCC TGA TTT AAG and reverse 5' AAT TCT TAA ATC AGG CCC AGG CCC AGG CCA AAC GCC AGA AAC ACC GCG CGG CCG CAC GGG CCC GCG CAG CCC CAG GCG, were ordered PAGE purified to duplex and were inserted into the vector flanked by 5' BamHI and 3' EcoRI.

Primer duplexing protocol was obtained from Integrated DNA Technologies. Primers were dissolved in 100 mM potassium acetate, 30 mM HEPES, pH 7.5 to A_{260} of 3.0 and 13 µL of each were mixed together. The mixture was heated to 94 °C and cooled to 4 °C on a gradient over 30 min. This duplex was inserted into a BamHI/EcoRI digested vector, transformed into Top10 competent cells, and plated on LB plates containing 100 µg/mL ampicillin. The pMAL vector was restriction digested with Fermentas restriction enzymes and buffers. 3 µg (3.4 µL) of pMAL vector was mixed with 3 µL BamH1 and 3 µL EcoR1 (20 U/µL), 5 µL 10X fast digest buffer with stain and 35.4 µL ddH_2O, which was incubated at 37 °C for 1.5 h. A 1% agarose gel was run and the digested pMAL fragment was purified with QIAquick Gel Extraction Kit (Qiagen). Ligation of PINK1 transmembrane duplex into the pMAL vector was carried out by T4 DNA ligase kit (Invitrogen) by mixing 13 µL of PINK1 duplex, 1 µL digested pMAL vector, 4 µL 5X ligase buffer and 1 µL T4 DNA ligase. The ligation was carried out at

room temperature for 1 h. Transformation was into Top10 competent cells and cells were plated on LB plates with 100 μg/mL ampicillin.

Colonies were screened for insertion of the TM sequence with screening primers that bound 5' within the MBP region and 3' of the inserted segment (Forward 5' TCG CTG ATT TAT AAC AAA GAT CTG C and reverse 5' TTA AAT CAG GCC CAG GCC). Four clones resulted in successful sequencing results from The Applied Genomics Center (TAGC) (University of Alberta).

2.3.2 Growth and Expression in *E.coli*

Expression in LB Medium

Medium used was LB + 0.4% glucose + 100 μg/mL ampicillin. PINK1-pMAL was transformed into DH5α and a fresh transformation was used to inoculate an overnight culture grown at 37 °C. Large cultures were inoculated with 2% of the overnight culture and grown at 37 °C to an A_{600} of 0.6 and induced to a final concentration of 0.5 mM IPTG. Expression was optimal after 3 days at 24 °C and 225 rpm. Cells were centrifuged at 8000 *g* for 10 minutes and used immediately or frozen at -20 °C.

Expression in Minimal Medium

Enriched M9 minimal medium was used for expression of MBP-PINK fusion construct. Using stock solutions (Table 2.1), combine autoclaved 100 mL 10X M9 minimal medium, 100 mL 10X phosphate buffer, 1 mL metal mix, 0.1% w/v NH_4Cl, 1% w/v D-glucose, 1% thiamine w/v, 100 μg/mL final concentration of ampicillin and ddH_2O to 1 L.

Table 2.1: Recipe for Components of Minimal Medium in g/L

Media Component	Chemical	Quantity (g/L)	Concentration (mM)
10X M9 Minimal Medium (pH 7.4)	NaH_2PO_4	120 g	1000 mM
	KH_2PO_4	60 g	440 mM
	NaCl	5 g	85 mM
10X Phosphate Buffer	KH_2PO_4	49.6 g	365 mM
	K_2HPO_4	106 g	608 mM
Metal Mix	$MnSO_4$	5 g	33 mM
	$FeSO_4 \cdot 7H_2O$	0.925 g	3 mM
	$MgSO_4 \cdot \cdot 7H_2O$	50 g	203 mM
	$CaCl_2 \cdot 2H_2O$	0.5 g	4 mM

A freshly transformed colony of MBP-PINK1 in DH5α was used to inoculate an overnight culture of LB with 100 ng/mL final ampicillin concentration, grown at 37 °C. Once the A_{600} has reached ~2, 50 mL of overnight culture was used to inoculate 1 L minimal medium culture grown at 37 °C and 225 rpm in a shaker. Expression was induced once the A_{600} was ~0.5 with 0.5 mM IPTG. Growth was continued for 40 h (37 °C, 225 rpm). Cells were centrifuged in Beckman centrifuge (rotor JLA 8.1) at 7000 *g* (4 °C, 10 min) and used immediately for cell lysis or stored at -20 °C.

2.3.3 Small Scale Expression Test of MBP-PINK1 in *E. coli*

Small cultures of 25 mL were grown overnight in either LB medium or M9 minimal medium. Growth conditions were varied by time (from 3 h – 72 h), concentration of IPTG (from 0.001 mM to 1 mM) and induction temperature (22 °C and 37 °C). Cell pellets from these experiments were

resuspended in buffer (1X PBS (pH 7.4), 1 mM EDTA, 1 mM PMSF) at 5X the volume of the pellet weight. 450 µL of each resuspension was collected . 1 µL of 10 mg/mL DNase was added to each tube and mixed well. 50 µL of 10% v/v Triton X-100 was added to each cell resuspension and tubes were incubated at 4 °C with rotation for 1.5 h. Cells were centrifuged at 4 °C with a benchtop centrifuge at 14 000 *g* for 15 min. 30 µL of each supernatant was set aside for SDS-PAGE gel. An approximate 2 µL fraction of the inclusion body was collected with a pipette tip and solubilized in 100 µL of 8 M urea. 30 µL of this sample was also set aside for SDS-PAGE gel. Both supernatant and inclusion body samples were mixed with 10 µL 4X SDS gel buffer, and 10 µL of this mixture was loaded onto 12 or 14% acrylamide SDS-PAGE gels with 4% stacking gels. Gels were stained with Coomassie stain, destained, and imaged with ImageQuant LAS4000 (GE healthcare, USA).

2.3.4 Cell Lysis

Cells were resuspended on ice in lysis buffer 5X the weight of the cell pellet (20 mM KPO_4 buffer (pH 8), 120 mM NaCl, 50 mM glycerol, 1 mM EDTA, 1 mM PMSF, 1 mM DTT) with protease inhibitor tablets (1 per 100 mL) and 10 µg/mL DNase. Cells were lysed in Constant System cell disrupter at 35 kPSI, and 0.5% Triton X-100 was added post-lysis. Lysate was centrifuged in the Beckman centrifuge (rotor JA 25.50) at 40,000 *g* for 30 min at 4 °C. The supernatant was collected carefully to avoid contamination of inclusion bodies and poured into chilled 50 mL Falcon tubes.

2.3.5 Amylose Purification of MBP-PINK1

The amylose resin (Amylose Resin High Flow, NEB) was equilibrated by running 10X the column volume of phosphate salt EDTA (PSE) buffer (20 mM KPO_4, 120 mM NaCl, 1 mM EDTA) through resin by gravity flow at 4 °C. MBP-PINK1 supernatant was mixed batch with resin and incubated on rotator for 2 h at 4 °C. 1 mM PMSF was added to continue proteolysis prevention. Batch resin was flowed through column and flow through was collected. The amylose resin was washed with ~1 L of PSE until A_{280} returned to ~0.03 or less. MBP-PINK1 was eluted with 50 mL of 40 mM maltose in PSE buffer. Fraction collection was monitored by A_{280} until A_{280} returned to baseline.

2.3.6 Tobacco Etch Virus (TEV) Digestion of MBP PINK1:

For TEV digestion 50 µL of purified TEV (30 mg/ml, recombinant TEV expressed and purified from pET vector prepared by Dr. Elena Arutyunova was used per 20-30 mg of fusion protein present, with 1 mM DTT at 20X TEV buffer (1 M Tris-HCl, pH 8.0, 10 mM EDTA) and left to digest at 16 °C. A second aliquot of TEV was added after 2-3 days of digestion, and continued until sufficient digestion was observed in the form of precipitation of the hydrophobic TM PINK1. Small digestions (~10 mL or less) would typically take approximately 4 days, and large (~20 mL or more) take up to 8 days.

2.3.7 Organic Extraction of PINK1 Transmembrane Segment

Corex glass tubes, 30 mL, were rinsed with methanol to pre-clean, and digested MBP-PINK1 was divided into equal fractions between tubes (~45 mL/4 tubes). 2.5 mL of 60% w/v Trichloroacetic Acid (TCA) was added to each tube and was incubated for 30 min on ice. The precipitant was centrifuged for 10 min at 10,000 *g* in Thermo Scientific Sorvall centrifuge (rotor SS-34) at 4 °C. The supernatant was decanted and the pellet was rinsed 3 times with ddH_2O. For the final rinse, the pellet was incubated with water on ice for 10 min. A 50:50 isopropanol:chloroform (100 mL) was mixed in a graduated cylinder and used to resuspend the pellets by carefully scratching them off the sides of the Corex tube. The resuspension in organic solvents was incubated on ice for 30 min. A glass homogenizer was used to homogenize the pellet, which was distributed equally into 16 X 100 mm glass tubes. 1-2 ml of ddH_2O was aliquoted into each tube and left to incubate in a fume hood overnight. The next day, the organic layer (bottom layer) was carefully removed with a glass Pasteur pipette and transferred it into a clean tube. 1-2 ml of ddH_2O was aliquoted into each new tube and left to incubate in a fume hood overnight at room temperature. This separation was repeated until all white precipitate was removed and organic phase was considered clean. At this point, organic layers were combined and dried down under nitrogen or argon gas.

2.3.8 High Performance Liquid Chromatography of PINK1 Transmembrane Segment

The PINK1 peptide was resuspended in ~6-8 mL of 7 M guanidine-HCl, 50 mM KPO_4 buffer (pH 8). This was injected through a 2.5 mL loop onto a Agilant Zorbax SB-300 C8 silica based, stainless steel 25 cm x 1 cm column which was preheated to 60 °C. The column ran at 60 °C with a flow rate of 1 ml/min. An isopropanol gradient against 0.05% TFA/water was used to elute the protein, where the gradient ran from 20% - 80% over 180 min. PINK1 TM typically eluted at ~50% isopropanol. Determination of fractions containing the peptide was established by running 6% urea gels, which were visualized through silver staining.

2.3.9 Analytical Gel Filtration of MBP-PINK1 Fusion Protein

Amylose-purified MBP-PINK1 fusion protein (300 µL of 1 mg/mL) was filtered in DURApore membrane filters (Millipore) with a benchtop centrifuge at 14,000 *g* for 5-10 min at 4 °C or until completely filtered. Analytical gel filtration was performed on a SEC 75 10/300 column (GE Healthcare, USA). The column was equilibrated with 2 column volumes of 20 mM KPO_4, 120 mM NaCl, 1 mM EDTA, pH 8.0. 250 µg of fusion protein was loaded and the column was run with the equilibration buffer. Samples were run at 0.8 ml/min and the absorbance values of the fractions were determined at 280 nm. Fractions were collected in 18 mm x 100 mm tubes.

2.3.10 6 M Urea Gels

Based off of Hermann Schägger's Nature Protocols "Tricine-SDS-Page" [89]

Table 2.2: Recipe of Components for 6% Urea Gel

Gel Component	Chemical	Composition
AB3 Stock Solution	Acrylamide	48% w/v
	Bis-acrylamide	1.5% w/v
AB6 Stock Solution	Acrylamide	46.5% w/v
	Bis-acrylamide	3% w/v
4X SDS Buffer	SDS	3% w/v
	βME	6% v/v
	Glycerol	30% w/v
	Coomassie blue dye	0.05% w/v
	Tris-HCl (pH 7)	150 mM
3X Gel Buffer (pH 8.45)	Tris Base	3 M
	Hydrochloric acid	1 M
	SDS	0.3% w/v
10X Anode Buffer (pH 8.9)	Tris Base	1 M
	Hydrochloric acid	0.225 M
10X Cathode Buffer (pH 8.25)	Tris Base	1 M
	Tricine	1 M
	SDS	1% w/v

Table 2.3: Silver Stain Solutions

Silver Stain Buffer	Chemical	Composition
Fixing Solution	Methanol	50% v/v
	Acetic acid	10% v/v
	Ammonium acetate	100 mM
Sensitizer Solution	Sodium thiosulfate	0.005% w/v
Silver Solution	Silver nitrate	0.1% w/v
Developing Solution	Formaldehyde	0.036% v/v
	Sodium carbonate	2% w/v

Stop Solution	EDTA	50 mM

The urea gel was composed by three layers, a 6 M urea gel layer, 10% spacer gel and a 4% stacking gel. The urea gel layer contained 10 mL AB6, 10 mL 3X gel buffer, 10.8 g urea, 10 mL ddH_2O, 100 µL 10% APS and 100 µL TEMED . The 10% spacer gel was made of 2.5 mL AB3, 3.3 mL 3X gel buffer, 0.5 mL glycerol, 3.7 mL ddH_2O, 50 µL 10% APS and 5 µL TEMED. The 4% stacking gel contained 1 mL AB3, 3.3 mL 3X gel buffer, 5.7 mL ddH_2O, 100 µL 10% APS and 10 µL TEMED. The gel was made layer by layer and used 95% ethanol to level each gel before adding each additional layer.

Most samples were in isopropanol or organic solvents. In regards to dealing with loading solvents incompatible with water, solvents were evaporated off by boiling or higher temperatures (>70 °C). Dried samples were resuspended in 10 µL – 15 µL of 4X SDS sample buffer. All samples were warmed at 37 °C before loading into the gel.

The gel was run in 1X cathode buffer and 1X anode buffer. The gel was run at 30 V until running front was seen to enter the urea gel layer, where the voltage was increased to 150 – 200 V.

The gel was run until the running front closely approached the end of the gel upon which it was soaked overnight in fixing solution. This step removed the dye front from the gel and prevented it from staining over the protein bands. The next day, it was washed twice with ddH_2O (20 min each),

washed once with sensitizer solution (30 min), washed once with silver solution (30 min) and wash once quickly with ddH_2O. The staining was started by washing the gel with developer solution until bands were appropriately visualized, and then stop solution was quickly added for at least 30 min. Gels were imaged using a ImageQuant LAS4000 apparatus (GE healthcare, USA)

2.3.11 NMR Spectroscopy of PINK1 Transmembrane

A synthetic peptide was obtained from Biomatik with a sequence of AGPCGRAVFLAFGLGLGLIEE at 95% purity (9 mg). The peptide was dissolved into deuterated DMSO to a concentration of 2 mM in 500 μL. The spectra were acquired with a Varian INOVA 600 MHz spectrometer at 30 °C.

2.4 *Pichia Pastoris* Experimental Protocols

2.4.1 Construction of GFP Fusion Vector and Cloning of PEMTs

A red shifted variant of enhanced GFP containing the mutations F64L and S65T (eGFP) was amplified from pEGFP-N1 (Clontech). To the 3' end of the coding sequence, codons corresponding to an 8 x His's-tag were added and to the 5' end cDNA coding for a Tobacco Etch Virus protease (TEV) cut site and a four amino acid linker sequence were added. The PCR product was then ligated into pPICZ-A (Invitrogen). Genes (cDNA) for human, and mouse PEMT were a kind gift of Dr. Dennis Vance (University of Alberta) and *Saccharomyces cerevisiae* PEMT (OPI3) were obtained from the Protein

Structure Initiative materials repository[90]. The genes were amplified using PCR and cloned into pPICZA-GFP.

2.4.2 Transformation of *Pichia pastoris*

Plasmids containing the PEMT gene were purified using maxi-prep kits (Qiagen), and 20 µg of DNA was linearized overnight at 37 °C with SacI (Fermentas, USA). Electrocompetent *P. pastoris* GS115 were prepared following the protocol outlined in the *Pichia* EasySelect^{Tm} Expression kit (Invitrogen, USA). Linearized plasmid DNA was incubated with 80 µl of electrocompetent GS115 on ice and electroporated using a BioRad Gene Pulser at 2.5 kV, 25 µF, 100 Ω. Cells were plated on YPDS (1% yeast extract, 2% peptone, 2% dextrose, 1 M sorbitol) medium, containing 100 µg/ml zeocin, and incubated at 30 °C until colonies appeared (approximately two days).

2.4.3 PCR Screening for Insert

To confirm genomic integration of the expression cassettes, individual colonies were picked into 10 µl of sterile water. To lyse the cells, 5 µl of 5 U/µl of lyticase (Sigma, USA) was added and the cells were incubated at 30 °C for 10 min, followed by freeze-thaw from -80 °C to RT. A hot start PCR was set up using TopTaq (Qiagen, USA). Briefly, 50 µl PCR reactions contained 5 µl 10X TopTaq buffer, 2.5 µl 10 mM dNTPs, 0.5 µl 25 mM Mg^{2+}, 1 µl of 10 mM forward and reverse primers, 5 µl of cell lysate, and 30 µl of sterile water. PCR samples were mixed thoroughly and placed in Eppendorf Thermocycler

at 95 °C for 5 min before 5 µl of 0.16 U/µl TopTaq polymerase was added. PCR cycled 30 X with a 1 min 95 °C denaturation, 1 min 54 °C annealing stage and 1 min 72 °C elongation. Samples were run on 1% agarose gels with 1% ethidium bromide.

2.4.4 Induction Plating and Imaging of *Pichia Pastoris* colonies

Following the appearance of colonies on YPDS-zeocin plates, a total of 50 colonies from each transformation were picked onto BMMY plates (1% yeast extract, 2% peptone 100 mM potassium phosphate buffer pH 6.0, 1.34% YNB (yeast nitrogen base), 40 µM biotin, 0.5% methanol) using a grid. As a negative control, two colonies of untransformed GS115 were also picked. Plates were incubated at 30 °C for 24 h and imaged, using an ImageQuant LAS4000 imager equipped with blue light (GE healthcare, USA). All exposures were taken at $1/8^{th}$ of a second. In order to quantify the intensity of the colonies, the mean gray value was determined, using ImageJ software

2.4.5 Culture Fluorescence, Small Scale Lysis and Protein Expression

Colonies were inoculated into 5 ml of BMGY (1% yeast extract, 2% peptone 100 mM potassium phosphate buffer pH 6.0, 1.34% YNB, 40 µM biotin , 1% glycerol) and grown overnight at 30 °C at 300 rpm. Cultures were sub-inoculated into 25 ml of BMGY with a starting A_{600} of 0.02 and grown for 24 h at 30 °C at 300 rpm. When the cells had reached at A_{600} of approximately 7, they were centrifuged (1500 *g*, 5 min) and induced by re-suspension of the

cell pellet in 25 ml of BMMY medium and incubated for 24 h at 24 °C at 300 rpm. In order to measure cell fluorescence, 5 ml of the cells were centrifuged (1500 *g*, 5 min) and re-suspended in 200 ml of PBS in a 96 well plate (Costar, USA). Fluorescence was measured, using a FluoroSTAR fluorescent plate reader at an excitation wavelength of 488 nm and emission wavelength of 509 nm with a gain of 800.

To correlate fluorescent measurements with protein expression, the remaining 20 ml of culture was harvested by centrifugation (1500 *g*, 5 min) and re-suspended in 50 mM KPO_4 Buffer, 0.3 M NaCl, 10% glycerol, pH 8.0 so that the final A_{600} was 150. 100 µl aliquots were taken from the re-suspended cells and lyticase was added to a final concentration of 2 U/µl and incubated for 30 min at 30 °C. The cells were then flash frozen in liquid nitrogen for 2 min, followed by heat shocking at 30 °C. The freeze thaw was repeated twice more, and insoluble material and unbroken cells were removed by centrifugation. The lysate was run on a 14% SDS PAGE gel and imaged using blue light on an ImageQuant LAS4000 apparatus (GE healthcare, USA).

2.4.6 Expression and Purification of mPEMT

A clone of mPEMT that appeared brightest under blue light was grown overnight (30 °C, 300 rpm) in 100 ml of BMGY medium to an A_{600} of 7. A total of 6L of culture was sub-inoculated into BMGY and grown for 24 h (30 °C, 300 rpm) to an A_{600} of 10. The cells were harvested by centrifugation (1500 *g*, 10 min) and re-suspended in an equal volume of BMMY induction

medium. The cultures were grown for 48 h (25 °C, 300 rpm), adding fresh methanol at 24 h (0.5%). The cells were harvested by centrifugation (1500 *g*, 10 min) and re-suspended in 300 ml of 50 mM Tris pH 8.0, 0.15 M NaCl, 5% glycerol and lysed by passage through a Constant Systems cell disruptor at 40,000 PSI. Cell debris was pelleted by centrifugation (3000 *g*, 10 min) and membranes were isolated by ultracentrifugation (100,000 *g*, 2 h). Membranes were homogenized in 50 mM Tris pH 8.0, 0.15 M NaCl, 5% glycerol, and solubilized in 1% Fos-choline-12. Insoluble material was pelleted (100,000 *g*, 30 min) and the supernatant batch bound to Ni-NTA agarose (Qiagen) for 2 h at 4 °C and washed and eluted using a step imidazole gradient of 30 mM to 1 M in 0.1% Fos-choline-12. The purified fusion protein was digested using TEV protease with a 1:1 w/w ratio. mPEMT was purified from GFP and TEV, using M2 FLAG tag resin (Sigma) according to the manufacturer's instructions. The final purified protein was injected onto a Superdex 200 16/60 column equilibrated in 20 mM Tris pH 8.0, 0.15 M NaCl, 5% glycerol, 0.15% FC-12 to assess the oligomeric state (Figure 8).

2.5 PARL Purification and Expression

2.5.1 Cloning of PARL-GFP into pPICZA – GFP vector

PARL was cloned into the pPICZA GFP fusion vector. Using the primers forward 5' TCG AAA CGA GGA ATT CAC CAT GGC GTG GCG AGG CTG G and reverse 5' ACA GGT TTT CCT CGA GCT TAG AGC CAC CTC CTT TTT TGG G PARL was amplified through standard PCR reaction (See protocol 2.). A 1% agarose gel was used to purify the PCR amplification, followed by gel

extraction by kit (Qiagen). The PARL PCR product was blunt ligated into pJET1.2 (Fermentas CloneJET PCR cloning kit) by following kit directions and was transformed into Top10 competent cells.

A PCR screen was used to assess successful ligation into the pJET1.2 vector. Successful clones were grown in 3 mL of LB medium and plasmid purified with a plasmid purification kit (Qiagen). Both the pPICZa GFP fusion vector and the PARL-pJET1.2 blunt vector were digested with Xho1 and Pml1 for 1 h at 37 °C. A 1% agarose gel was run and the digested fragments were purified from the gel with a gel extraction kit (Qiagen). A ligation with T4 DNA ligase (Invitrogen, USA) was set up, following the kit protocol. The ligation was transformed into Top10 competent cells and colonies with successful insert were screened for insert by PCR screening and verified with sequencing by TAGC (University of Alberta).

2.5.2 Expression and Purification of PARL-GFP

A brightly fluorescing PARL-GFP colony (colony 14) was selected for overexpression in large scale (6 L) cultures. PARL-GFP was grown overnight (28 °C, 300 rpm) in 100 mL of BMGY medium to an A_{600} of 7. A total of 6 L of culture was sub-inoculated into BMGY and grown for 24 h (28 °C, 250 rpm) to an A_{600} of 10. The cells were harvested by centrifugation (1500 *g*, 10 min) and re-suspended in an equal volume of BMMY induction medium. The cultures were grown for 72 h (25 °C, 250 rpm), adding fresh methanol at 24 h (0.5%) and ampicillin (100 ng/mL). The cells were harvested by

centrifugation (1500 *g*, 10 min) to a final weight of 145.45 g. Cells were resuspended in 400 mL of 50 mM KPO_4 (pH 8), 0.1 M NaCl, 5% glycerol and 10 mM βME, with 5 protease inhibitor tablets (Roche, EDTA-free) and 10 ng/mL DNase. Cells were pre-homogenized with a hand mixer and then lysed in the Constant cell disruptor with a single pass at 40 kPSI. Cell lysates had PSMF added to a final concentration of 1 mM after lysis and were centrifuged in a Beckman centrifuge (rotor JLA 8.1) 3000 *g* for 5 min (4 °C) to remove cell wall debris. The supernatant was transferred into tubes for ultracentrifugation (Beckman, rotor TI-45) and centrifuged at 100,000 *g* for 2 h (4 °C). The supernatant was discarded and the membrane fraction was isolated. The membrane fraction (25.5 g) was homogenized in 250 mL of a high salt buffer, 50 mM KPO_4 (pH 8), 0.8 M NaCl, 5% glycerol, 10 mM βME and 1 mM PMSF. Membranes were isolated by ultracentrifugation again (38,000 rpm, 30 min, 4 °C).

Purified membranes (20.7 g) were homogenized in 200 mL of 50 mM KPO_4, 0.1 M NaCl, 5% glycerol, 10 mM βME, 1 mM PMSF, pH 8.0 and two protease inhibitor tablets. The fusion protein was solubilized on ice in 0.2% Fos-choline 12 for 30 min at 4 °C. Insoluble protein was removed by ultracentrifugation (Beckman, rotor TI-45) at 100,000 *g*, 4 °C, for 30 min. The supernatant was transferred into pre-chilled 50 mL falcon tubes with Ni-NTA agarose (Qiagen) (6 tubes, 1 mL of 50% Ni-NTA resin (Qiagen) with ethanol removed). PARL-GFP was bound to the resin for 2 h with rotation at 4 °C. Protein was washed and eluted, using a step imidazole gradient from 30 mM

to 1 M in 0.2% Fos-choline-12 (Anatrace). Samples were collected from washes and elutions and assessed on SDS-PAGE acrylamide gels. The flow through collected was subjected to a repeat batch Ni-NTA binding with fresh resin for 2 h more and was washed and eluted as described above.

2.5.3 Detergent Optimization of PARL-GFP

Using 3 g of crude membranes containing PARL-GFP, homogenized with a glass homogenizer in 30 mL of resuspension buffer (50 mM KPO_4, 10% glycerol, 0.3 M NaCl, 10 mM βME, 1 protease inhibitor tablet). Separated homogenized membranes into 7 x 2.7 mL aliquots and added 0.3 mL of the following detergents to each: 20% neopentyl glycol, 10% n-decyl-β-D-maltopyranoside, 10% n-dodecyl-β-D-maltopyranoside, 10% dodecyl octaethylene glycol ether, 10% lauryldimethylamine-N-oxide, 10% Triton X-100, 10% Foscholine-12. A blank sample with water added was also included. Each aliquot of homogenized membrane with its detergent was incubated on a rotator at 4 °C for 30 min. Aliquots (0.5 mL) were then set aside which would be used to measure relative fluorescence and for a running an SDS-PAGE gel. The remaining 2.5 mL samples were centrifuged in a Beckman Optima micro-ultracentrifuge (fixed angle rotor TLA-110) at 50,000 *g* for 30 min. Aliquots of the solubilized protein were removed for relative fluorescence measurement and for SDS-PAGE gel. Aliquots (200 µL) were used of homogenized and detergent solubilized membranes for relative fluorescence comparison. Fluorescence was measured using a FluoroSTAR

fluorescent plate reader, at an excitation wavelength of 488 nm and emission wavelength of 509 nm with a gain of 1600. Each sample (7.5 µL) was mixed with SDS loading dye and electrophoresed on 14% acrylamide SDS-PAGE gels.

2.5.4 Fluorescence Size Exclusion Chromatography of PARL-GFP.

Solubilized PARL-GFP (1 mL) in 0.1% foscholine-12 from crude membranes was centrifuged in DURApore membrane filters (Millipore) with a benchtop centrifuge at 4 °C until completely filtered. Analytical gel filtration was done on a SEC 200 10 x 300 column (GE Healthcare, USA). The column was equilibrated with 2 column volumes of 50 mM KPO_4, 5% glycerol, 0.1 M NaCl, 10 mM βME, 0.1% foscholine-12. Fusion protein (100 µL) was loaded and the column was run with the equilibration buffer. Samples were run at 0.5 ml/min and the absorbance values of the fractions were determined at 280 nm. Fractions were collected in 18 mm x 100 mm tubes. Aliquots of each collected fraction (200 µL) was measure in a 96 well plate for relative fluorescence. Fluorescence was measured using a FluoroSTAR fluorescent plate reader, at an excitation wavelength of 488 nm and emission wavelength of 509 nm with a gain of 1595.

Chapter 3

Structural studies of PINK1 transmembrane domain with NMR spectroscopy

Contributions:

I would like to acknowledge the help and contributions of Dr. Brian Sykes and Brian Lee from the Sykes group at University of Alberta. All NMR experiments were performed by Brian Lee, and strategizing and data analysis carried out by Brian Lee and Brian Sykes.

3.1 Introduction:

The mitochondrial PTEN-induced kinase (PINK1) is a dynamic protein which acts as a molecular checkpoint in mitochondrial health[55]. The interest to uncover its molecular mechanisms and interactions has been peaked due to the protein's role in early-onset Parkinson's disease[4,17,60,63,91]. The introduction chapter to this thesis provided a comprehensive assessment of the protein as a whole, and this chapter's introduction will aim to provide a more thorough discussion specifically of the PINK1 transmembrane domain.

As mentioned in the introduction, PINK1 is composed of three domains; an N-terminal domain, containing the mitochondrial targeting sequence, putative transmembrane domain and PTEN kinase domain[4,42,48] (Figure 1.4). The boundaries of transmembrane domain are weakly predicted, probably due to its dynamic nature in mitochondria. However, several transmembrane prediction programs predict a boundary consensus of the domain. Domain boundaries marked by residues 91-111 were determined by TMPRED and TopPred, and boundaries with 89-111 were determined by TMHMM and SACS MEMSAT. The sequence was predicted to be (89)AWGCAGPCGRAVFLAFGLGLGLI(111).

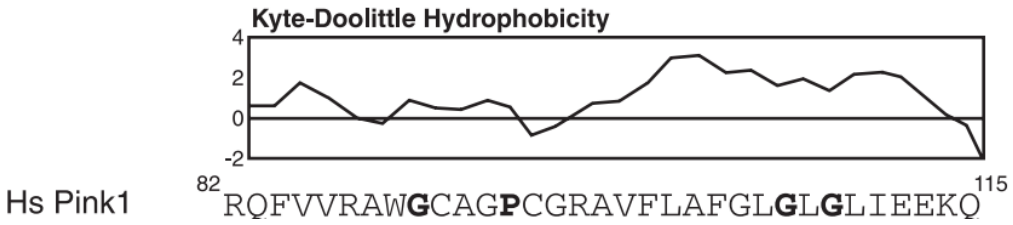

Figure 3.1: Kyte-Doolittle hydrophobicity plot of PINK1 transmembrane domain. Human PINK1 transmembrane domain was assessed its hydrophobicity using the Kyte and Doolittle scale, where regions above zero are considered more hydrophobic in nature[48]. Adapted from Meissner, C., Lorenz, H., Weihofen, A., Selkoe, D. J., and Lemberg, M. K. (2011) The mitochondrial intramembrane protease PARL cleaves human Pink1 to regulate Pink1 trafficking. *Journal of Neurochemistry 117*, 856–867.

Among many PINK1 mutations located throughout the protein leading to PARK6 and the onset of Parkinsonism (Table 1.1), only four known mutations are located in the transmembrane domain: C92F, P95A, R98W and I111S. All have been reported in relation to Parkinson's disease (Figure 3.2 and 5.2). C92F (along with R464H in the kinase domain) was found when a genetic analysis of a 60 year old woman with PD was performed. She presented with a resting tremor of the right upper limb, which began at age 37 years[92]. A Parkinson's mutation database, PDmutDB, considers this mutation pathogenic for PD.

A recent publication characterizing the interactions with PINK1 and PARL *in vivo* also analyzed the effect of the mutation on PINK1 behavior. The C92F mutation resulted in accumulation of full length PINK1, but no information was available regarding the localization of the C92F mutant PINK1[59].

The next reported mutations R98W and I111S were found in 2008 by a retrospective genetic analysis of over 1126 sporadic and familial cases of PD. Among assessed patients with confirmed clinical PD, R98W and I111S were identified as statistically significant mutations, ranked probably damaging and possibly damaging respectively[92] (Figure 3.2). The PDmutDB has marked these mutations as having an unclear pathogenic nature. A thorough review suggests that these residues may be essential for structural integrity of the TM domain or that they may destabilize the TM due to

changes in hydrophobicity[42]. These mutations may result in misfolding or improper localization of the protein[42]. Their characterization *in vivo* demonstrated that both R98W and I111S abolished cleavage of PINK1 by PARL, resulting in full length PINK1 accumulation[48].

The final mutation worth discussing is the P95A (Figure 3.2). This mutation has a profound effect on the protein's ability to interact with PARL. The mutation allows proper localization of PINK1 to the inner mitochondrial membrane, but abolished cleavage by PARL[59]. It also results in the same accumulation of full length PINK1 as seen in mutations C92F, R98W and I111S. The P95A mutation has not been found in a genetic screen of a patient with PD, and remains a potential PD promoting mutation. It is still worth investigating, since it has detrimental effects on the proper functioning of PINK1 and parallels the same behavior as known PD mutations.

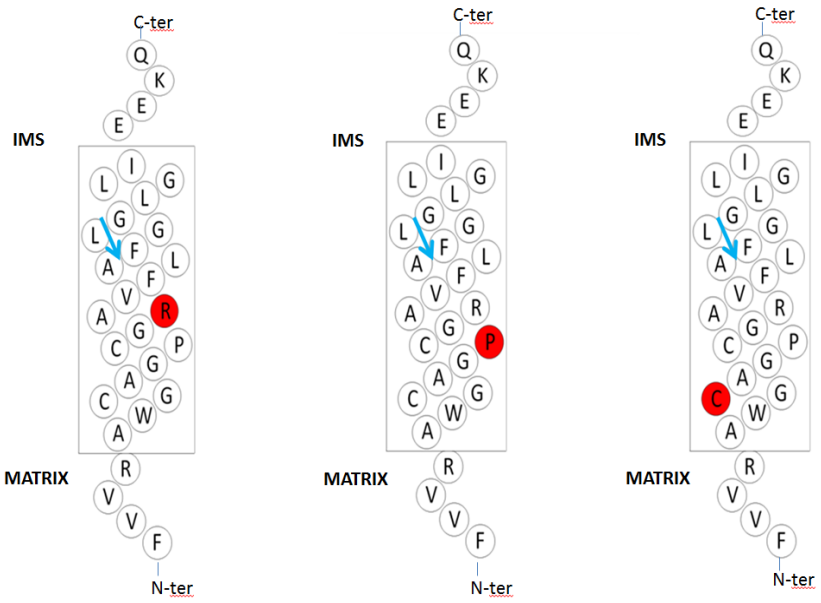

Figure 3.2: Mutations in the transmembrane domain of PINK1. The mutations in the PINK1 transmembrane domain; R98W, P95A, and C92F, respectively. Mutations are marked in red circles. Blue arrow designates PARL cleavage site. The transmembrane domain is shown with boundaries A89 - I111.

3.1.1 Objective

PINK1 has a highly conserved transmembrane domain, which is prone to Parkinson's disease causal mutations. Weakly characterized PD mutations within transmembrane domain of PINK1 and the recent insights of cleavage of this domain by PARL attracted our interest. It is tempting to speculate that PINK1 TMD mutations could affect three aspects of its behavior. Firstly, mutations may alter the structure of PINK1, possibly impairing cleavage of PINK1 by PARL. Secondly, mutations may prevent its ability to localize correctly due to aggregation or its inability to interact with import proteins properly. And finally, if the mutations do not affect the secondary structure of the transmembrane domain, they still may prevent PARL from correctly interacting or recognizing the PINK1 substrate, thus preventing PINK1 cleavage resulting in accumulation.

Since there is no structural information about PINK1 transmembrane domain, our goal was to solve the structure of this domain and assess whether the PINK1 transmembrane domain undergoes secondary structure changes in the presence of PD mutations, which prevent interaction with PARL. Our strategy was to express and purify the TM domain of PINK1 and analyze its structure using solution nuclear magnetic resonance (NMR). A structure of the transmembrane domain of PINK1 may also be insightful into the shape and behavior of substrates of rhomboid intramembrane proteases such as PARL.

3.2 Results

3.2.1 PINK1 Transmembrane Domain Expression

The PINK1 transmembrane domain was cloned into a pMAL vector, containing an N-terminal maltose binding protein (MBP), followed by a tobacco etch virus (TEV) cleavage site and C-terminal PINK1 transmembrane domain. The TM domain of PINK1 consisted of residues 89 to 111. The construct was expressed in *E. coli*. The strain of *E. coli* which yielded the most soluble protein with the least amount in the inclusion body was DH5α, when compared to BL21-DE3, Top10 and C43 cells. Expression of the MBP-PINK1 construct was also optimized for expression in both LB and M9 minimal medium. This was done in preparation for N^{15} and C^{13} labeling which may be necessary for NMR spectroscopy. Expression in LB medium was highest when cells at A_{600} of 0.6 were induced with 0.5 mM IPTG, and grown at 22 °C for 72 h. However, it was determined that protein yield was higher in M9 minimal medium. Expression in minimal medium was optimal when cells were induced with 0.5 mM IPTG at A_{600} of 0.4 - 0.5, and induction was carried out at 37 °C for 40 h. Yield of MBP-PINK1 grown in 6L of LB was 75 – 100 mg, while 150-200 mg was obtained from minimal medium.

3.2.2 Purification and Isolation of the PINK1 Transmembrane Domain

MBP-PINK1 was isolated from *E. coli* cells through high pressure lysis and insoluble cell components were pelleted by centrifugation. The isolated supernatant containing the soluble MBP-PINK1 protein was applied to amylose affinity columns. The unbound and weakly bound proteins were

washed out and the protein of interest was eluted with 40 mM maltose. The purity was checked on Coomassie stained SDS-PAGE gels (Figure 3.3). Purified MBP-PINK1 was immediately digested with TEV protease, for 3-8 days for optimal digestion depending on the amount of fusion protein. Conveniently, the hydrophobic PINK1 TM domain precipitated upon cleavage by TEV, which provided a means to gauge the degree of digestion. Also, a simple centrifugation step enabled isolation of mostly the precipitated TM segment away from the soluble MBP and TEV and undigested MBP-PINK1.

The precipitate was collected for an organic extraction, a step which would act to eliminate any TEV or MBP from the precipitated transmembrane fragment. Trichloroacetic acid (TCA) was added to solution to precipitate all the protein. The mixture then was centrifuged and washed with water to remove all TCA. An organic mixture of 50% isopropanol and 50% chloroform was added to the pellet, which was homogenized in the organic solvents. Water was added to the resuspension, which acted to segregate soluble proteins - TEV and MBP - which would separate into the aqueous phase, while the hydrophobic peptide would partition into the organic phase. This process was repeated two or three times to ensure adequate separation. Urea gels were used to monitor the purity of the organic phase (Figure 3.4).

The purified peptide was either kept in organic solvent or dried down, and the pellet was resuspended in deuterated DMSO. The solution NMR

spectroscopy was performed by collaborators (Brian Lee) for both conditions but neither of them yielded satisfactory spectra, and it was suggested that the sample was not pure enough for NMR. To further purify the protein, reverse phase high performance liquid chromatography was added to the purification protocol. The peptide sample was dried down, resuspended in a phosphate buffer, containing 7 M guanidine-HCl, loaded on SB-300 C8 silica based column and eluted with isopropanol gradient. The disadvantage of this step was a yield insufficient for NMR. With purifying a very hydrophobic and sticky peptide, major losses occurred after reverse phase HPLC. Unfortunately, due to problems drying and resuspending the peptide in guanidine, as well as losses in HPLC columns, we were unable to purify sufficient amounts for NMR spectroscopy.

3.2.3 Synthetic PINK1 Peptide for NMR Spectroscopy

As an alternative strategy, a synthetic peptide was ordered from Biomatik. The peptide had slightly different boundaries for strategic reasons. Instead of ordering the expressed peptide with (89)AWGCAGPCGRAVFLAFGLGLGLI(111), the synthetic peptide was marked by (93)AGPCGRAVFLAFGLGLGLIEE(113) boundaries. This was to remove one of the N-terminal cysteines, which may have helped stabilize the peptide by preventing disulfide bridge formation. Peptide in a quantity of 9 mg was ordered at 95% purity. The purity was verified by mass spectroscopy at the Institution of Biomolecular Design (IBD) at the University of Alberta (Figure 3.5).

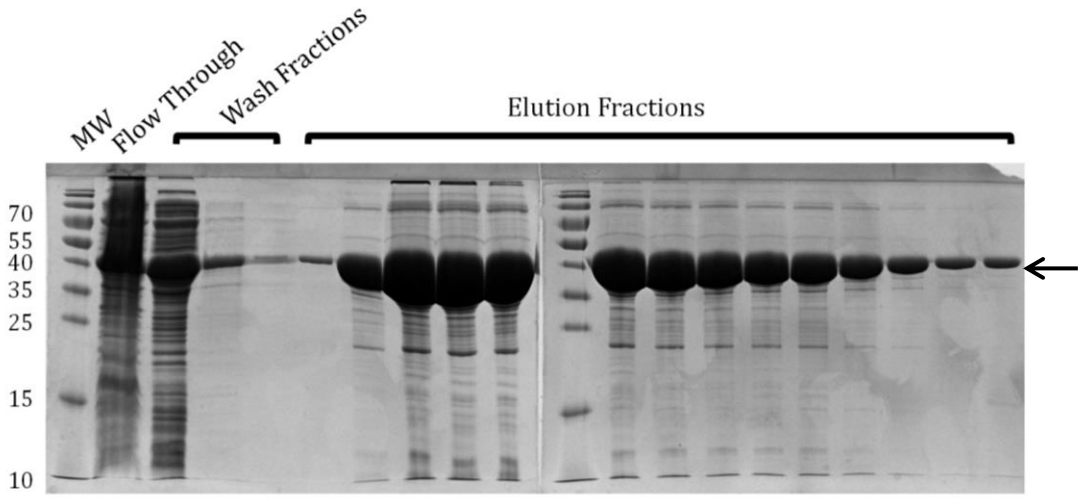

Figure 3.3: SDS_PAGE of MBP-PINK1 transmembrane segment fusion purification. 14% SDS-PAGE of MBP-PINK1-fractions after amylose-column purification. 3.75 µL of eluted fractions were loaded with Coomassie loading dye. Arrow represents MBP-PINK1 fusion protein.

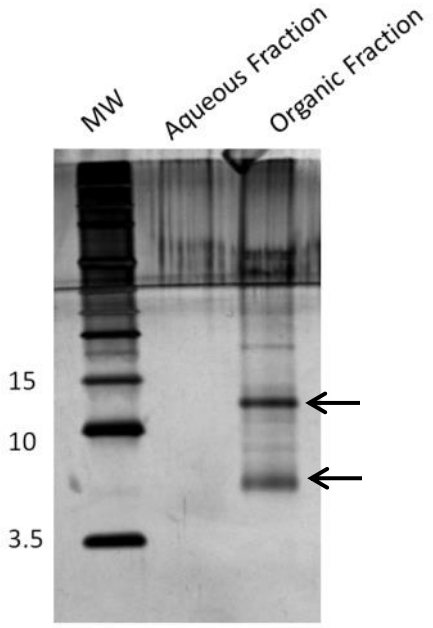

Figure 3.4: 6% Urea gel of PINK1 transmembrane domain purification by organic extraction. 6% urea gels were run composed of a 4% stacking and 10% spacer, with the 6% urea phase for separation. 1 µL of Novex (Life Technologies) MW ladder was used containing low MW bands. 100 µL of the aqueous fraction and organic fraction were evaporated and resuspended in 10 µL of SDS Coomassie buffer. Gels were run at 30 V through the stacking and spacer gel phases, and 150 V for the separating urea gel. Arrows represents the oligomers of the PINK1 transmembrane in the gel.

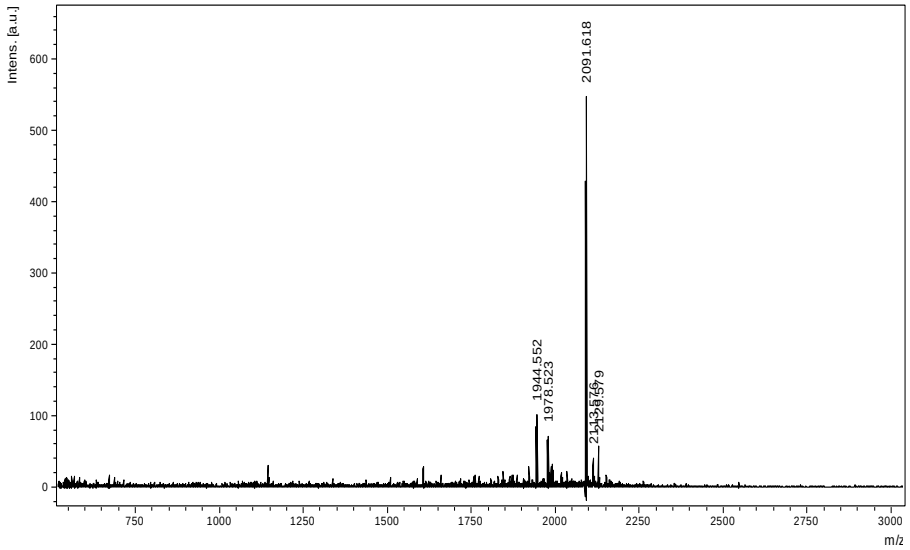

m/z	Intensity	Area
1944.552	101.92	31
1978.523	71.46	21
2091.618	548.00	186
2113.576	40.90	14
2129.579	57.84	19

Figure 3.5: Maldi-TOF mass spectrometry of PINK1 synthetic peptide. Routine Maldi-TOF(matrix assisted laser desorption/ionization – time of flight) mass spectroscopy was used to verify the quality of the synthetic peptide. The correct molecular weight was 2092 Da , which was observed to be the middle peak at m/z of 2091.618. The two peaks below were assumed to be small contaminants, and the two peaks above were determined to be ion adducts of the peptide. Experiments were performed by the Institute for Biomolecular Design at the University of Alberta.

3.2.4 Solution NMR Spectroscopy of PINK1 Transmembrane Domain

Synthetic peptide was easily dissolved into deuterated DMSO to a final concentration of 2 mM. With our collaborator's help, we were able to obtain 1D proton spectra with well separated peaks (Figures 3.6, 3.7, 3.8). This warranted three 2D NMR spectroscopy experiments: a correlation spectroscopy (COSY), total correlation spectroscopy (TOCSY) and nuclear overhauser effect spectroscopy (NOESY) (Figure 3.9). These spectra were all utilized to understand different information about the peptide. COSY identifies basic connectivity and determines which protons are spin coupled. TOCSY correlates all protons in a spin system. NOESY investigates the conformation and proximity of adjacent spin systems. The three spectra were used to associate observed peaks with amino acids connected down the peptide backbone (Figures 3.9 and 3.10). This determination allowed a chemical shift index to be generated for each amino acid[93,94] (Figure 3.11). Analysis of the chemical shift index demonstrated that the peptide had no significant secondary structure, and was classified as a random coil[95]. This was presumed due to the fact that the chemical shift index does not deviate lower than -0.1 (lower than -0.1 represents significance alpha helical structure) or higher than +0.1 (greater than +0.1 represents significant beta-sheet nature) (Figure 3.11).

Experiments with the synthetic PINK1 peptide were attempted to be repeated in detergent DPC/fos-choline12 and SDS. Neither led to clear 1D spectra, and were not carried further for 2D NMR proton-proton analysis.

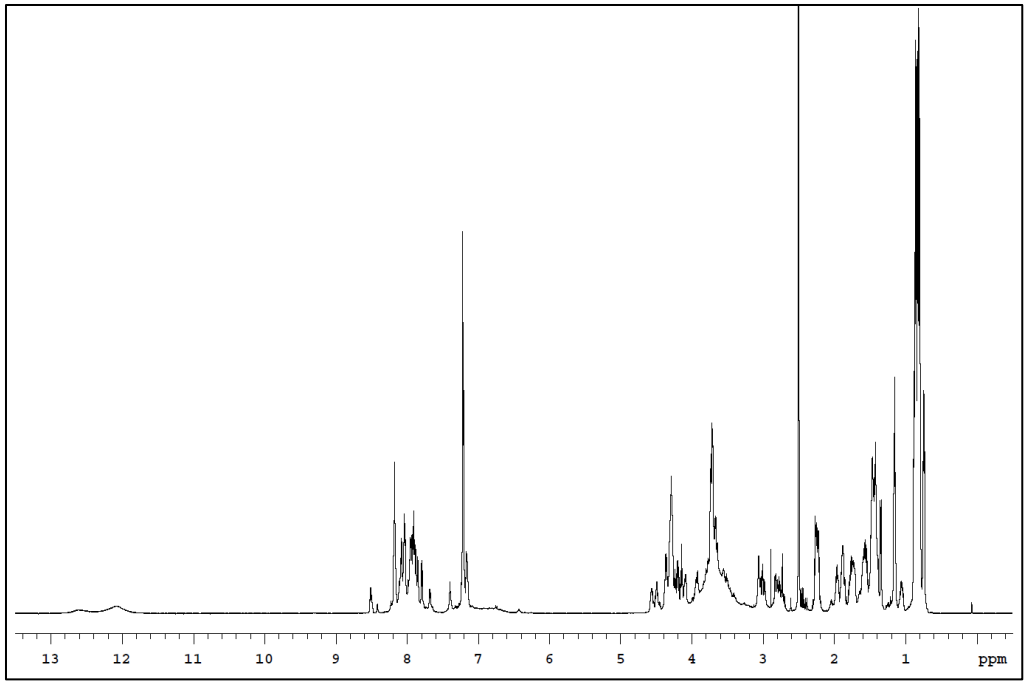

Figure 3.6: 1D H^+-H^+ spectrum of PINK1 transmembrane segment. Synthetic peptide (2 mM) of PINK1 transmembrane segment dissolved in deuterated DMSO and was acquired at 600 MHz at 30 °C. Sequence corresponds to peptide sequence of human PINK1, AGPCGRAVFLAFGLGLGLIEE. Peptide was obtained from Biomatik at 95% purity.

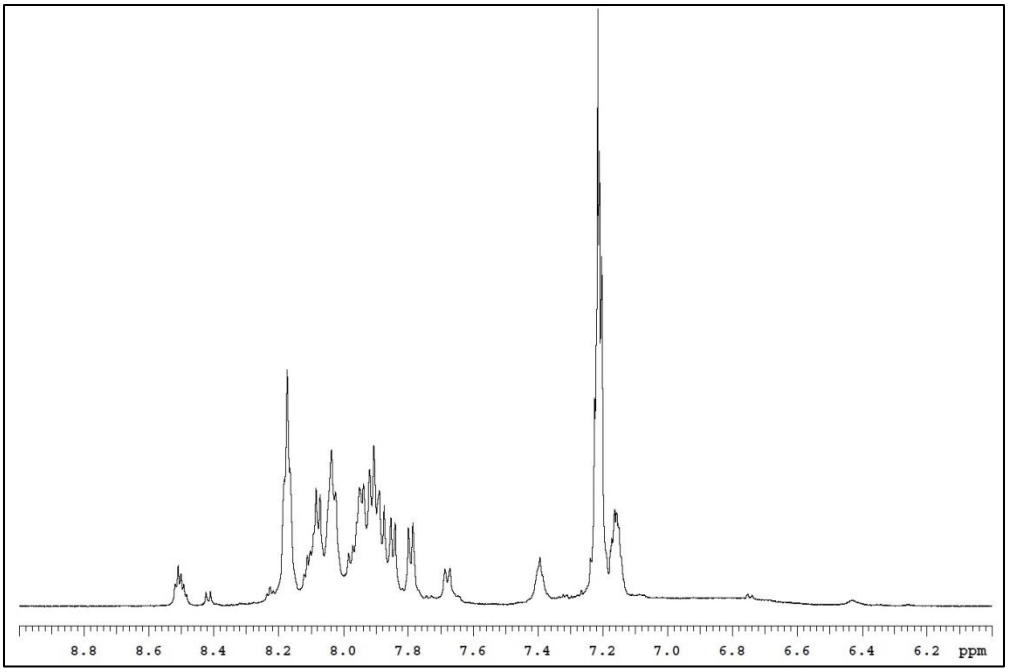

Figure 3.7: Amide/Aromatic region of a 1D H^+-H^+ spectrum of PINK1 transmembrane segment. Synthetic peptide (2 mM) of PINK1 transmembrane segment dissolved in deuterated DMSO and was acquired at 600 MHz at 30 °C. Sequence corresponds to peptide sequence of human PINK1, AGPCGRAVFLAFGLGLGLIEE. Peptide was obtained from Biomatik at 95% purity.

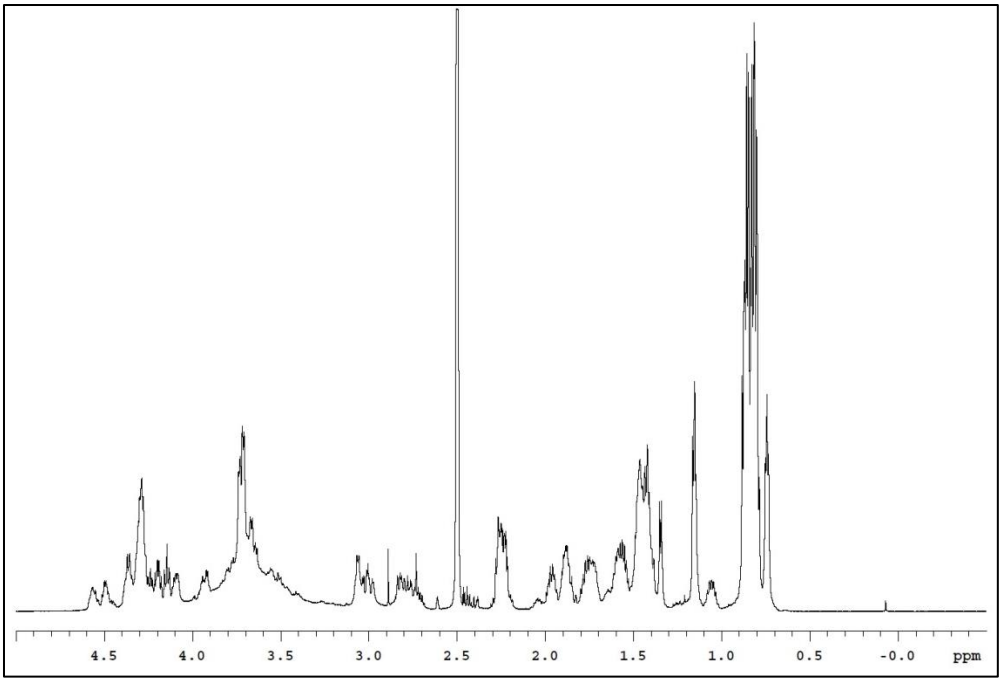

Figure 3.8: Aliphatic region of a 1D ^{1}H spectrum of PINK1 transmembrane segment. Synthetic peptide (2 mM) of PINK1 transmembrane segment dissolved in deuterated DMSO and was acquired at 600 MHz at 30 °C. Sequence corresponds to peptide sequence of human PINK1, AGPCGRAVFLAFGLGLGLIEE. Peptide was obtained from Biomatik at 95% purity.

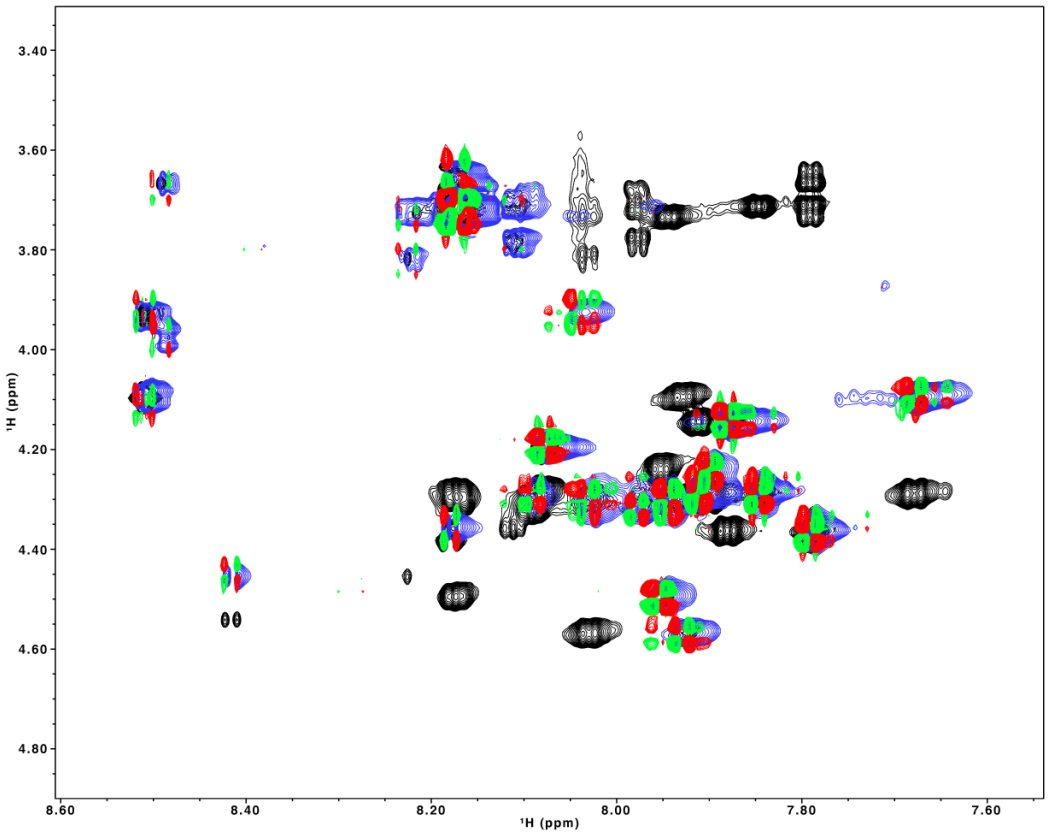

Figure 3.9: Overlay of 2D H^+-H^+ spectras COSY-TOCSY-NOESY of PINK1 transmembrane segment. Synthetic peptide (2 mM) of PINK1 transmembrane segment dissolved in deuterated DMSO and was acquired at 600 MHz at 30 °C. Black peaks are associated with the NOESY spectra, blue peaks represent the TOCSY spectra and the red/green peaks represent the COSY spectra. Sequence corresponds to peptide sequence of human PINK, AGPCGRAVFLAFGLGLGLIEE. Peptide was obtained from Biomatik at 95% purity.

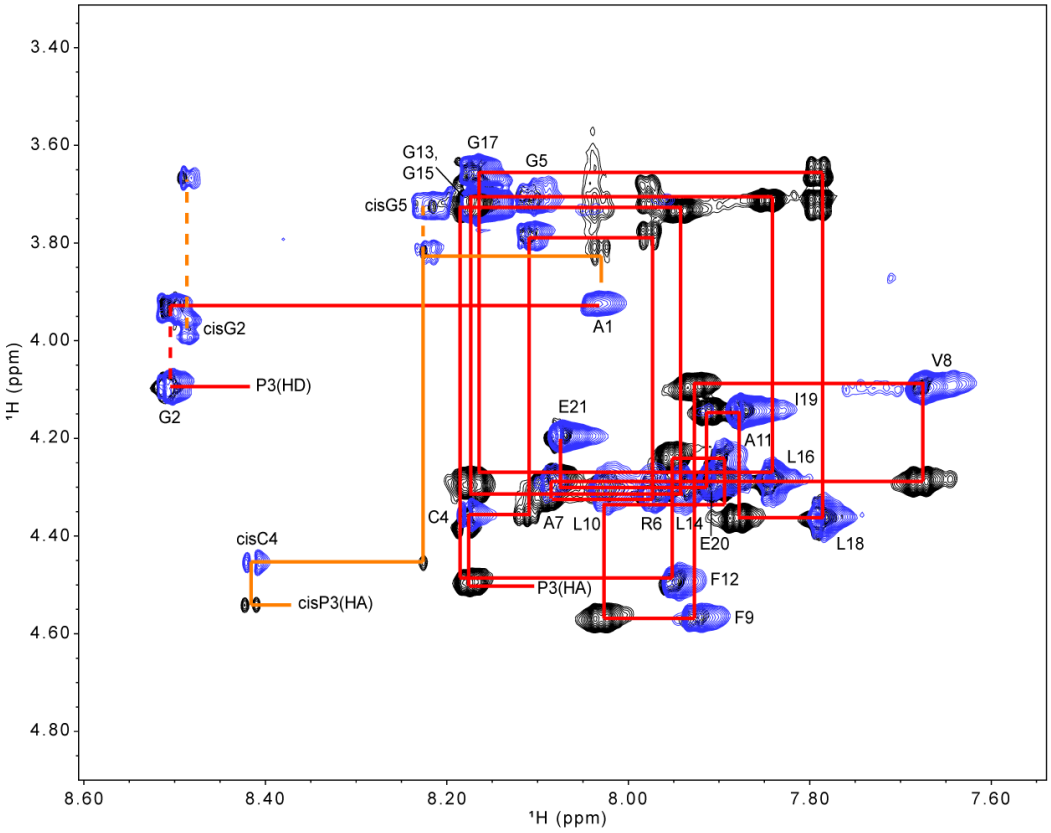

Figure 3.10: Amino acid assignment of PINK1 tranmembrane using overlay of 2D H⁺-H⁺ spectras TOCSY-NOESY. Synthetic peptide (2 mM) of PINK1 transmembrane segment dissolved in deuterated DMSO and was acquired at 600 MHz at 30 °C. Black peaks are associated with the NOESY spectra, blue peaks represent the TOCSY spectra. Red lines connect consecutive amino acids peaks. Yellow lines represent peaks associated with the cis-conformation of the proline 95. Sequence corresponds to peptide sequence of human PINK1, AGPCGRAVFLAFGLGLGLIEE. Peptide was obtained from Biomatik at 95% purity.

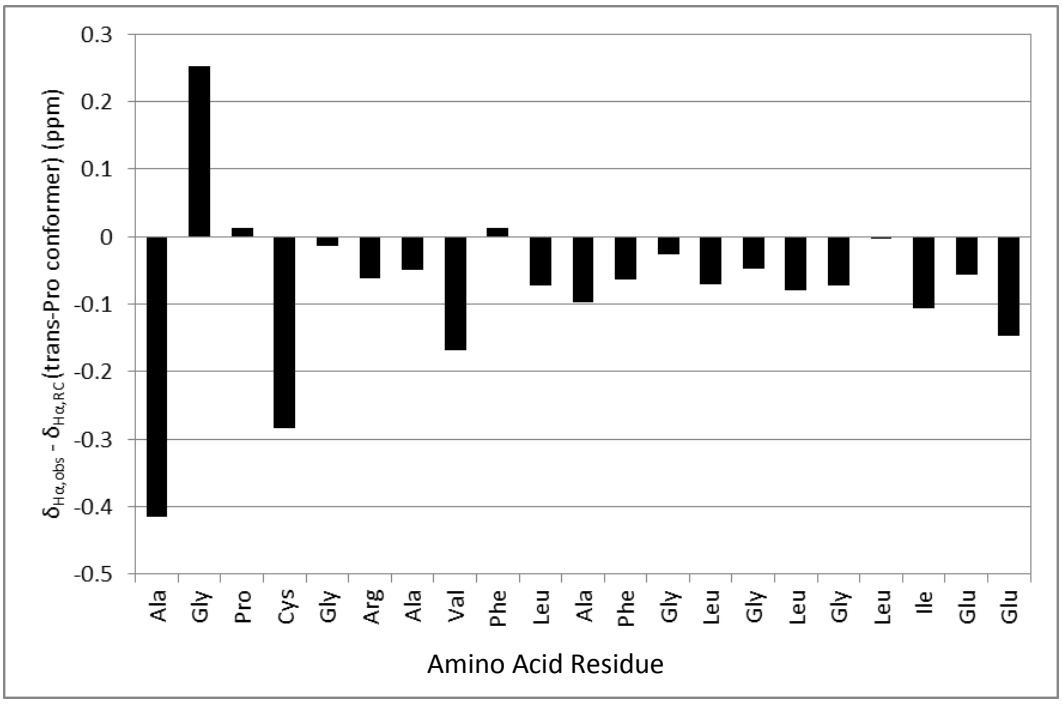

Figure 3.11: Chemical shift index (CSI) of the PINK1 transmembrane domain. Chemical shift of PINK1 transmembrane domain were compared to the chemical shifts of amino acids in a random coil conformation. Secondary chemical shifts lower than -0.1 are considered α-helical in nature and shifts greater than +0.1 are considered to be of β-sheet nature.

3.3 Discussion

A complete protocol for the expression and purification of the PINK1 transmembrane domain has been developed. This was carried out by tagging a hydrophobic peptide to the large soluble maltose binding protein (MBP). Purification of the peptide to high purity was accomplished through the specificity of the MBP to an amylose affinity column. The final purification steps of TEV digestion and organic extraction utilize the hydrophobic nature of the peptide: its ability to precipitate once released from the large soluble moiety and its separation into an organic phase.

The peptide became very unstable once solubilized in solutions compatible for NMR or further HPLC purification buffers. In part, this may be due to the nature of the peptide and its sequence. After working through this protocol many times, the major limitation was successfully solubilizing the peptide into new buffers. Including NMR compatible detergents, such as DPC/fos-choline12, in the peptide sample when drying with liquid nitrogen may help resuspending the peptide pellet[96,97]. The drying-resuspension cycle in the presence of detergent should be repeated multiple times, so that in the final aqueous solution the peptide is completely surrounded with detergent micelles.

As explained in the results, use of a synthetic peptide had a double edged intent. It offered an alternative source of pure peptide, but more importantly, it was designed with a different delineation of the predicted

membrane boundaries. The synthetic peptide was soluble in DMSO and yielded interpretable NMR spectra. Secondary structure determination for the peptide was unsuccessful due to the fact that it was a random coil in DMSO solution.

Although this was not the initial anticipated result, it does fit with several pieces of information known in the field of rhomboid protease substrates. There is little concrete evidence in the literature about how substrates interact with the proteases, and what defines the specificity in terms of sequence and secondary structure. One hypothesis in the literature suggests that the membrane environment defines the helical structure of the transmembrane domain. Recent preliminary data suggest that rhomboid substrates are meta-stable transmembrane helices, which require a membrane to have structure[98]. Furthermore, the substrate's transmembrane domain loses its helical propensity when it transitions from the lipid environment to the active site of the rhomboid, which contains water. This cleavage-site-specific unraveling is necessary for hydrolysis of the peptide backbone, especially if it was α-helical in the membrane. This complicates structural analysis, as in theory it is unfavorable to unravel a helix within the membrane. The requirement for unraveling suggests that residues surrounding the cleavage site have a duality in their helical propensity, which is dependent on the environment[98,99].

The only other rhomboid substrate with known structural information is TatA (Twin arginine transport protein A), a native substrate of rhomboid AarA from *Providencia stuartii*. The solution NMR structure of TatA in *Bacillus subtilis* was determined in the detergent DPC. NMR analysis of this 70 amino acid single pass transmembrane domain indicated TatA has an L-shaped helix; a helical transmembrane segment connected by a kink to an amiphipathic helix[100]. This is consistent with the hypothesis that rhomboid substrates are helical in a membrane environment.

The PINK1 transmembrane domain results show a random coil, which follows the hypothesis that substrate structure is governed by the membrane. The NMR experiments were carried out in DMSO, a small polar aprotic solvent, which is adequate for stabilizing membrane substrates. DMSO is not a membrane mimetic environment however. It follows along with the hypothesis that, in these conditions which do not resemble a lipid environment, the peptide would be unstructured. The NMR structure of TatA, which was found to be helical, was solved in detergent DPC which is more suggestive of a membrane environment. Unfortunately, attempts to study PINK1 TM domain in DPC and SDS did not yield spectra with well separated peaks.

There is a counter perspective, which reasons that the transmembrane domain of PINK1 is unstructured. Although there is only one structure of a rhomboid protease substrate, comparisons between TatA and

the TM domain of PINK1 may not be valid. TatA is a stable single pass transmembrane with a second peripheral hydrophibic extension, and therefore double the size of the PINK1 TM domain expressed. It is possible that in order to form a helical structure PINK1's TM requires a larger region flanking the transmembrane domain to induce a helix on either side of the cleavage site. There is another obvious difference in the behavior of both proteins: whereas TatA is located in the membrane from its synthesis, PINK1 must be able to localize to two different membranes and also is found on occasion in the cytosol. It could be that the weakly predicted transmembrane domain is just enough to hold the protein in the membrane, and may not be a true or metastable helix.

Although these results are still preliminary, we return to our original hypothesis regarding the behavior of this protein for the future directions. With the preliminary results presented, one of the options left to further analyze the structure of the PINK1 TM domain within the methods presented is to try shifting the membrane boundaries. Lengthening the protein on both sides may add stability and possibly allow for secondary structure formation on the ends of the peptide. A more difficult but comprehensive alternative would be to use micelles or bicelles in NMR analysis. This would be ideal as it would create a true membrane environment to observe the structure of the peptide. Another approach could be to express a longer version without an MBP tag and allow the TM domain to be solubilized from the lipid bilayer. This procedure is used for the TatA substrate in our lab[101].

It may be more insightful to analyze the other components of our hypothesis of how Parkinson's disease mutations in the TM affect PINK1 behavior. If, in fact, the transmembrane domain is unstructured (unpublished data); it may be that mutations in the domain do not alter its secondary structure but affect its behavior in other ways. It could alter its ability to localize, either preventing its interactions with TIM or TOM, or resulting in aggregation of the protein. Alternatively, it may be that the PD mutations prevent cleavage by PARL by altering its recognition, or prohibiting effective cleavage kinetics.

The next phase of experiments to answer these questions will be an *in vitro* cleavage assay. Our laboratory is equipped to study intramembrane protease enzyme kinetics. We developed the kinetic assay based on fluoresce resonance energy transfer (FRET) between CyPet (cyan fluorescent protein) and YPet (yellow fluorescent protein) (also called donor and acceptor) with the rhomboid substrate cloned between them (Unpublished data). Upon cleavage of the substrate by the rhomboid protease two fluorophores are separated, the energy transfer is disrupted and the full quantum yield of the donor is restored. Enzyme activity is linearly related to the increase of fluorescence. FRET assays are very accurate and sensitive, and, most significantly allow measurement of steady-state kinetics of rhomboid proteases. PINK1 transmembrane domain would be cloned into a FRET pair and the activity of PARL against it would be measured. Once the cleavage assay is optimized for the native TM domain, PD-associated mutations could

be introduced and analyzed to see their effect on cleavage sensitivity. Other questions regarding localization could be answered by observing full length PINK1 behavior by high resolution confocal microscopy. If the PD mutations in the transmembrane were introduced to the full length protein, it could be observed to what mitochondrial membrane they localize to. It is only known that the P95A mutation localizes to the IMM. Other mutations are only observed to result in accumulation of full length PINK1, presumably meaning that they are unable to be cleaved by PARL. This would answer whether the accumulation of full length PINK1 is due to localization or interactions with PARL.

The NMR analysis of the PINK1 transmembrane domain has been insightful in determining the manner in which Parkinson disease mutations affect the behavior of this protein. Although complete conclusions cannot be drawn about the secondary structure of this protein's domain, it appears that it may be so dynamic that it is probable that mutations do not influence a predictable structure. The future experiments outlining cleavage and localization hope to be insightful to provide new perspective on PD mutations and protein behavior.

Chapter 4

Rapid Expression Screening of Eukaryotic Membrane Protein in *Pichia Pastoris*

***A version of this chapter was published in:**

Brooks, C. L., Morrison, M. and Joanne Lemieux, M. (2013), Rapid expression screening of eukaryotic membrane proteins in *Pichia pastoris*. Protein Science, 22: 425–433.

†Cory L. Brooks and Melissa Morrison contributed equally to this work.

Contributions:

All cloning, plate screening, liquid culture and cell lysis experiments were carried out by Melissa Morrison. Purification of mPEMT was carried out by Dr. Cory Brooks (University of Alberta). The paper was written by both Dr. Cory Brooks and Melissa Morrison.

4.1 Introduction

Membrane proteins play vital roles in a wide variety of cellular processes, with an estimated 20-30% of prokaryotic and eukaryotic genomes coding for membrane proteins[102]. In addition to the important physiological roles these proteins play in cellular biology, they also make an enormous impact in the area of human health, with disease arising from abnormalities in their function. Membrane proteins have thus become critical targets for pharmaceutical development with an estimated 50% of all current drugs being targeted to membrane proteins[103]. Despite the obvious importance of these proteins for both biology and disease, relatively few X-ray crystals structures have been determined. In particular, there is a clear deficiency in the number of eukaryotic membrane protein structures available. There are many challenges and bottlenecks associated with membrane protein crystallography, and one of the greatest challenges is obtaining sufficient quantities of the protein for structural studies[104].

Recombinant membrane proteins are frequently poorly expressed, for example examination of the expression of over a hundred membrane proteins from *Mycobacterium tuberculosis* revealed that only 25% of the proteins tested were overexpressed, and that only 1/3 of these were properly inserted into the membrane[105]. In order to bypass the high degree of failure associated with membrane protein overexpression, numerous groups have taken the approach of screening a large number of homologues in order to maximize the probability of obtaining sufficient protein for

structural studies[106-109]. One recent tool developed to facilitate screening of homologues for expression and stability, is addition of GFP to the C-terminus of the target protein[110]. This technique has numerous advantages for expression screening, as it allows direct measurement of membrane protein expression by measuring in cell fluorescence; protein stability in detergents can be assessed using fluorescent size exclusion chromatography (FSEC), and correct protein localization using confocal microscopy[111,112]. The technique of using GFP fusions for expression screening was initially developed for use in *E. coli*, but has since been adapted for use in eukaryotic expression systems, like that of the yeast *Saccharomyces cerevisiae*[113]. The use of GFP fusions for expression screening has greatly accelerated the process of target selection for membrane protein structural biology and has already paid dividends in terms of novel membrane protein structures[114-116].

The *in vitro* study of eukaryotic membrane proteins has been especially problematic, with the frequent requirement for a eukaryotic heterologous host for overexpression, including Sf9 insect cells, HEK cells, CHO cells, and yeasts such as *Pichia pastoris* and *Saccharomyces cerevisiae.* The yeast expression system *Pichia pastoris* has been successfully used to produce many eukaryotic membrane proteins for X-ray crystallography studies including; G-protein coupled receptors[76,77], ion channels[78,79], aquaporins[80,81] and ABC transporters[82]. It is an attractive system for membrane protein expression as it maintains many of the advantages associated with prokaryotic protein expression, including inexpensive

medium components; a simple drug based selection system (Zeocin), a strong inducible promoter (AOX1), simple genetics, high cell density and rapid growth yet has the complex folding machinery found in eukaryotic systems.

In this chapter, a simple method to identify highly expressed eukaryotic membrane proteins in *P. pastoris* using a fluorescent-based induction plate assay is described. Human aquaporin 4 (AQP4) is known to express to high levels in *P. pastoris* (~20 mg/L)[80] and was thus used a positive control to demonstrate the validity of the plate screening assay for the identification of high expressing clones. The method was also applied to identify high expressing clones of three homologues of the membrane protein phosphatidylethanolamine N-methyltrasferase (PEMT). PEMT is predicted to have four transmembrane helices and localizes to the ER (Figure 4.1). This enzyme plays an important role in the biosynthesis of phosphotidylcholine and is involved in lipid homeostasis[117]. PEMT deficient mice are deficient in diet-induced obesity and atherosclerosis suggesting PEMT is a crucial target for structural studies to facilitate inhibitor design[118,119].

Human AQP4 and the PEMT homologues from human, mouse and yeast *Saccharomyces cerevisiae* were cloned as C-terminal GFP fusions and making use of a simple fluorescent induction plate method, we demonstrate that the measured fluorescence on the induction plate correlates with

protein expression, thus facilitating the rapid identification of high expressing clones. A high expressing clone of mouse PEMT was further targeted for large scale expression yielding ~5 mg/L of fusion protein after purification.

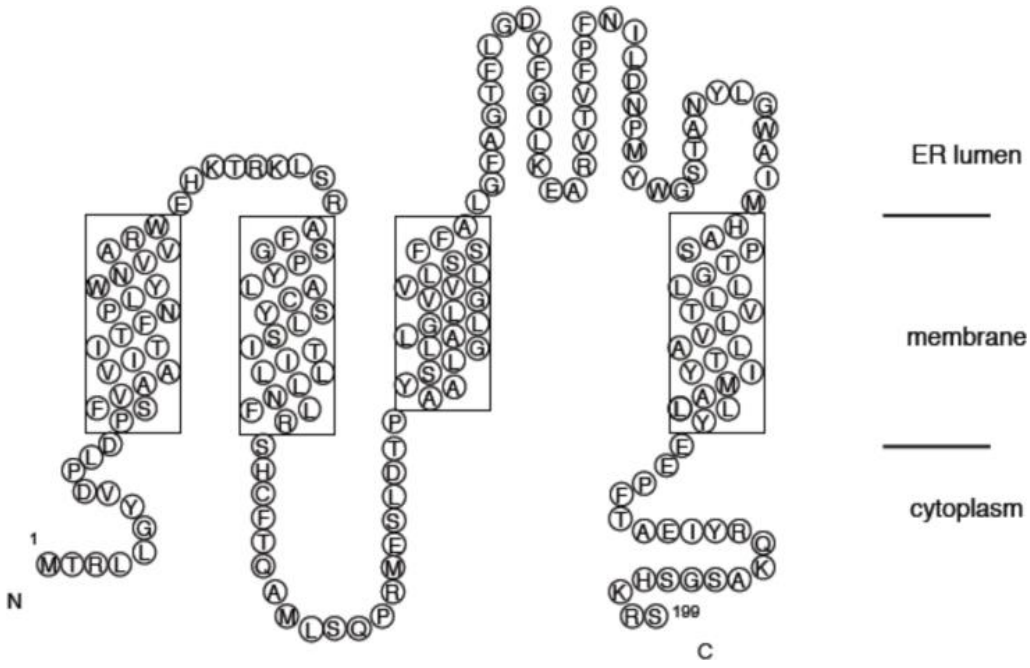

Figure 4.1: Predicted membrane topology of the ER membrane protein phosphatidyl ethanolamine-N-methyl transferase (PEMT). Transmembrane helices were predicted using the TMHMM server.

4.1.1 Phosphatidylethanolamine-N-methyltransferase (PEMT)

Phosphatidylethanolamine N-methyl transferase (PEMT) is a membrane protein responsible for catalyzing the conversion of phosphatidylethanolamine (PE) to phosphatidylcholine (PC). This enzyme performs three transmethylations, transferring three methyl groups from S-adenosylmethionine (AdoMet) to PE[88]. It is a 22.3 kDa protein localized to the membranes of the endoplasmic reticulum (ER) and mitochondrial associated membranes, which are a subfraction of the ER. Topological studies suggest that it is composed of four transmembrane helices with both N-terminus and C-terminus on the cytosolic side of the ER[120] (Figure 4.1).

PEMT is responsible for generating 30% of total hepatic PC. The remaining 70% is generated via the choline pathway and is dependent on being derived from the diet[121]. When PEMT knockout mice are fed a choline-deficient diet, they abnormally accumulate fats, resulting in conditions like steatohepatitis also known as “fatty liver disease” and steatosis. This leads to liver failure within three days due to a 50% decrease in hepatic PC, followed by mouse death in 4-5 days[118]. However, when PEMT double knockout mice were fed a high fat diet, weight gain was prevented and oxygen consumption increased, suggesting PEMT may provide protection from diet-induced obesity and insulin resistance[122].

4.2 Results

4.2.1 Induction Plate-based Expression Screening of Human Aquaporin 4 and PEMTs

Human AQP4 and PEMT homologues from mouse, human and yeast (*S. cerevisiae*) were cloned as in-frame C-terminal GFP fusions to facilitate expression screening. The constructs were preceded by a Kozak consensus sequence (ACCATGG) and a FLAG tag epitope. The PEMT genes were linked to GFP-His^8 by a tobacco etch virus (TEV) protease cut site, with a small peptide linker (GGGS). Constructs were transformed into electrocompetent *P. pastoris* GS115, and the selection for genomic integration of the constructs was performed on YPDS plates containing the antibiotic Zeocin. Human AQP4 is known to have high expression in *P. pastoris*[80] and was used as a proof of principle that the method could identify a high expressing clone. For AQP4, 50 clones of the transformation were chosen along with two untransformed GS115 negative controls and plated onto BMMY to induce protein expression directly on plates. For the PEMT homologues, 48 clones were plated, along with two negative GS115 controls and two high expressing AQP4 clones as positive controls. Plates, imaged under blue light (Figure 4.2), revealed a distribution of fluorescence related to protein expression, ranging from low to high. Colony fluorescence was quantified using Mean Gray Values (MGV) (Figure 4.3). Given that several clones gave background expression (Figures 4.2, 4.3), the presence of genomic integration of the constructs was confirmed for each of the clones using a colony PCR.

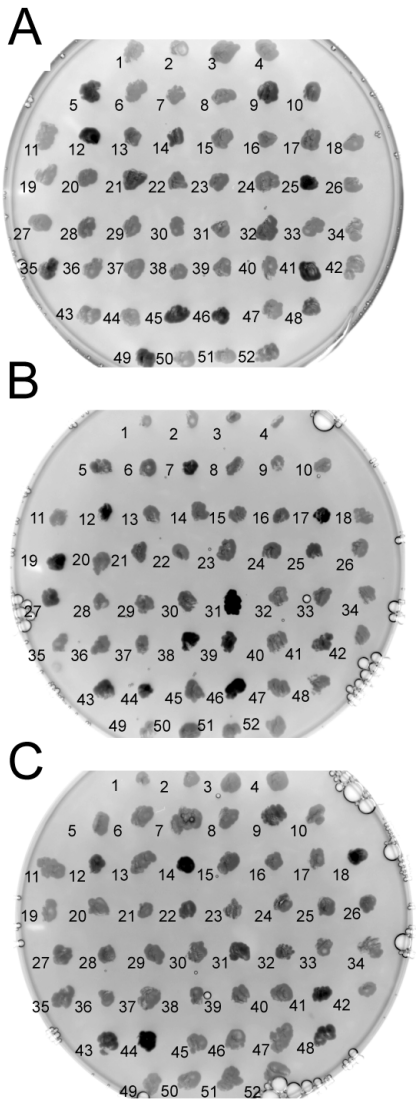

Figure 4.2: Induction plate expression screening. Yeast transformed with plasmids encoding (A) AQP4; (B) human PEMT; (C) mouse PEMT; (D) yeast PEMT (OPI3), were spotted onto BMMY plates and incubated for 24 h at 30 °C. *P. pastoris* GS115 was spotted onto position 1 and 2 as a negative control. High expressing clones of AQP4 (clones 25, 42) were included as positive controls in positions 3 and 4 on plates B-D. Plates were imaged under blue light using an ImageQuant LAS 4000 with a 1/8th of a second exposure.

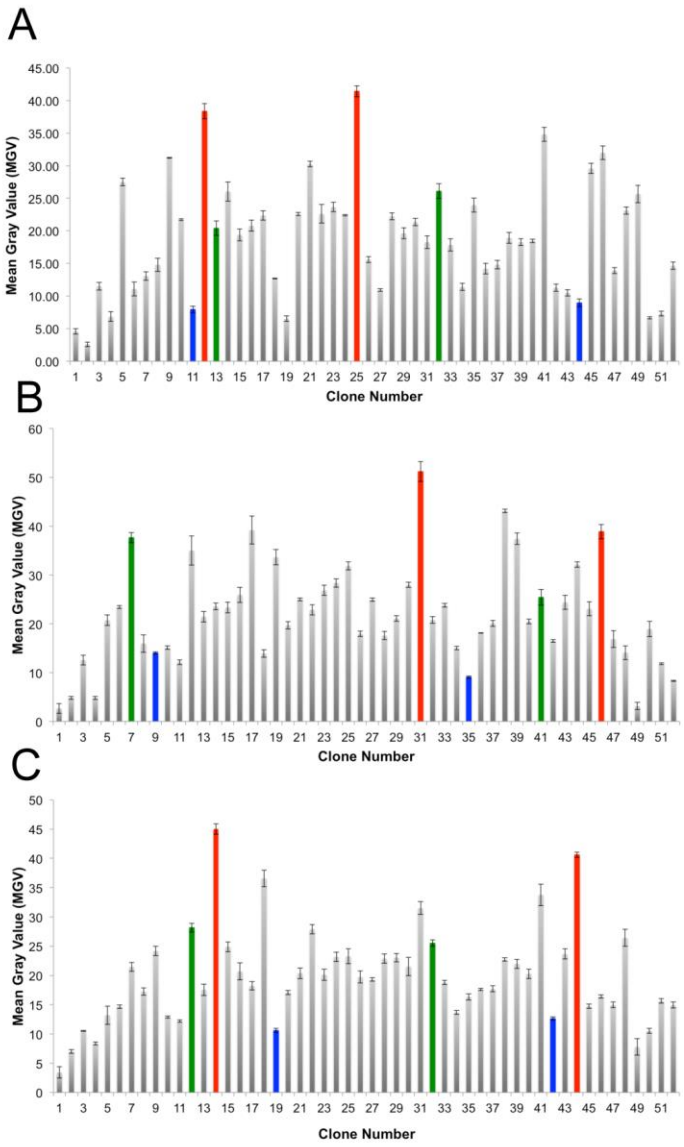

Figure 4.3: **Quantification of plate screening by mean gray value (MGV)**. (A) AQP4; (B) human PEMT; (C) mouse PEMT; (D) yeast PEMT (OPI3). Mean gray value was determined using ImageJ. Colored bars represent clones chosen for further characterization. Blue bars represent low expressing clones, green bars represent medium expressing clones, red bars represent high expressing clones.

4.2.2 Correlation Between Assessment of Expression on Plates in Liquid Culture

To evaluate the reproducibility of the level of protein expression observed on plates with that in liquid culture, two clones each of weak expressers, medium expressers and high expressers (Figure 4.3) cultured in liquid medium. The fluorescence was measured 24 h post-induction with methanol (Figure 4.4), and small-scale lysis of the cultures was carried out for visualization of the total fusion protein through in-gel fluorescence (Figure 4.5).

Both liquid culture fluorescence and total protein analysis show a clear distribution of low, medium and highly expressing clones (Figure 4.2-4.4). This distribution correlates well with the MGV measurements of the initial induction plate colonies, validating this method as a rapid means to test initial expression of GFP tagged membrane proteins in *Pichia*.

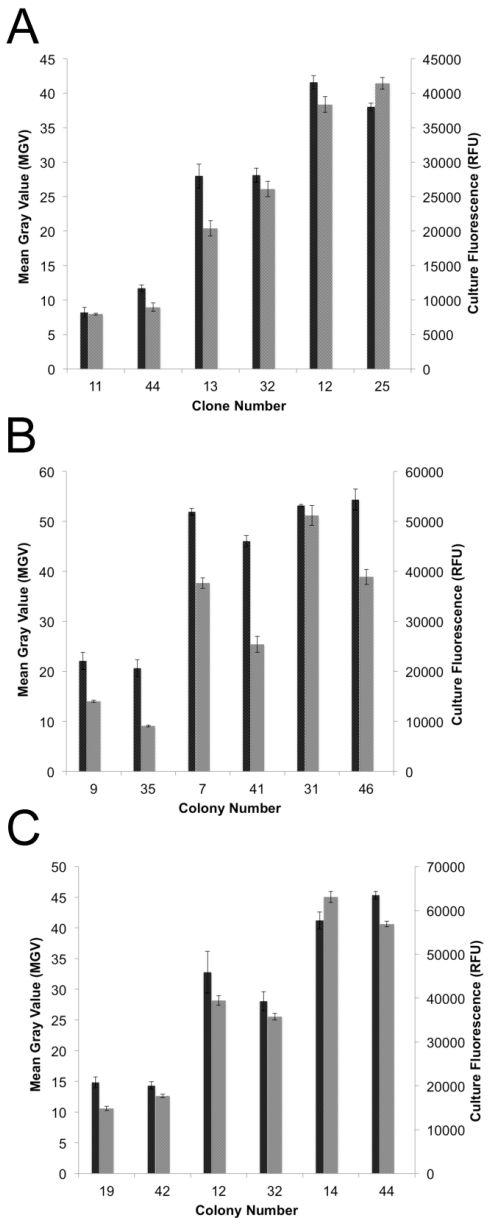

Figure 4.4: Correlation of expression. Measured from plate (MGV) with expression measured (Right axis, gray bars) in liquid culture (right axis, black bars). (A) human PEMT; (B) mouse PEMT; (C) yeast PEMT (OPI3). Error bars represent the standard error of the mean from three separate experiments.

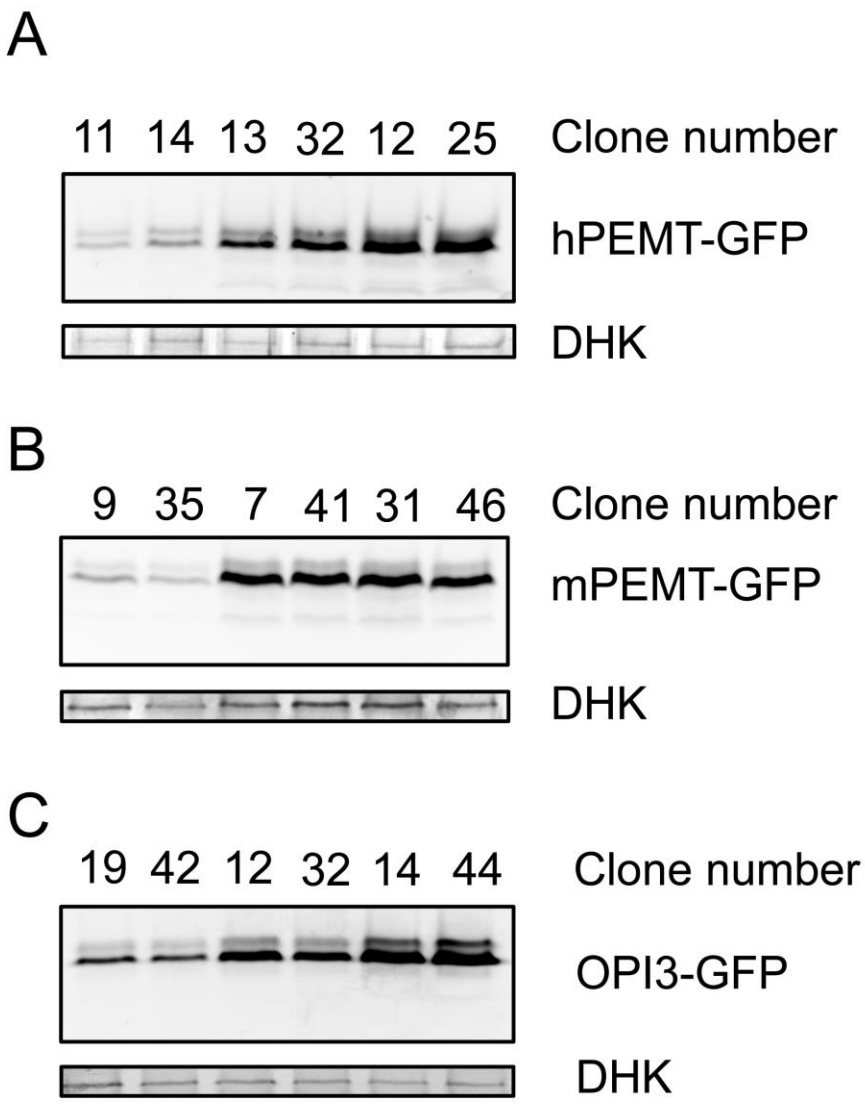

Figure 4.5: In gel fluorescence of PEMT lysates showing variable protein expression in different clones. (A) AQP4; (B) human PEMT; (C) mouse PEMT; (D) yeast PEMT (OPI3). Equal amounts of protein were loaded; dihydroxy acetone kinase (DHK) was used as a loading control (bottom).

4.2.3 Expression and Purification of mouse PEMT (mPEMT)

To demonstrate whether a clone identified by the plate screening method can be used to purify milligram quantities of a eukaryotic membrane protein, clone 48 of mPEMT was selected for large-scale purification. The fusion protein was purified using Ni^{2+} affinity chromatography (Figure 4.6A). The fusion protein was cleaved, using TEV protease and further purified using FLAG tag resin (Figure 4.6B). The final protein purified mPEMT was ~90% pure, the final yield of mPEMT-GFP fusion protein was approximately 5 mg/L of culture, and the yield of purified mPEMT after removal of the GFP tag was 2 mg/L of culture. The final purified protein eluted as a single monodisperse peak from gel filtration chromatography (Figure 4.7), an indication that the protein was not aggregated and is suitable for future crystallization trials.

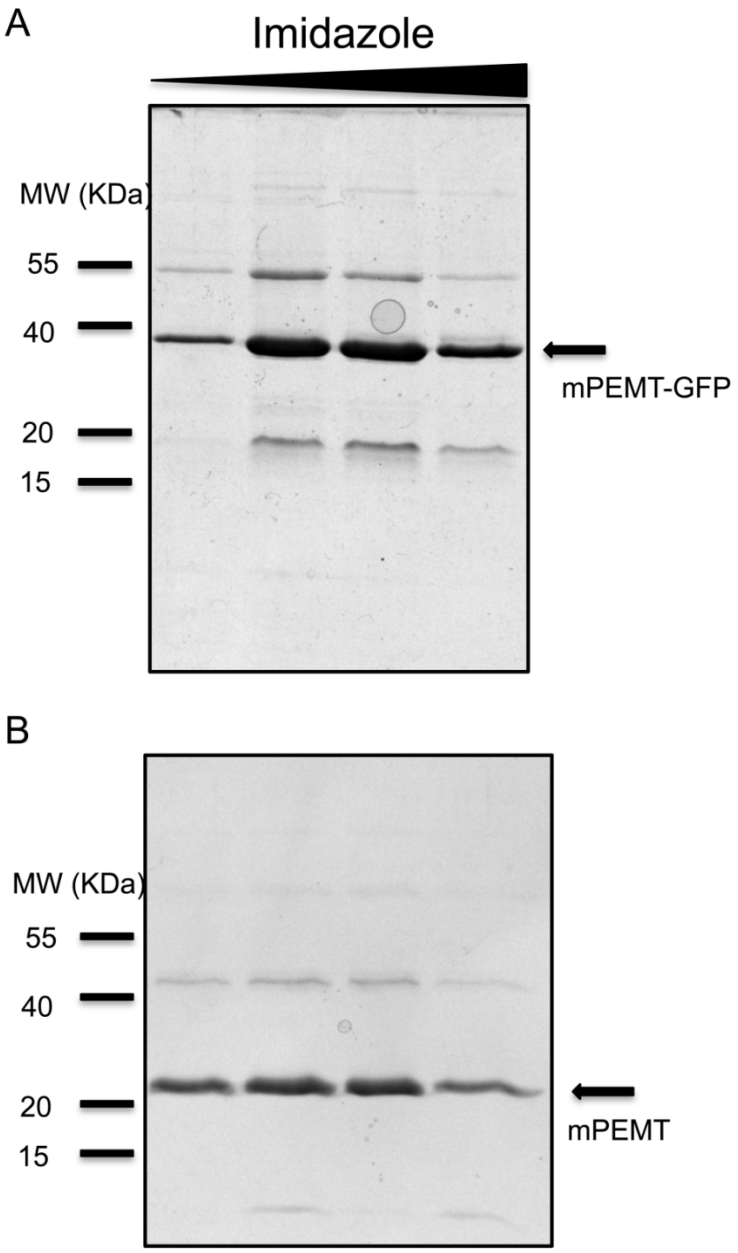

Figure 4.6: Purification of mPEMT. (A) Ni^{2+} affinity chromatography of mPEMT-GFP fusion protein, protein was eluted in a step imidazole gradient. (B) M2 FLAG resin affinity chromatography of mPEMT after TEV cleavage of the fusion protein. Protein eluted in pH 3.5 glycine buffer.

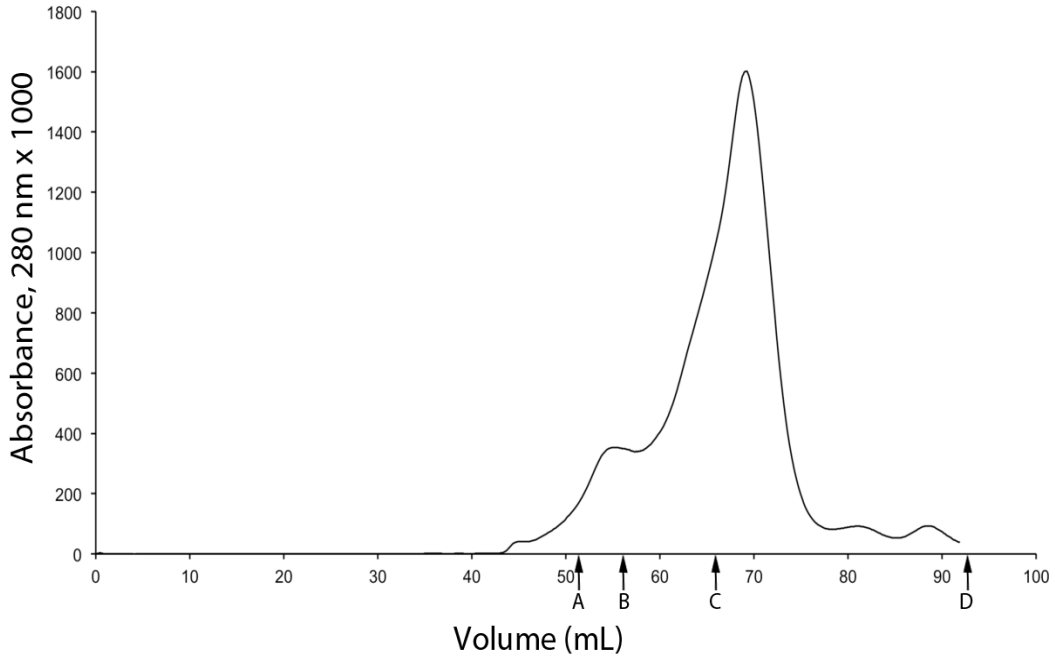

Figure 4.7: Size exclusion chromatography of purified mPEMT. Injected onto a Superdex 200 16 x 160 column equilibrated in 20 mM Tris pH 8.0, 0.15M NaCl, 5% glycerol, 0.15% FC-12. The protein eluted as a single monodisperse peak with minimal aggregation. Elutions for standard proteins are marked by arrows. A) Thyroglobulin 50.7 mL (MW, 670 kDa; Stokes radius 85 Å); B) γ-globulin 56.8 mL (MW 158 kDa; Stokes radius 52.9 Å); C) Ovalbumin 66.8 mL (MW 44 kDa; Stokes radius 30.5 Å); D) myoglobin 93.4 mL (MW 17 kDa, Stokes radius 20.7 Å).

4.3 Discussion

4.3.1 Protein Induction on a Plate is Indicative of Overall Expression Levels

For induction plate screening to be used for large-scale expression screening, it is important that the fluorescent measurements taken from the plate correlate well with protein expression in liquid culture. For both the control AQP4 and the PEMT homologues there is good correlation with the low, medium, and highly expressing colonies in both liquid culture fluorescence and the intensity of the PEMT-GFP fusion protein band on SDS-PAGE (Figure 4.4 and 4.5). Interestingly, mouse PEMT deviates slightly from this observed correlation, with the medium expressers chosen giving relatively high expression in liquid culture (Clones 22 and 30, Figure 4.4B). This trend indicates that the plate screen is most effective at distinguishing between very high and very poor expressers, while the medium expressions could give inconsistent results in liquid culture growth. Thus, the screen is of greatest utility for rapidly identifying the highest expressing clones, while care must be taken in cases where highly variable expression on the plate is not observed.

Colony blot based screening procedures have been used successfully to find high expressing bacterial membrane proteins in *E. coli*[90], as well as soluble protein expression in *E. coli*[80] permitting high throughput expression screening in bacteria. Despite the utility of such methods for protein

expression screening, this is the first time such a method has been applied to expression screening of eukaryotic membrane proteins in a eukaryotic host.

4.3.2 Variable Protein Expression in *Pichia pastoris*

The typical strategy when expressing proteins in *P. pastoris* is to choose several clones (typically 5-10) to screen for expression, owing to variable expression of clones in *P. pastoris*. Examination of levels of expression measured on a plate for the control AQP4 and the three homologues of PEMT (Figure 4.3) indicates a wide variety of expression, ranging from essentially background expression to highly expressing clones (Figure 4.3). An examination of the distribution of expression of the three PEMT homologues shows that only a small fraction of the clones express to relatively high levels, while a handful of clones (5-10 per plate) give essentially no protein expression (Figure 4.3). Thus using conventional liquid culture based screening approaches it may be necessary to screen 50-100 clones to find the best expressing clone, or if insufficient clones are chosen for screening, no high-expressing clone may be found. Given this highly variable protein expression observed in the *Pichia* clones, the induction plate based screening method is a highly efficient way of screening a very large number of clones for expression.

Interestingly, all of the clones tested for expression had successful genomic integration of the expression cassette (Figure 4.8), thus differences in protein expression must be the result of other factors. During the

integration of the expression cassette into the *Pichia* genome there exists the possibility of multi-copy integration that occurs at a rate of 1-10%. It has been suggested that a general strategy to increase protein expression in *Pichia* is to increase the gene dosage[123], although the effects of increasing gene dosage does not increase protein yields. There has been only a single systematic study examining the effect of gene dose in membrane protein expression, where the effect of increasing gene dose increased the expression recombinant aquaporins[124]. In addition to the possible expression variation owing to multi-copy genomic integration of different clones, it has also been suggested that differences in the unfolded protein response (UPR) may contribute to increased protein expression in both *P. pastoris* and *S. cerevisiae*[125].

4.3.3 Induction plate screening permits rapid assessment of expression

A critical variable for success in membrane protein structural biology is the generation of sufficient protein for structural studies[83]. Numerous strategies have been suggested to maximize the possibility of obtaining highly expressing clones. For example screening of homologues for high level expression and crystallization has been successful in many examples[126]. Given the variable protein expression between clones, homologue screening in *Pichia* would become a very laborious process, requiring perhaps hundreds of individual clones to be screened for expression. In addition to homologue screening, other approaches including truncations, codon

optimization, co-expression with chaperones, and gene dosage could all be assessed in a rapid and efficient manner using the method established here. Given that AQP4, a protein known to express to high levels in *P. pastoris* and the very different class of PEMT protein exhibit identical trends in the plate screening assay it could be generally applied for the identification of high expressing membrane proteins of a variety of types. Furthermore the correlation between plate fluorescence, liquid culture fluorescence and protein expression suggests that the plate screen can be used without further testing in liquid culture to identify potential clones for high-level expression. We have used this simple screen to identify express and purify to milligram quantities a PEMT homologue. Rapid plate based expression screening has the potential to simplify and accelerate the search for high expressing eukaryotic membrane proteins.

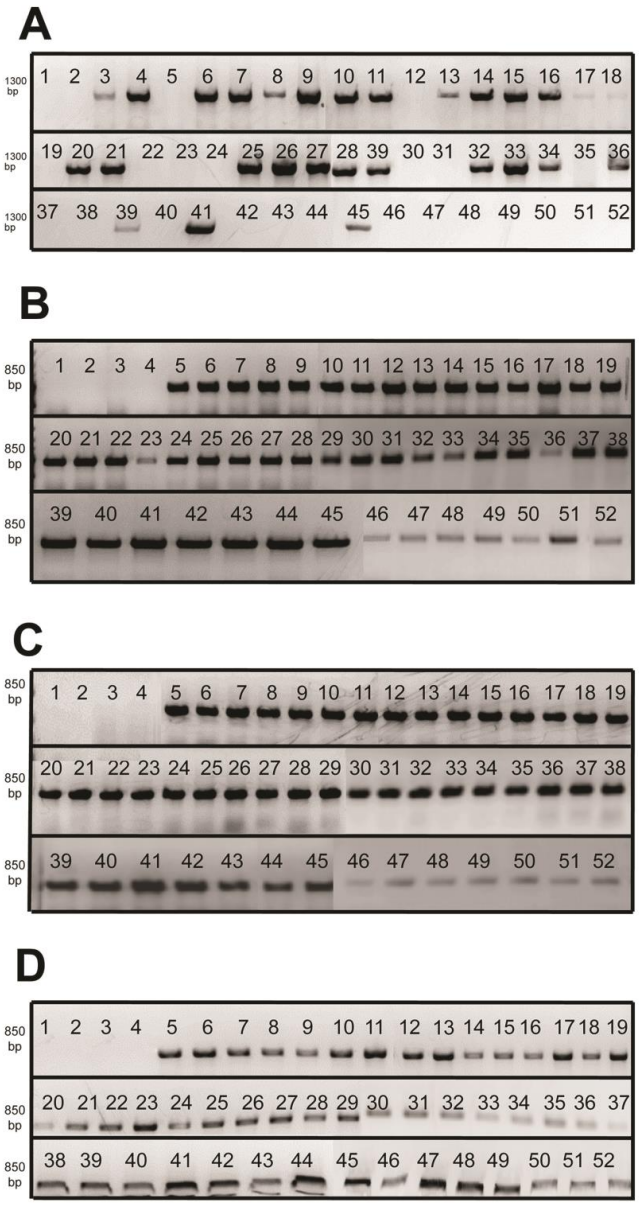

Figure 4.8: PCR screen to ensure genomic integration of expression cassette for human PEMT (A), mouse PEMT (B) and yeast PEMT (OPI3) (C). Lane numbers refer to colony number picked from plates in Fig 2. Positions 1 and 2 are negative controls (untransformed GS115).

Chapter 5

Overexpression of Human PARL in *Pichia Pastoris*

5.1 Introduction

5.1.1 Presenilin-Associated Rhomboid-Like protein (PARL)

PARL is a mitochondrial member of the rhomboid family of intramembrane proteases[127]. Rhomboids cleave membrane anchored substrates through hydrolysis of the peptide backbone in a transmembrane spanning domain[99,128]

PARL was discovered in a yeast two hybrid screen and presumed to be a protease associated with the presenilin protein complex involved in αβPP plaque formation in Alzheimer's disease. Based on sequence homology PARL was classified as a member of the rhomboid family of proteases[99] with the name PARL given from its discovery. However, it was later found not to be involved in the presenilin complex, but instead plays a role in mitochondrial dynamics[99].

PARL possesses the characteristic rhomboid protease topology, consisting of a six transmembrane helical core, however PARL (and other mitochondrial rhomboids) has an additional N-terminal transmembrane helix that is referred to as a "1+6" structures[129]. The protein is 379 amino acids long with its core six TM segments spanning from residues 178-353[99]. It contains the prototypic rhomboid catalytic dyad consisting of residues S277 and H335 on TM helix 4 and 6 respectively[130,131].

5.1.2 N-terminal Cleavage and Regulation of PARL

PARL localizes to the inner mitochondrial membrane with a membrane orientation of the N-terminus in the matrix and the C-terminus in the inner membrane space (IMS). The N-terminus of the protein is proteolytically regulated, with several cleavage events (Figure 5.1) [99,131-133]. The first cleavage event is the proximal α-cleavage, which generates MAMP (mature mitochondrial PARL). This constitutively happens between residues G52 and F53 and is associated with the removal of the mitochondrial targeting sequence (MTS), presumably mediated by the matrix metallopeptidase MPP (mitochondrial processing protein)[133]. The second cleavage event is the distal β-cleavage which occurs between residues S77 and A78, forming PACT (PARL C-terminal fragment)[132]. This event is not constitutive and is thought to be self-regulating[99,133].

This hypothesis comes from several pieces of data, first, that catalytically inactive S277G PARL did not undergo β-cleavage unless wild type PARL was introduced *in vivo*[99]. Secondly, mutations in the β-cleavage residues 76-79, RSAL, to glutamate abolished β-cleavage while PARL was still active. Finally, deletion of region 84-87 resulted in constitutive β-cleavage (unpublished results from the Pellegrini group). The region of the protein containing this site, often called the Pβ domain (residues 40-100), are invariant with conservation among mammals and vertebrates. Four of the known five mammalian PARLs [128] show 58/62 residues completely invariable[99]. The β-cleavage releases a 25 amino acid fragment into the

matrix which acts as a bioactive peptide which is presumed to affect transcription that is nuclear-targeted through the mitochondrial retrograde signaling pathway *in vivo*[99,133]. Phosphorylation dependent regulation may also enable this β-cleavage of PARL[99]. This is due to evidence that the additive effect of multiple phosphorylation events at sites S65, S69 and S70 all abolish β-cleavage[132]. A third cleavage site, classified as γ-cleavage which generates PARL-rhomboid domain (PROD) was identified[131]. This cleavage event happens between residues 155-159. This was observed in HeLa cells and HEK293 cells, and is predicted to disrupt the 1+6 PARL topology, converting the protein to a 6 TM core structure characteristic of rhomboid proteases. It was found that α-cleaved PACT can be directly cleaved into both β-cleaved MAMP and γ-cleaved PROD, respectively. Further, β-cleaved MAMP was found not to be prerequisite to forming PROD[131].

Based on analysis of a structural model of PARL derived from the rhomboid GlpG structures, PARL is speculated to have a third catalytic residue, D319 on TM helix 5, which may exist in the plane of the catalytic dyad. Removal of PARL's additional +1 helix may result in a rotation of helix 5 to turn the D319 away from the catalytic dyad, thereby destabilizing the active site and negatively regulating its activity[131]. This is a new hypothesis in the field which warrants a three dimensional structure of PARL for its conformation.

The proteolytic regulation of PARL may have important consequences in the onset of Parkinson's disease. The observation of a mutation at the β-cleavage site (S77N) has been presumed to play a role in Parkinson's disease[134]. This has been disputed as there has only been one patient detected to have the S77N PARL mutation out of 230 screened in late-onset PD patients, with one additional carrier found in 2,353 late-onset patients of various ethnicities[130,135]. The evidence is of such low frequency that it is doubtful that PARL would be responsible for a PARK form of PD, although as will be discussed PARL plays in indirect role in PD by mediated the activity of the protein PINK1 [130].

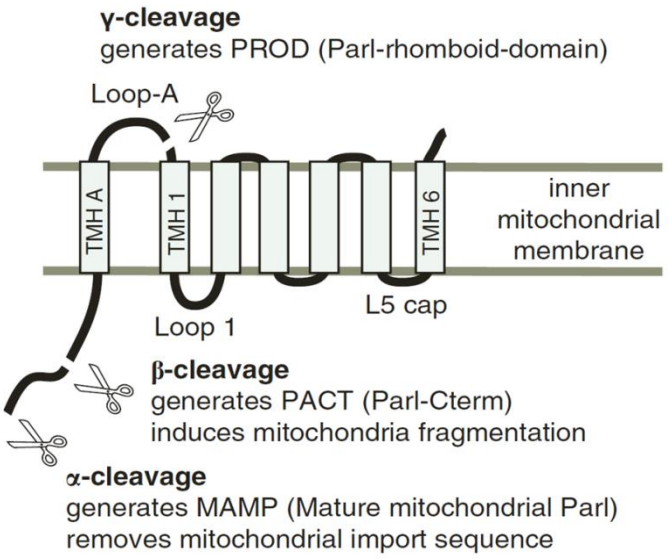

Figure 5.1: Cleavage events in the PARL rhomboid protease. Cleavage of PARL generates 3 forms of the enzyme through α-cleavage, β-cleavage and γ-cleavage. α-cleavage is responsible for removal of the mitochondrial targeting sequence. β-cleavage is suspected to release a 25 amino acid bioactive peptide. γ-cleavage removes the additional helix of PARL, returning the protein to an original rhomboid domain[131]. Adapted from Jeyaraju, D. V., McBride, H. M., Hill, R. B., and Pellegrini, L. (2011) Structural and mechanistic basis of Parl activity and regulation. *Cell Death and Differentiation 18*, 1531–1539.

5.1.3 PARL's Involvement in Governing Mitochondrial Dynamics

PARL appears to be important in the regulation of mitochondrial dynamics and morphology; however the extent of this role is largely unexplored. Heterozygous *parl*$^{+/-}$ mice have no distinguishing phenotype which suggests that the protein's compensates through functional complementation[99]. However, ablation of PARL in mice has detrimental effects on growth and lifespan, and PARL knockout mice die from cachexia due to multiple system atrophy (MSA)[136]. Cellular analyses of PARL knockdown in mouse embryonic fibroblast (MEF) cells were observed to increase apoptosis. This was linked to PARL's downstream ability to modulate cytochrome c release, where its release into the cytosol triggers apoptosis[136]. It can be further speculated that PARL mediated proteolysis of the transmembrane domain of PINK1 releases a PTEN kinase domain in the IMS[55]. The PTEN kinase phosphorylates TRAP1, a protein which prevents cytochrome c release[56,57,137] (Chapter 1). PARL and OPA1 were also placed in the same anti-apoptotic pathway due to their ability to mediate apoptosis[136]. PARL is one of the proteases that releases membrane bound fusion protein OPA1 as a soluble protein into the mitochondrial IMS, which acts to stabilize cristae and impede cytochrome c release[99,136,138].

PARL also mediates cleavage of high temperature regulated A2 (HtrA2), a mitochondrial serine protease also known as Omi1[99,134]. An interaction between Hax1 and HtrA2 was mediated by PARL, suggesting that Hax1 (a member of the B-cell lymphoma 2 (Bcl-1) family), associates with

PARL on the IMM, creating an interface where inactive pre-protein HtrA2 can be cleaved by PARL into an active peptidase[139].

5.1.4 PARL Catalyzes the Cleavage of PINK1

Arguably the most highly analyzed substrate of PARL is PINK1. PINK1 is a PARK6 protein, whose compromised proteolytic processing is strongly linked to the onset of Parkinson's disease[4] (Table 1.1). In a landmark study of the interaction of PARL and PINK1, PINK1 was found to be cleaved by PARL between A103 and F104 to form a 53 kDa N-terminal truncated form of PINK1. This was verified by mutagenesis where F104 substitutions in PINK1 (F104A, F104D) abrogated cleavage, while proper targeting to the IMM was maintained[59]. The transmembrane segment of PINK1 (containing the PARL cleavage site) is highly conserved in mammals and some vertebrates[42] (Figure 5.2). Initially, PARL was identified as the primary protease responsible for generating the PINK1 cleavage product of 53 kDa. Using siRNA to knock down the mitochondrial proteases Afg3L2, ClpP, Oma1, HtrA2/Omi, Paraplegin, Yme1 and PARL, it was observed that PARL had the greatest effect on PINK1 behavior and cleavage[34]. However, later studies have observed that knockdown of PARL allows for "compensating" degradation of PINK1 by other proteases. Without PARL, other cleavage events result in aberrant cleavage of PINK1 and do not release the 53 kDa product[59,140].

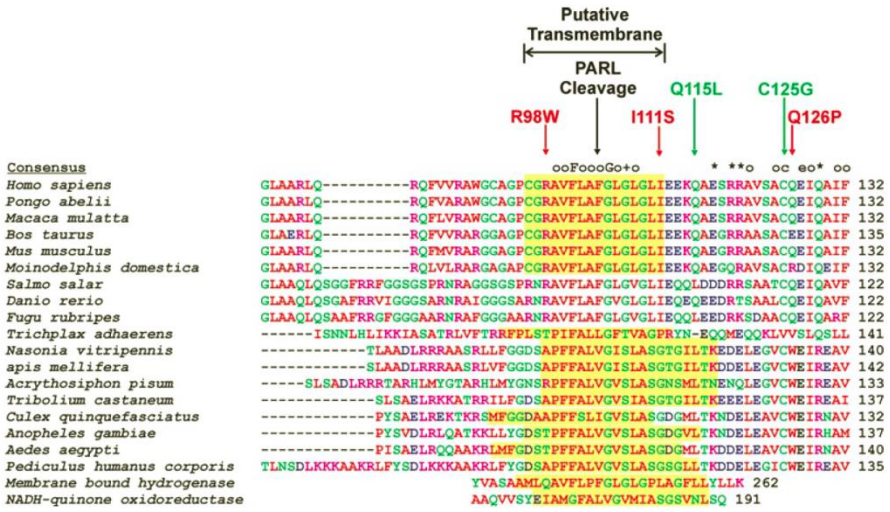

Figure 5.2: Alignment of PINK1 orthologue's transmembrane domains and Parkinson's disease missense mutations. Yellow regions represent predicted transmembrane domains determined using TopPred. The underlined region marks the transmembrane predicted by prediction program, HMMTOP. Dashes represent gaps in sequence. The colors represent the following: green - polar residue; red - hydrophobic residue; magenta - basic residue; blue - acidic residue. Parkinson's associated mutations are marked by red arrows. Green arrows mark the positions of missense mutations with potential association to Parkinson's disease[42]. Taken from Sim, C. H., Gabriel, K., Mills, R. D., Culvenor, J. G., and Cheng, H. (2012) Analysis of the regulatory and catalytic domains of PTEN-induced kinase-1 (PINK1). *Human mutation 33*, 1408–1422.

5.1.5 Objective

PARL is a unique member of the rhomboid protease family. With its topology of a 1+6 transmembrane bundle, N-terminal regulatory cleavage events, and important putative roles in mitochondrial dynamics and PD, a high-resolution crystal structure of PARL would be highly informative to further understand its interaction with substrate, its complex and unusal proteolytic regulation and its distinctive membrane topology. Heterologous expression and purification of PARL is critical for the development of *in vitro* assays of substrate proteolysis and to further understand the regulation of the protein by N-terminal self-cleavage. In addition to *in vitro* analyses, structural studies warrant the development of a heterologous overexpression and purification system for the protein.

The following chapter will explore the overexpression and purification of full length human PARL in *Pichia pastoris* facilitated with an N-terminal green fluorescent protein fusion. The development of this method was facilitated by techniques developed in Chapter 4, particularly the rapid expression screening of eukaryotic membrane proteins using an inducing colony blot plate screening assay.

5.2 Results

5.2.1 Expression and Purification of human PARL-GFP.

The human PARL cDNA was cloned into *Pichia pastoris*. As described in Chapter 4, a GFP tag was incorporated to help to identify *in vivo* conditions for overexpression. *In vivo* fluorescence was observed by transferring transformed *P. pastoris* colonies onto plates containing methanol, in order to induce expression of recombinant PARL. High expressing clones were identified, using fluorescence under blue light (Figure 5.3).

The GFP tag also permitted rapid identification of optimal expression conditions, simply by monitoring fluorescence in the cell during growth (Table 5.1). Maximal overexpression of PARL was obtained following 72 h of induction. Confocal microscopy confirmed the localization of PARL to the mitochondrial membrane (images not taken; visualized). Dense cell pellets were collected and lysed and membranes were isolated by ultracentrifugation. The membranes were washed with a high salt buffer and re-isolated, a step which helped to remove a contaminant protein alcohol dehydrogenase. The protein was also overexpressed in *Pichia* to process the methanol as a carbon source. Since purification was also on a Ni-NTA column, high salt washes have also been used to eliminate proteins with a propensity to bind and interfere with the His-tag binding[141]. Ni-NTA agarose purification resulted in ~3 mg/ 5 L of PARL-GFP. Two to three bands were observed which may represent PARL self-cleavage (Figure 5.4).

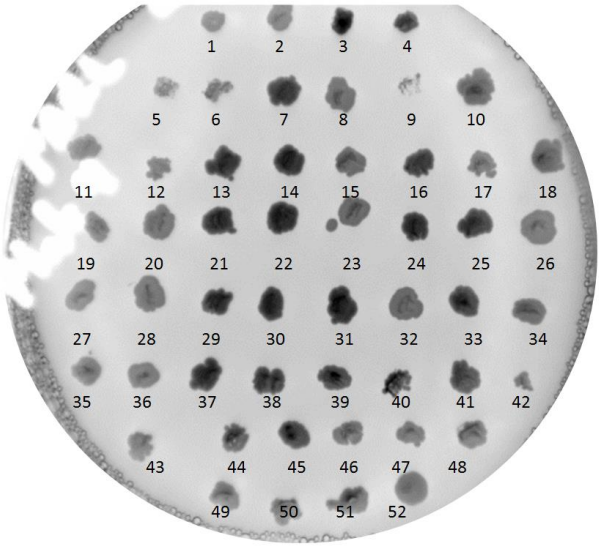

Figure 5.3: Plate Screening Assay of Human PARL-GFP. PARL-GFP colonies were plated onto a methanol containing plate to induce expression. Two negative controls of untransformed GS115 were included in colony positions 1 and 2. Colony 14 was selected for the culture growth as an overexpressing colony.

	Relative Fluorescence Units		
PARL Liquid Culture Flask #	24 h post induction	48 h post induction	72 h post induction
1	3717	7611	22341
2	8657	12903	16917
3	14928	39202	43929
4	14496	29668	45629
5	4507	28873	28105

Table 5.1: Relative fluorescence of PARL-GFP liquid cultures. 5 mL of liquid culture was centrifuged and resuspended in 200 µL of buffer for each flask. Resuspended cells were placed in a multiwell plate and measured for relative fluorescence units in a fluorimeter with gain set to 843.

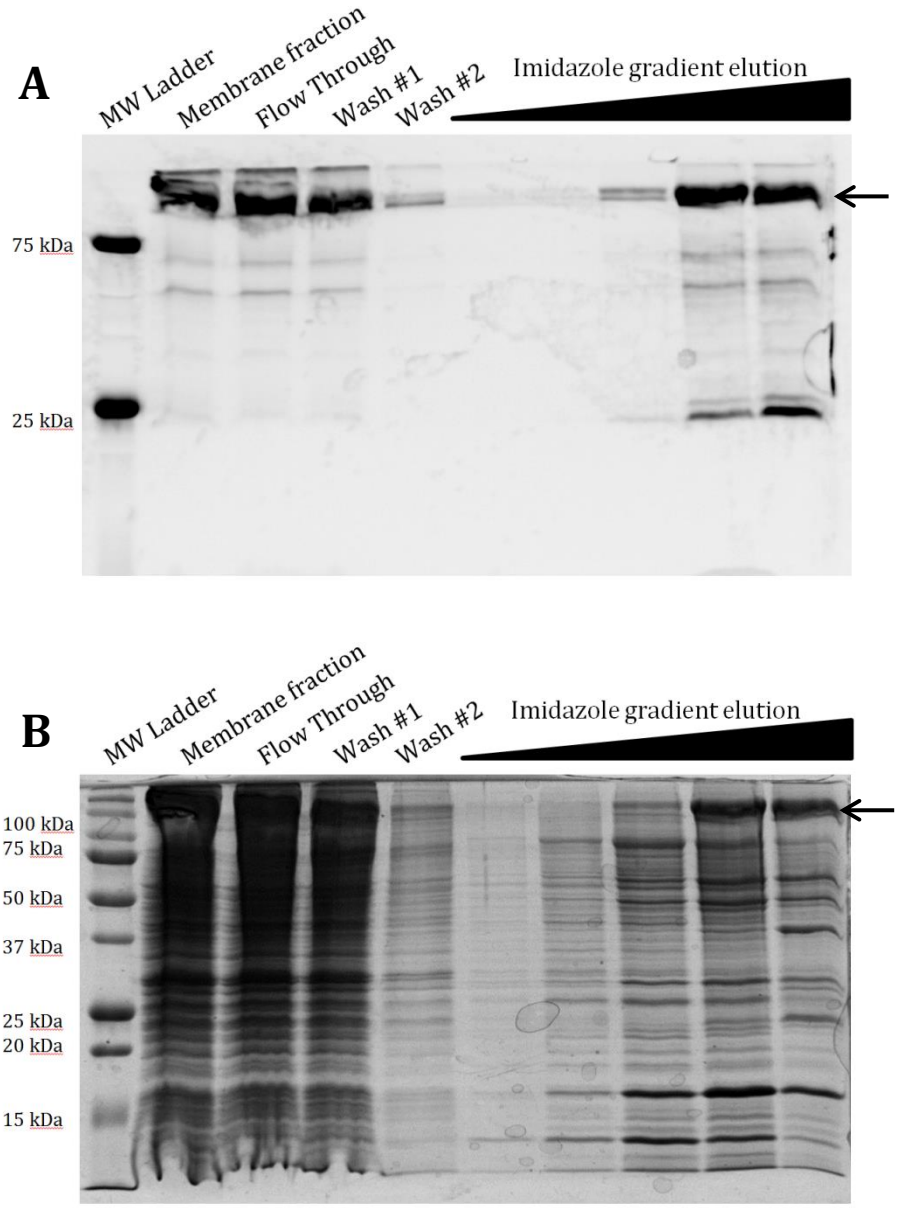

Figure 5.4: Purification of human PARL-GFP. PARL-GFP was purified on a NiNTA agarose column in 50 mM KPO_4, 10% glycerol, 0.3 M NaCl, 10 mM βME, 1 mM PMSF, 0.2% foscholine12 and eluted with an 1 M imidazole gradient. 7.5 µL of protein was loaded per well. A) In-gel fluorescence of 14% acrylamide SDS-PAGE gel. B) Coomassie stained 14% SDS-PAGE gel. Arrows represent human PARL-GFP

5.2.2 Detergent Optimization of PARL-GFP

A key parameter in the purification of membrane proteins is the choice of detergent[69,141]. Optimization of membrane protein solubility in detergents can be a laborious and time consuming endeavor, however in this case detergent optimization experiments were facilitated by the presence of the fluorescent tag GFP. Homogenized PARL-GFP membranes were solubilized in seven different detergents: DM, DDM, NG, LDAO, Triton X-100, $C_{12}E_8$, and FC-12. The selection of detergents was to determine which class of detergent was most preferable for the protein. OG represents glucosides, DDM and DM are maltosides, FC12 is a lipid-like detergent, LDAO is zwitterionic, and $C_{12}E_8$ and Triton X-100 are polyoxyethylenes (Anatrace). Solubility was assessed from three perspectives: an SDS-PAGE gel combined with in gel fluorescence for assessment of irreversible protein aggregation and proteolysis. Secondly, relative fluorescence units were measured before and after solubilization in order to obtain a quantitative measure of solubilization (Table 5.2) and finally, promising detergents from the first two means were selected for fluorescence size exclusion chromatography (FSEC) to determine the monodispersity of the protein in detergent (Figure 5.6, 5.7, 5.8) [112]. PARL-GFP fusion was found at the correct molecular weight of ~76 kDa with some proteolysis and free GFP. Based on the percent solubilization (Table 5.2) and the homogeneity of the protein in an SDS-PAGE gel (Figure 5.4) it was concluded that LDAO and foscholine-12 were the most efficient detergents for the solubilization of PARL. The commonly used detergent

DDM was also selected for analysis in FSEC due to its successful history in solubilizing membrane proteins and its compatibility for crystallization[142].

Analytical FSEC was carried out on PARL-GFP in 0.1% foscholine-12. The FSEC revealed PARL to be 40% homogenous, suggesting that PARL-GFP may not be best solubilized in foscholine-12. Detergent exchange FSEC was done from FC12 to detergents DDM and LDAO. The protein aggregated in LDAO, as seen by the large fluorescent peak coming off the column at its void volume, and DDM was only slightly better with about 70% aggregated.

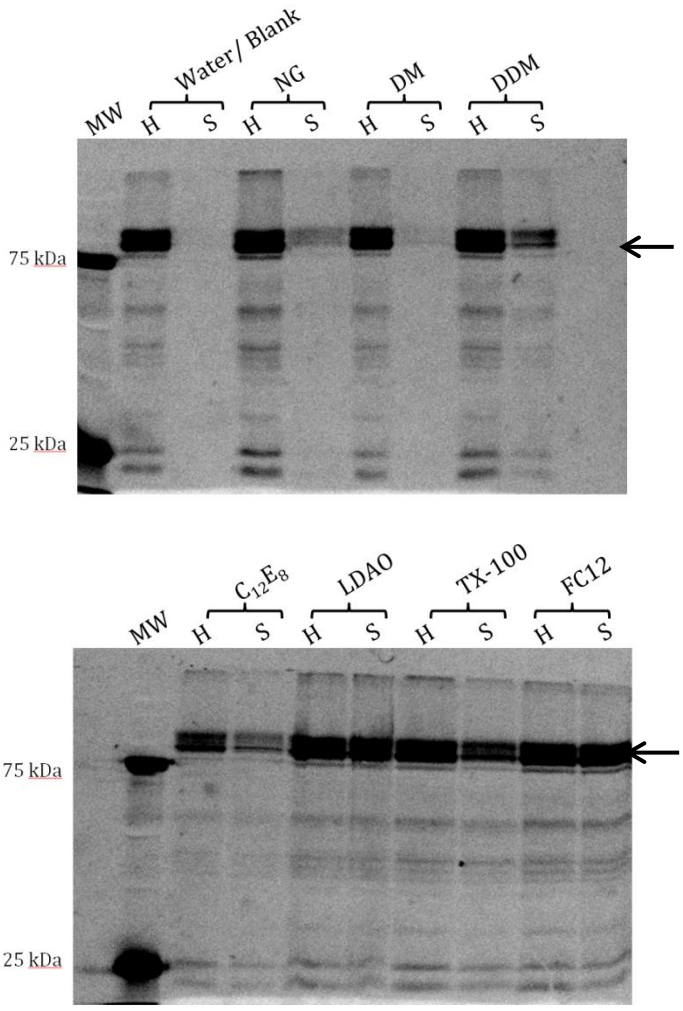

Figure 5.5: In-gel Fluorescence of PARL-GFP Solubility Test. PARL-GFP membranes were homogenized and solubilized in different detergents (NG: neopentyl glycol, DM: n-decyl-β-D-maltopyranoside, DDM: n-dodecyl-β-D-maltopyranoside, $C_{12}E_8$: dodecyl octaethylene glycol ether, LDAO: lauryldimethylamine-N-Oxide, Tx-100: Triton X-100, FC12: foscholine-12) . 14% acrylamide SDS-PAGE gels were loaded alternating homogenized fractions (H) and solubilized fractions (S). 7.5 µL of each sample were loaded with SDS loading dye. Gel was imaged under blue light in the ImageQuant Imager. Arrows represent human PARL-GFP.

Relative Fluorescence	Water/ Blank	NG	DM	DDM	$C_{12}E_8$	LDAO	Tx-100	FC12
Homogenized	9576	9398	9636	8405	9570	7449	6896	8614
Solubilized	117	1112	169	4718	4780	7944	4973	7297
% Solubilized	1.2	11.8	1.8	56.1	49.9	106.6	72.1	84.7

Table 5.2: Solubility of PARL-GFP in Various Detergents. Samples of PARL-GFP were analyzed for solubility in several detergents. Aliquots of each detergent sample were taken once homogenized and solubilized. Relative fluorescence was measured in a fluorimeter to assess the percent solubility in the following detergents. (NG: neopentyl glycol, DM: n-decyl-β-D-maltopyranoside, DDM: n-dodecyl-β-D-maltopyranoside, $C_{12}E_8$: dodecyl octaethylene glycol ether, LDAO: lauryldimethylamine-N-Oxide, Tx-100: Triton X-100, FC12: foscholine-12).

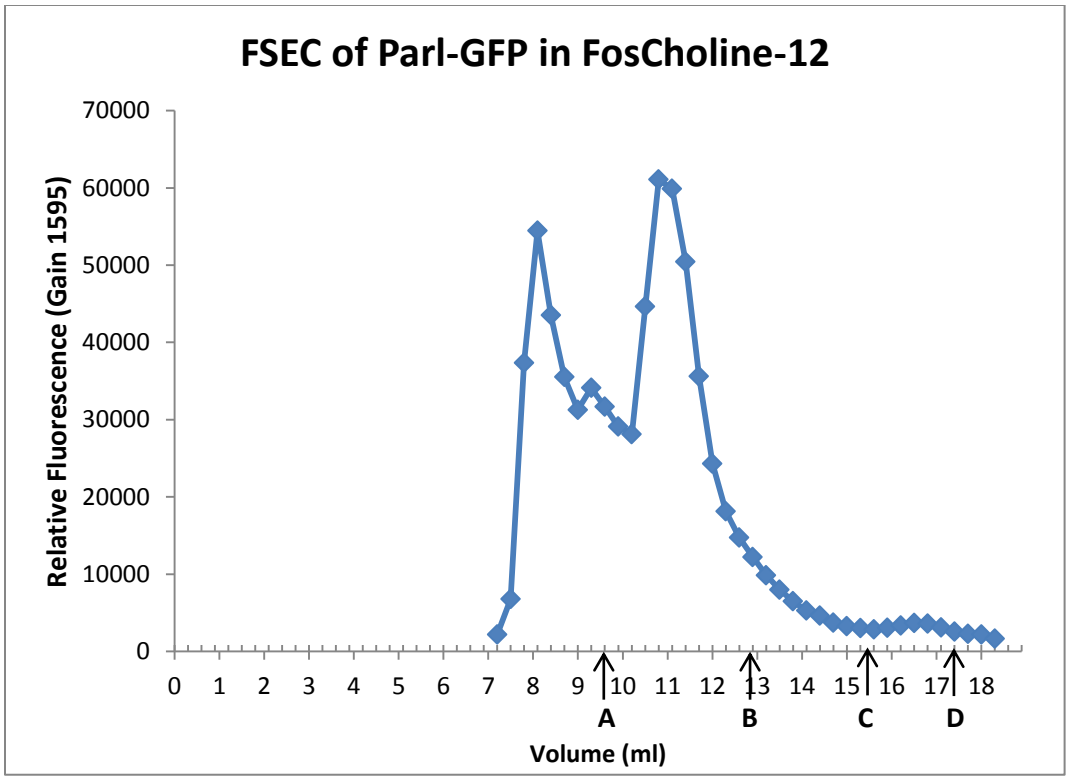

Figure 5.6: Fluorescence Size Exclusion Chromatography of PARL-GFP in foscholine-12. Analytical fluorescent size exclusion chromatography was used to analyze the optimal detergent solubilization. Filter-centrifuged crude membranes (100 µL) solubilized PARL-GFP was loaded on a Superdex 200 10x300 in 50 mM KPO_4, 5% glycerol, 0.1 M NaCl, 10 mM βME, 0.1% foscholine12. Void volume was 8.32 mL. Fractions were collected every 300 µL. Relative fluorescence was measured separately in a fluorimeter. A) Thyroglobulin 50.7 mL (MW, 670 kDa; Stokes radius 85 Å); B) γ-globulin 56.8 mL (MW 158 kDa; Stokes radius 52.9 Å); C) Ovalbumin 66.8 mL (MW 44 kDa; Stokes radius 30.5 Å); D) myoglobin 93.4 mL (MW 17 kDa, Stokes radius 20.7 Å).

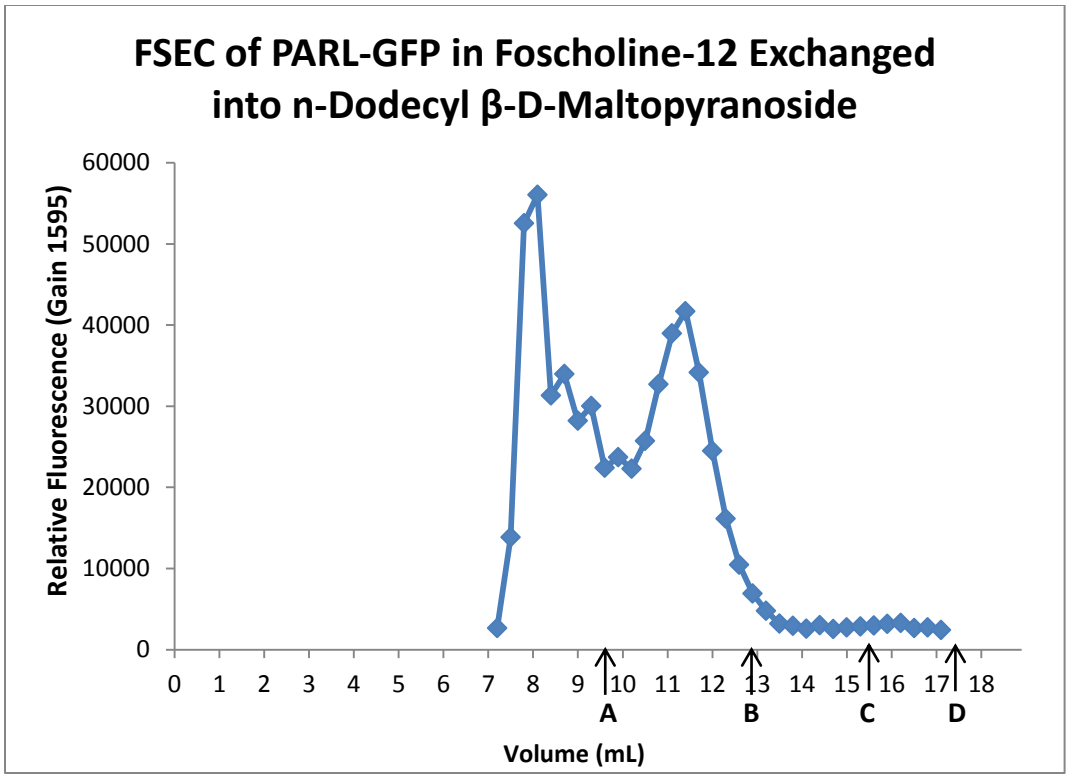

Figure 5.7: Fluorescence Size Exclusion Chromatography of PARL-GFP in foscholine-12 exchanged into n-dodecyl β-D-maltopyranoside. Analytical fluorescent size exclusion chromatography was used to analyze the optimal detergent solubilization. Filter-centrifuged crude membranes (100 µL) of PARL-GFP solubilized in 0.1% foscholine12 was loaded on a Superdex 200 10x300 in 50 mM KPO_4, 5% glycerol, 0.1 M NaCl, 10 mM βME, 0.1% n-Dodecyl β-D-Maltopyranoside. Void volume was 8.32 mL. Fractions were collected every 300 µL. Relative fluorescence was measured separately in a fluorimeter. A) Thyroglobulin 50.7 mL (MW, 670 kDa; Stokes radius 85 Å); B) γ-globulin 56.8 mL (MW 158 kDa; Stokes radius 52.9 Å); C) Ovalbumin 66.8 mL (MW 44 kDa; Stokes radius 30.5 Å); D) myoglobin 93.4 mL (MW 17 kDa, Stokes radius 20.7 Å).

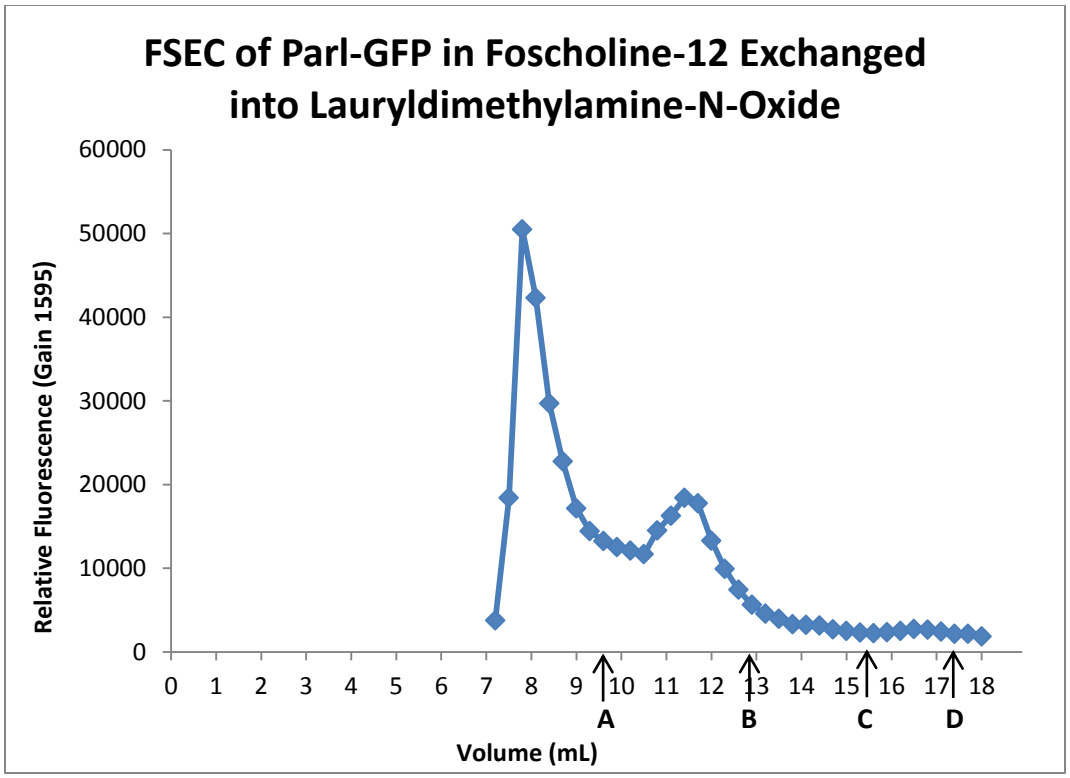

Figure 5.8: Fluorescence Size Exclusion Chromatography of PARL-GFP in foscholine-12 exchanged into lauryldimethylamine-N-oxide. Analytical fluorescent size exclusion chromatography was used to analyze the optimal detergent solubilization. Filter-centrifuged crude membranes (100 µL) of PARL-GFP solubilized in 0.1% foscholine12 were loaded on a Superdex 200 10x300 in 50 mM KPO_4, 5% glycerol, 0.1 M NaCl, 10 mM βME, 0.1% lauryldimethylamine-N-oxide. Void volume was 8.32 mL. Fractions were collected every 300 µL. Relative fluorescence was measured separately in a fluorimeter. A) Thyroglobulin 50.7 mL (MW, 670 kDa; Stokes radius 85 Å); B) γ-globulin 56.8 mL (MW 158 kDa; Stokes radius 52.9 Å); C) Ovalbumin 66.8 mL (MW 44 kDa; Stokes radius 30.5 Å); D) myoglobin 93.4 mL (MW 17 kDa, Stokes radius 20.7 Å).

5.3 Discussion

This chapter represents the first reported overexpression and purification of human PARL that represents a significant step in further understanding this important rhomboid protease. This protein is an interesting target for *in vitro* characterization and structural analysis by x-ray crystallography. The fact that we were able to obtain a few milligrams of PARL fusion protein is an achievement unreported in the literature. However, there is much optimization needed to carry out full purification of this protein.

The expression of PARL-GFP in culture is modest in comparison to that of mouse PEMT, as can be seen by the lower relative fluorescence in culture (Chapter 4). Fluorescence of PARL-GFP in Table 5.1 reached a maximum of ~45,000 R.F.U in comparison to those seen with the PEMT's (Chapter 4) which would reach greater than 60,000 R.F.U. within 24 h of induction. This was also seen by only mildly dark colonies in the plate screening assay of PARL-GFP by comparison (Figure 4.2 vs Figure 5.3). There was an 85% efficiency of solubilization for PARL into fos-choline12 (Table 5.2), but the success of this was diminished when the protein was shown to be ~60% aggregated with FSEC on a gel filtration column.

However, the largest difficulty faced so far in the purification of this protein was purification on a nickel column, where the expressed protein failed to bind efficiently to the resin. This may be due to the fact that a large

fraction of the protein was not well solubilized. Affinity purification has been documented to be a common problem when overexpressing membrane proteins in yeast, as presented in a thorough analysis of membrane protein overexpressing in *Saccharomyces cerevisiae*[141]. After overcoming many hurdles presented by lysis of the thick cell wall and countering the rich protease environment of yeast, affinity purification was often the most difficult[141]. Affinity tags binding to IMAC and IgG-sepharose which often bound extremely effectively when attached to soluble protein, resulted in very poor binding with a membrane protein. The reason for this may be due to excess detergent interference or protein aggregation. The ability of detergents to affect the oligomerization state of proteins may also interfere with affinity purification[141].

As seen in the purification gels, approximately 3 mg were purified from 5 L of liquid culture. In comparison to mPEMT (Chapter 4), 6 L of protein yielded 30 mg of clean fusion protein. In working with other proteins in *Pichia pastoris* expression system with the construct outlined in Chapter 4, some of the greatest difficulties came from the TEV digestion, protein exchange into a new detergent for compatible digestion and losses with binding the nickel column as already discussed.

At this stage, further attempts to complete the purification of PARL require larger culture preparations or optimization of the genetic construct. The cultures of *P. pastoris* to express PARL took 6-7 days to grow, so in order

to carry out large preparations, considerable growing time of the culture would be required. Another option not explored was the use of a fermenter to grow high density cultures in a lower volume of medium[143,144].

Optimization of the expression construct will prove useful for future stages of purification. First, adding or exchanging of the 8X histadine tag for a flag tag would be worth investigating. A flag tag was used in addition to the His tag in mouse PEMT, which allowed better binding, as well as enabling removal of the GFP from the His-tagged TEV. It also may be worthwhile to examine removing the TEV site for another protease site, such as thrombin or HRV 3C protease. Large amounts of TEV were required for mPEMT purification at a 1:1 ratio, and the removal of TEV after proteolysis was very difficult and resulted in large losses of protein due to excessive gel filtration runs. This emphasizes the need to optimize which protease will be most successful in cleaving the PARL-GFP construct in detergent[141]. It is also an option to remove the MTS and allow the protein to reach the plasma membrane as opposed to the mitochondrial membrane. On a further note, it has been suggested that detergent concentrations must also be optimized to be at a minimal critical micellar concentration (CMC) as by their observation, detergent can counter successful cleavage[141].

The beginning steps characterizing a way to overexpress heterologous mitochondrial membrane protein PARL has been explored. There is much more work required to completely purify this protein, such as optimizing the

expression vector or reworking the purification conditions. However, with membrane proteins being so difficult to overexpress, this represents exciting first step towards large scale purification. Most exciting this amount of protein will be useful to examine *in vitro* expression of PINK1 by PARL, a step that has not yet been carried out. Large scale expression will be a prerequisite for structural studies including both 2D and 3D crystallography.

Chapter 6

Conclusions

Conclusions

This thesis set out to study two interacting proteins: the intramembrane protease PARL and the transmembrane domain of the dynamic mitochondrial protein PINK1. Membrane proteins and membrane domains are very difficult to study; significant amounts of protein must be produced and purified, and stabilizing them outside their lipid environment is difficult. The expression and purification of PARL fused to a green fluorescent protein outlined in Chapter 5 was part of an optimization and screening protocol for rapid determination of high expressing clones in *Pichia pastoris* in Chapter 4. These chapters outline the difficulties of overexpressing membrane proteins and the tedious optimization involved in their expression. The use of green fluorescent protein was shown to be a powerful tool in rapidly identifying high expressing colonies in a plate screening assay, as well used to assess protein in liquid culture, detergent optimization and purification.

The expression, purification, and solution NMR spectra of mitochondrial kinase PINK1's single pass transmembrane domain was outlined in Chapter 3. The purpose was to determine the secondary structure of the PINK1 transmembrane domain in order to assess how it changes when Parkinson's disease missense mutations occur. A strategy to obtain milligram quantities of the membrane domain was outlined, where the transmembrane domain of PINK1 was fused to maltose binding protein. Although the purified transmembrane domain was not used for NMR studies, a synthetic peptide

did lead to analysis of the TM domain. It was determined to have no helical structure and was classified as a random coil. This is in following with a hypothesis in the field that substrates of rhomboid intramembrane proteases are metastable helixes that have structures dependent on the presence of a membrane. Unfortunately, if the transmembrane domain is unstructured, further analysis of the effect of mutations on the secondary structure may not be warranted.

The next goal of these projects converges on a cleavage assay of the PINK1 TM domain by the protein PARL. This assay would be used to assess if Parkinson's disease mutations in that domain affect its ability to be cleavage by PARL. This *in vitro* cleavage assay has been optimized in our lab for steady-state kinetic analysis of rhomboid proteases. The PINK1 TM domain will be cloned into a FRET pair where cleavage of the TM disrupts energy transfer. In order for this experiment to move forward, the optimization of the purification of PARL would need improvement.

To further analyze the effect of Parkinson's mutations in the transmembrane domain of PINK1 is to study localization of the protein under confocal microscopy. This would be facilitated through collaboration with Dr. Nicolas Touret (University of Alberta). We would hope to analyze if the localization of PINK1 to the IMM is impeded by the presence of mutations in its transmembrane domain. Together these studies work to dissecting the molecular mechanism of the PARK6 phenotype of Parkinson's disease.

Bibliography

References

(1) Pilsl, A., and Winklhofer, K. F. (2012) Parkin, PINK1 and mitochondrial integrity: emerging concepts of mitochondrial dysfunction in Parkinson's disease. *Acta Neuropathologica 123*, 173–188.

(2) Martin, I., Dawson, V., and Dawson, T. (2011) Recent advances in the genetics of Parkinson's disease. *Annual Review of Genomics and Human Genetics 12*, 301–325.

(3) Vries, R., and Przedborski, S. (2013) Mitophagy and Parkinson's disease: Be eaten to stay healthy. *Molecular and Cellular Neurosciences 55*, 37–43.

(4) Mills, R. D., Sim, C. H., Mok, S. S., Mulhern, T. D., Culvenor, J. G., and Cheng, H. (2008) Biochemical aspects of the neuroprotective mechanism of PTEN-induced kinase-1 (PINK1). *Journal of Neurochemistry 105*, 18–33.

(5) Belin, A. C., and Westerlund, M. (2008) Parkinson's disease: a genetic perspective. *The FEBS Journal 275*, 1377–1383.

(6) Langston, J., and Ballard, P. (1983) Parkinson's disease in a chemist working with 1-methyl-4-phenyl-1,2,5,6-tetrahydropyridine. *The New England Journal of Medicine 309*, 310.

(7) Houlden, H., and Singleton, A. B. (2012) The genetics and neuropathology of Parkinson's disease. *Acta Neuropathologica 124*, 325–338.

(8) Cookson, M. R., Dauer, W., Dawson, T., Fon, E. A., Guo, M., and Shen, J. (2007) The roles of kinases in familial Parkinson's disease. *The Journal of Neuroscience 27*, 11865–11868.

(9) Cookson, M. R. (2012) Parkinsonism due to mutations in PINK1, parkin, and DJ-1 and oxidative stress and mitochondrial pathways. *Cold Spring Harbor Perspectives in Medicine 2*, a009415.

(10) Blackinton, J. G., Anvret, A., Beilina, A., Olson, L., Cookson, M. R., and Galter, D. (2007) Expression of PINK1 mRNA in human and rodent brain and in Parkinson's disease. *Brain Research 1184*, 10–16.

(11) Gandhi, S., Muqit, M., Stanyer, L., Healy, D., Abou-Sleiman, P., Hargreaves, I., Heales, S., Ganguly, M., Parsons, L., Lees, A., Latchman, D., Holton, J., Wood, N., and Revesz, T. (2006) PINK1 protein in normal human brain and Parkinson's disease. *Brain 129*, 1720–1731.

(12) Lin, W., and Kang, U. (2008) Characterization of PINK1 processing, stability, and subcellular localization. *Journal of Neurochemistry 106*, 464–474.

(13) Samaranch, L., Lorenzo-Betancor, O., Arbelo, J. M., Ferrer, I., Lorenzo, E., Irigoyen, J., Pastor, M. A., Marrero, C., Isla, C., Herrera-Henriquez, J., and Pastor, P. (2010) PINK1-linked parkinsonism is associated with Lewy body pathology. *Brain 133*, 1128–1142.

(14) Polymeropoulos, M. H., Lavedan, C., Leroy, E., Ide, S. E., Dehejia, A., Dutra, A., Pike, B., Root, H., Rubenstein, J., Boyer, R., Stenroos, E. S., Chandrasekharappa, S., Athanassiadou, A., Papapetropoulos, T.,

Johnson, W. G., Lazzarini, A. M., Duvoisin, R. C., Iorio, G., Golbe, L. I., and Nussbaum, R. L. (1997) Mutation in the alpha-synuclein gene identified in families with Parkinson's disease. *Science 276*, 2045–2047.

(15) Singleton, A. B., Farrer, M., Johnson, J., Singleton, A., Hague, S., Kachergus, J., Hulihan, M., Peuralinna, T., Dutra, A., Nussbaum, R., Lincoln, S., Crawley, A., Hanson, M., Maraganore, D., Adler, C., Cookson, M. R., Muenter, M., Baptista, M., Miller, D., Blancato, J., Hardy, J., and Gwinn-Hardy, K. (2003) alpha-Synuclein locus triplication causes Parkinson's disease. *Science 302*, 841.

(16) Kitada, T., Asakawa, S., Hattori, N., Matsumine, H., Yamamura, Y., Minoshima, S., Yokochi, M., Mizuno, Y., and Shimizu, N. (1998) Mutations in the parkin gene cause autosomal recessive juvenile parkinsonism. *Nature 392*, 605–608.

(17) Valente, E. M., Abou-Sleiman, P. M., Caputo, V., Muqit, M. M., Harvey, K., ispert, S., Ali, Z., Turco, D., Bentivoglio, A. R., Healy, D. G., Albanese, A., Nussbaum, R., González-Maldonado, R., Deller, T., Salvi, S., Cortelli, P., Gilks, W. P., Latchman, D. S., Harvey, R. J., Dallapiccola, B., Auburger, G., and Wood, N. W. (2004) Hereditary early-onset Parkinson's disease caused by mutations in PINK1. *Science 304*, 1158–1160.

(18) Bonifati, V., Rizzu, P., Baren, M. J., Schaap, O., Breedveld, G. J., Krieger, E., Dekker, M. C., Squitieri, F., Ibanez, P., Joosse, M., Dongen, J. W., Vanacore, N., Swieten, J. C., Brice, A., Meco, G., Duijn, C. M., Oostra, A., and Heutink, P. (2003) Mutations in the DJ-1 gene associated with autosomal recessive early-onset parkinsonism. *Science 299*, 256–259.

(19) Paisán-Ruíz, C., Jain, S., Evans, E. W., Gilks, W. P., Simón, J., Brug, M., Munain, A. L., Aparicio, S., Gil, A. M., Khan, N., Johnson, J., Martinez, J. R., Nicholl, D., Carrera, I. M., Pena, A. S., Silva, R., Lees, A., Martí-Massó, J. F., Pérez-Tur, J., Wood, N. W., and Singleton, A. B. (2004) Cloning of the gene containing mutations that cause PARK8-linked Parkinson's disease. *Neuron 44*, 595–600.

(20) Zimprich, A., Biskup, S., Leitner, P., Lichtner, P., Farrer, M., Lincoln, S., Kachergus, J., Hulihan, M., Uitti, R. J., Calne, D. B., Stoessl, A. J., Pfeiffer, R. F., Patenge, N., Carbajal, I. C., Vieregge, P., Asmus, F., Müller-Myhsok, B., Dickson, D. W., Meitinger, T., Strom, T. M., Wszolek, Z. K., and Gasser, T. (2004) Mutations in LRRK2 cause autosomal-dominant parkinsonism with pleomorphic pathology. *Neuron 44*, 601–607.

(21) Ramirez, A., Heimbach, A., Gründemann, J., Stiller, B., Hampshire, D., Cid, L. P., Goebel, I., Mubaidin, A. F., Wriekat, A., Roeper, J., Al-Din, A., Hillmer, A. M., Karsak, M., Liss, B., Woods, C. G., Behrens, M. I., and Kubisch, C. (2006) Hereditary parkinsonism with dementia is caused by mutations in ATP13A2, encoding a lysosomal type 5 P-type ATPase. *Nature Genetics 38*, 1184–1191.

(22) Paisán-Ruíz, C., Bhatia, K. P., Li, A., Hernández, D., Davis, M., Wood, N. W., Hardy, J., Houlden, H., Singleton, A., and Schneider, S. A. (2009) Characterization of PLA2G6 as a locus for dystonia-parkinsonism. *Annals of Neurology 65*, 19–23.

(23) Fonzo, A., Dekker, M. C., Montagna, P., Baruzzi, A., Yonova, E. H., Guedes, L. C., Szczerbinska, A., Zhao, T., Dubbel-Hulsman, L. O., Wouters, C. H., Graaff, E., Oyen, W. J., Simons, E. J., Breedveld, G. J., Oostra, B. A., Horstink, M. W., and Bonifati, V. (2009) FBXO7 mutations cause autosomal recessive, early-onset parkinsonian-pyramidal syndrome. *Neurology 72*, 240–245.

(24) Vilariño-Güell, C., Wider, C., Ross, O. A., Dachsel, J. C., Kachergus, J. M., Lincoln, S. J., Soto-Ortolaza, A. I., Cobb, S. A., Wilhoite, G. J., Bacon, J. A., Behrouz, B., Melrose, H. L., Hentati, E., Puschmann, A., Evans, D. M., Conibear, E., Wasserman, W. W., Aasly, J. O., Burkhard, P. R., Djaldetti, R., Ghika, J., Hentati, F., Krygowska-Wajs, A., Lynch, T., Melamed, E., Rajput, A., Rajput, A. H., Solida, A., Wu, R., Uitti, R. J., Wszolek, Z. K., Vingerhoets, F., and Farrer, M. J. (2011) VPS35 mutations in Parkinson disease. *American Journal of Human Genetics 89*, 162–167.

(25) Zimprich, A., Benet-Pagès, A., Struhal, W., Graf, E., Eck, S. H., Offman, M. N., Haubenberger, D., Spielberger, S., Schulte, E. C., Lichtner, P., Rossle, S. C., Klopp, N., Wolf, E., Seppi, K., Pirker, W., Presslauer, S., Mollenhauer, B., Katzenschlager, R., Foki, T., Hotzy, C., Reinthaler, E., Harutyunyan, A., Kralovics, R., Peters, A., Zimprich, F., Brücke, T., Poewe, W., Auff, E., Trenkwalder, C., Rost, B., Ransmayr, G., Winkelmann, J., Meitinger, T., and Strom, T. M. (2011) A mutation in VPS35, encoding a subunit of the retromer complex, causes late-onset Parkinson disease. *American Journal of Human Genetics 89*, 168–175.

(26) Thomas, M., Hayflick, S. J., and Jankovic, J. (2004) Clinical heterogeneity of neurodegeneration with brain iron accumulation (Hallervorden-Spatz syndrome) and pantothenate kinase-associated neurodegeneration. *Movement Disorders 19*, 36–42.

(27) Zhou, B., Westaway, S. K., Levinson, B., Johnson, M. A., Gitschier, J., and Hayflick, S. J. (2001) A novel pantothenate kinase gene (PANK2) is defective in Hallervorden-Spatz syndrome. *Nature Genetics 28*, 345–349.

(28) Youle, R. J., and Narendra, D. P. (2011) Mechanisms of mitophagy. *Nature reviews. Molecular Cell Biology 12*, 9–14.

(29) Ferree, A., and Shirihai, O. (2012) Mitochondrial dynamics: the intersection of form and function. *Advances in Experimental Medicine and Biology 748*, 13–40.

(30) Ashrafi, G., and Schwarz, T. L. (2013) The pathways of mitophagy for quality control and clearance of mitochondria. *Cell Death and Differentiation 20*, 31–42.

(31) Koppen, M., and Langer, T. (2007) Protein degradation within mitochondria: versatile activities of AAA proteases and other peptidases. *Critical Reviews in Biochemistry and Molecular Biology 42*, 221–242.

(32) Soubannier, V., McLelland, G., Zunino, R., Braschi, E., Rippstein, P., Fon, E. A., and McBride, H. M. (2012) A vesicular transport pathway shuttles cargo from mitochondria to lysosomes. *Current biology* 135–141.

(33) Lemasters, J. J., Nieminen, A. L., Qian, T., Trost, L. C., Elmore, S. P., Nishimura, Y., Crowe, R. A., Cascio, W. E., Bradham, C. A., Brenner, D. A., and Herman, B. (1998) The mitochondrial permeability transition in cell death: a common mechanism in necrosis, apoptosis and autophagy. *Biochimica et Biophysica Acta 1366*, 177–196.
(34) Jin, S. M., Lazarou, M., Wang, C., Kane, L. A., Narendra, D. P., and Youle, R. J. (2010) Mitochondrial membrane potential regulates PINK1 import and proteolytic destabilization by PARL. *The Journal of Cell Biology 191*, 933–942.
(35) Jin, S. M., and Youle, R. J. (2012) PINK1- and Parkin-mediated mitophagy at a glance. *Journal of Cell Science 125*, 795–799.
(36) Wang, X., Winter, D., Ashrafi, G., Schlehe, J., Wong, Y. L., Selkoe, D., Rice, S., Steen, J., LaVoie, M. J., and Schwarz, T. L. (2011) PINK1 and Parkin target Miro for phosphorylation and degradation to arrest mitochondrial motility. *Cell 147*, 893–906.
(37) Lazarou, M., Jin, S. M., Kane, L. A., and Youle, R. J. (2012) Role of PINK1 binding to the TOM complex and alternate intracellular membranes in recruitment and activation of the E3 ligase Parkin. *Developmental Cell 22*, 320–333.
(38) Poole, A. C., Thomas, R. E., Yu, S., Vincow, E. S., and Pallanck, L. (2010) The mitochondrial fusion-promoting factor mitofusin is a substrate of the PINK1/parkin pathway. *PloS one 5*, e10054.
(39) Chan, N. C., Salazar, A. M., Pham, A. H., Sweredoski, M. J., Kolawa, N. J., Graham, R. L., Hess, S., and Chan, D. C. (2011) Broad activation of the ubiquitin-proteasome system by Parkin is critical for mitophagy. *Human Molecular Genetics 20*, 1726–1737.
(40) Chu, C. T. (2010) Tickled PINK1: mitochondrial homeostasis and autophagy in recessive Parkinsonism. *Biochimica et Biophysica Acta 1802*, 20–28.
(41) Arena, G., Gelmetti, V., Torosantucci, L., Vignone, D., Lamorte, G., Rosa, P., Cilia, E., Jonas, E. A., and Valente, E. M. (2013) PINK1 protects against cell death induced by mitochondrial depolarization, by phosphorylating Bcl-xL and impairing its pro-apoptotic cleavage. *Cell Death and Differentiation*.
(42) Sim, C. H., Gabriel, K., Mills, R. D., Culvenor, J. G., and Cheng, H. (2012) Analysis of the regulatory and catalytic domains of PTEN-induced kinase-1 (PINK1). *Human mutation 33*, 1408–1422.
(43) Gautier, C. A., Kitada, T., and Shen, J. (2008) Loss of PINK1 causes mitochondrial functional defects and increased sensitivity to oxidative stress. *Proceedings of the National Academy of Sciences of the United States of America 105*, 11364–11369.
(44) Park, J., Lee, S. B., Lee, S., Kim, Y., Song, S., Kim, S., Bae, E., Kim, J., Shong, M., Kim, J., and Chung, J. (2006) Mitochondrial dysfunction in Drosophila PINK1 mutants is complemented by parkin. *Nature 441*, 1157–1161.
(45) Kato, H., Lu, Q., Rapaport, D., and Kozjak-Pavlovic, V. (2013) Tom70 is

essential for PINK1 import into mitochondria. *PloS one 8*, e58435.
(46) Zhou, C., Huang, Y., Shao, Y., May, J., Prou, D., Perier, C., Dauer, W., Schon, E. A., and Przedborski, S. (2008) The kinase domain of mitochondrial PINK1 faces the cytoplasm. *Proceedings of the National Academy of Sciences of the United States of America 105*, 12022–12027.
(47) Lin, W., and Kang, U. (2010) Structural determinants of PINK1 topology and dual subcellular distribution. *BMC Cell Biology 11*, 90.
(48) Meissner, C., Lorenz, H., Weihofen, A., Selkoe, D. J., and Lemberg, M. K. (2011) The mitochondrial intramembrane protease PARL cleaves human Pink1 to regulate Pink1 trafficking. *Journal of Neurochemistry 117*, 856–867.
(49) Silvestri, L., Caputo, V., Bellacchio, E., Atorino, L., Dallapiccola, B., Valente, E., and Casari, G. (2005) Mitochondrial import and enzymatic activity of PINK1 mutants associated to recessive parkinsonism. *Human Molecular Genetics 14*, 3477–3492.
(50) Takatori, S., Ito, G., and Iwatsubo, T. (2008) Cytoplasmic localization and proteasomal degradation of N-terminally cleaved form of PINK1. *Neuroscience Letters 430*, 13–17.
(51) Beilina, A., Brug, M., Ahmad, R., Kesavapany, S., Miller, D. W., Petsko, G. A., and Cookson, M. R. (2005) Mutations in PTEN-induced putative kinase 1 associated with recessive parkinsonism have differential effects on protein stability. *Proceedings of the National Academy of Sciences of the United States of America 102*, 5703–5708.
(52) Imai, Y. (2012) Mitochondrial Regulation by PINK1-Parkin Signaling. *ISRN Cell Biology 2012*, 1–15.
(53) Kondapalli, C., Kazlauskaite, A., Zhang, N., Woodroof, H., Campbell, D., Gourlay, R., Burchell, L., Walden, H., Macartney, T., Deak, M., Knebel, A., Alessi, D., and Muqit, M. (2012) PINK1 is activated by mitochondrial membrane potential depolarization and stimulates Parkin E3 ligase activity by phosphorylating Serine 65. *Open Biology 2*, 120080.
(54) Greene, A. W., Grenier, K., Aguileta, M. A., Muise, S., Farazifard, R., Haque, M. E., McBride, H. M., Park, D. S., and Fon, E. A. (2012) Mitochondrial processing peptidase regulates PINK1 processing, import and Parkin recruitment. *EMBO reports 13*, 378–385.
(55) Koh, H., and Chung, J. (2012) PINK1 as a molecular checkpoint in the maintenance of mitochondrial function and integrity. *Molecules and Cells 34*, 7–13.
(56) Pridgeon, J. W., Olzmann, J. A., Chin, L., and Li, L. (2007) PINK1 protects against oxidative stress by phosphorylating mitochondrial chaperone TRAP1. *PLoS Biology 5*, e172.
(57) Zhang, L., Karsten, P., Hamm, S., Pogson, J. H., Lutz, A. K., Exner, N., Haass, C., Whitworth, A., Winklhofer, K., Schulz, J. B., and Voigt, A. (2013) TRAP1 rescues PINK1 loss-of-function phenotypes. *Human Molecular Genetics*.
(58) Butler, E. K., Voigt, A., Lutz, A. K., Toegel, J. P., Gerhardt, E., Karsten, P., Falkenburger, B., Reinartz, A., Winklhofer, K. F., and Schulz, J. B. (2012)

The mitochondrial chaperone protein TRAP1 mitigates α-Synuclein toxicity. *PLoS Genetics 8*, e1002488.
(59) Deas, E., Plun-Favreau, H., Gandhi, S., Desmond, H., Kjaer, S., Loh, S. H., Renton, A. E., Harvey, R. J., Whitworth, A. J., Martins, L. M., Abramov, A. Y., and Wood, N. W. (2011) PINK1 cleavage at position A103 by the mitochondrial protease PARL. *Human Molecular Genetics 20*, 867–879.
(60) Gandhi, S., Wood-Kaczmar, A., Yao, Z., Plun-Favreau, H., Deas, E., Klupsch, K., Downward, J., Latchman, D., Tabrizi, S., Wood, N., Duchen, M., and Abramov, A. (2009) PINK1-associated Parkinson's disease is caused by neuronal vulnerability to calcium-induced cell death. *Molecular Cell 33*, 627–638.
(61) Sim, C., Lio, D., Mok, S., Masters, C., Hill, A., Culvenor, J., and Cheng, H. (2006) C-terminal truncation and Parkinson's disease-associated mutations down-regulate the protein serine/threonine kinase activity of PTEN-induced kinase-1. *Human Molecular Genetics 15*, 3251–3262.
(62) Okatsu, K., Oka, T., Iguchi, M., Imamura, K., Kosako, H., Tani, N., Kimura, M., Go, E., Koyano, F., Funayama, M., Shiba-Fukushima, K., Sato, S., Shimizu, H., Fukunaga, Y., Taniguchi, H., Komatsu, M., Hattori, N., Mihara, K., Tanaka, K., and Matsuda, N. (2012) PINK1 autophosphorylation upon membrane potential dissipation is essential for Parkin recruitment to damaged mitochondria. *Nature Communications 3*, 1016.
(63) Gandhi, S., Vaarmann, A., Yao, Z., Duchen, M. R., Wood, N. W., and Abramov, A. Y. (2012) Dopamine induced neurodegeneration in a PINK1 model of Parkinson's disease. *PloS one 7*, e37564.
(64) Sinclair, D. A., and Guarente, L. (2006) Unlocking the secrets of longevity genes. *Scientific American 294*, 48–51– 54–7.
(65) Koh, H., Kim, H., Kim, M., Park, J., Lee, H., and Chung, J. (2012) Silent information regulator 2 (Sir2) and Forkhead box O (FOXO) complement mitochondrial dysfunction and dopaminergic neuron loss in Drosophila PTEN-induced kinase 1 (PINK1) null mutant. *The Journal of Biological Chemistry 287*, 12750–12758.
(66) Shiba-Fukushima, K., Imai, Y., Yoshida, S., Ishihama, Y., Kanao, T., Sato, S., and Hattori, N. (2012) PINK1-mediated phosphorylation of the Parkin ubiquitin-like domain primes mitochondrial translocation of Parkin and regulates mitophagy. *Scientific reports 2*, 1002.
(67) Öberg, F., Sjöhamn, J., Conner, M. T., Bill, R. M., and Hedfalk, K. (2011) Improving recombinant eukaryotic membrane protein yields in Pichia pastoris: the importance of codon optimization and clone selection. *Molecular Membrane Biology 28*, 398–411.
(68) Bernaudat, F., Frelet-Barrand, A., Pochon, N., Dementin, S., Hivin, P., Boutigny, S., Rioux, J., Salvi, D., Seigneurin-Berny, D., Richaud, P., Joyard, J., Pignol, D., Sabaty, M., Desnos, T., Pebay-Peyroula, E., Darrouzet, E., Vernet, T., and Rolland, N. (2011) Heterologous expression of membrane proteins: choosing the appropriate host. *PloS one 6*, e29191.
(69) Wagner, S., Bader, M. L., Drew, D., and Gier, J. (2006) Rationalizing

membrane protein overexpression. *Trends in Biotechnology 24*, 364–371.
(70) Freigassner, M., Pichler, H., and Glieder, A. (2009) Tuning microbial hosts for membrane protein production. *Microbial Cell Factories 8*, 69.
(71) Alguel, Y., Leung, J., Singh, S., Rana, R., Civiero, L., Alves, C., and Byrne, B. (2010) New tools for membrane protein research. *Current Protein & Peptide Science 11*, 156–165.
(72) Ramón, A., and Marín, M. (2011) Advances in the production of membrane proteins in Pichia pastoris. *Biotechnology Journal 6*, 700–706.
(73) Mizutani, K., Yoshioka, S., Mizutani, Y., Iwata, S., and Mikami, B. (2011) High-throughput construction of expression system using yeast Pichia pastoris, and its application to membrane proteins. *Protein Expression and Purification 77*, 1–8.
(74) Macauley-Patrick, S., Fazenda, M. L., McNeil, B., and Harvey, L. M. (2005) Heterologous protein production using the Pichia pastoris expression system. *Yeast 22*, 249–270.
(75) Li, P., Anumanthan, A., Gao, X., Ilangovan, K., Suzara, V. V., Düzgüneş, N., and Renugopalakrishnan, V. (2007) Expression of recombinant proteins in Pichia pastoris. *Applied Biochemistry and Biotechnology 142*, 105–124.
(76) Hino, T., Arakawa, T., Iwanari, H., Yurugi-Kobayashi, T., Ikeda-Suno, C., Nakada-Nakura, Y., Kusano-Arai, O., Weyand, S., Shimamura, T., Nomura, N., Cameron, A. D., Kobayashi, T., Hamakubo, T., Iwata, S., and Murata, T. (2012) G-protein-coupled receptor inactivation by an allosteric inverse-agonist antibody. *Nature 482*, 237–240.
(77) Shimamura, T., Shiroishi, M., Weyand, S., Tsujimoto, H., Winter, G., Katritch, V., Abagyan, R., Cherezov, V., Liu, W., Han, G. W., Kobayashi, T., Stevens, R. C., and Iwata, S. (2011) Structure of the human histamine H1 receptor complex with doxepin. *Nature 475*, 65–70.
(78) Miller, A. N., and Long, S. B. (2012) Crystal structure of the human two-pore domain potassium channel K2P1. *Science 335*, 432–436.
(79) Long, S. B., Campbell, E. B., and Mackinnon, R. (2005) Crystal structure of a mammalian voltage-dependent Shaker family K^+ channel. *Science 309*, 897–903.
(80) Ho, J. D., Yeh, R., Sandstrom, A., Chorny, I., Harries, W. E., Robbins, R. A., Miercke, L. J., and Stroud, R. M. (2009) Crystal structure of human aquaporin 4 at 1.8 A and its mechanism of conductance. *Proceedings of the National Academy of Sciences of the United States of America 106*, 7437–7442.
(81) Törnroth-Horsefield, S., Wang, Y., Hedfalk, K., Johanson, U., Karlsson, M., Tajkhorshid, E., Neutze, R., and Kjellbom, P. (2006) Structural mechanism of plant aquaporin gating. *Nature 439*, 688–694.
(82) Aller, S. G., Yu, J., Ward, A., Weng, Y., Chittaboina, S., Zhuo, R., Harrell, P. M., Trinh, Y. T., Zhang, Q., Urbatsch, I. L., and Chang, G. (2009) Structure of P-glycoprotein reveals a molecular basis for poly-specific drug

binding. *Science 323*, 1718–1722.
(83) Nordén, K., Agemark, M., Danielson, J. Å., Alexandersson, E., Kjellbom, P., and Johanson, U. (2011) Increasing gene dosage greatly enhances recombinant expression of aquaporins in Pichia pastoris. *BMC Biotechnology 11*, 47.
(84) Cereghino, J. L., and Cregg, J. M. (2000) Heterologous protein expression in the methylotrophic yeast Pichia pastoris. *FEMS Microbiology Reviews 24*, 45–66.
(85) Ellis, S. B., Brust, P. F., Koutz, P. J., Waters, A. F., Harpold, M. M., and Gingeras, T. R. (1985) Isolation of alcohol oxidase and two other methanol regulatable genes from the yeast Pichia pastoris. *Molecular and Cellular Biology 5*, 1111–1121.
(86) Cregg, J. M., Barringer, K. J., Hessler, A. Y., and Madden, K. R. (1985) Pichia pastoris as a host system for transformations. *Molecular and Cellular Biology 5*, 3376–3385.
(87) Gellissen, G. (2000) Heterologous protein production in methylotrophic yeasts. *Applied Microbiology and Biotechnology 54*, 741–750.
(88) Sarramegna, V., Demange, P., Milon, A., and Talmont, F. (2002) Optimizing functional versus total expression of the human mu-opioid receptor in Pichia pastoris. *Protein Expression and Purification 24*, 212–220.
(89) Schägger, H. (2006) Tricine-SDS-PAGE. *Nature protocols 1*, 16–22.
(90) Cormier, C. Y., Mohr, S. E., Zuo, D., Hu, Y., Rolfs, A., Kramer, J., Taycher, E., Kelley, F., Fiacco, M., Turnbull, G., and LaBaer, J. (2010) Protein Structure Initiative Material Repository: an open shared public resource of structural genomics plasmids for the biological community. *Nucleic Acids Research 38*, D743–9.
(91) Kumar, K. R., Djarmati-Westenberger, A., and Grünewald, A. (2011) Genetics of Parkinson's disease. *Seminars in Neurology 31*, 433–440.
(92) Valente, E. M., Salvi, S., Ialongo, T., Marongiu, R., Elia, A. E., Caputo, V., Romito, L., Albanese, A., Dallapiccola, B., and Bentivoglio, A. R. (2004) PINK1 mutations are associated with sporadic early-onset parkinsonism. *Annals of Neurology 56*, 336–341.
(93) Wishart, D. S., Sykes, B. D., and Richards, F. M. (1991) Simple techniques for the quantification of protein secondary structure by 1H NMR spectroscopy. *FEBS letters 293*, 72–80.
(94) Wishart, D. S., Sykes, B. D., and Richards, F. M. (1992) The chemical shift index: a fast and simple method for the assignment of protein secondary structure through NMR spectroscopy. *Biochemistry 31*, 1647–1651.
(95) Tremblay, M., Banks, A. W., and Rainey, J. K. (2010) The predictive accuracy of secondary chemical shifts is more affected by protein secondary structure than solvent environment. *Journal of Biomolecular NMR 46*, 257–270.
(96) Killian, J. A., Trouard, T. P., Greathouse, D. V., Chupin, V., and Lindblom, G. (1994) A general method for the preparation of mixed micelles of

hydrophobic peptides and sodium dodecyl sulphate. *FEBS letters 348*, 161–165.
(97) Kocherla, H., Marino, J., Shao, X., Graf, J., Zou, C., and Zerbe, O. (2012) Biosynthesis and Spectroscopic Characterization of 2-TM Fragments Encompassing the Sequence of a Human GPCR, the Y4 Receptor. *ChemBioChem 13*, 818–828.
(98) Moin, S., and Urban, S. (2012) Membrane immersion allows rhomboid proteases to achieve specificity by reading transmembrane segment dynamics. *eLife 1*, e00173.
(99) Hill, R. B., and Pellegrini, L. (2010) The PARL family of mitochondrial rhomboid proteases. *Seminars in Cell & Developmental Biology 21*, 582–592.
(100) Hu, Y., Zhao, E., Li, H., Xia, and Jin, C. (2010) Solution NMR structure of the TatA component of the twin-arginine protein transport system from gram-positive bacterium *Bacillus subtilis*. *Journal of the American Chemical Society 132*, 15942–15944.
(101) Lazareno-Saez, C., Arutyunova, E., Coquelle, N., and Lemieux, M. J. (2013) Domain swapping in the cytoplasmic domain of the Escherichia coli rhomboid protease. *Journal of Molecular Biology 425*, 1127–1142.
(102) Liu, J., and Rost, B. (2001) Comparing function and structure between entire proteomes. *Protein science 10*, 1970–1979.
(103) Sanders, C. R., and Myers, J. K. (2004) Disease-related misassembly of membrane proteins. *Annual Review of Biophysics and Biomolecular Structure 33*, 25–51.
(104) Bill, R. M., Henderson, P. J., Iwata, S., Kunji, E. R., Michel, H., Neutze, R., Newstead, S., Poolman, B., Tate, C. G., and Vogel, H. (2011) Overcoming barriers to membrane protein structure determination. *Nature Biotechnology 29*, 335–340.
(105) Korepanova, A., Gao, F. P., Hua, Y., Qin, H., Nakamoto, R. K., and Cross, T. A. (2005) Cloning and expression of multiple integral membrane proteins from *Mycobacterium tuberculosis* in *Escherichia coli*. *Protein Science 14*, 148–158.
(106) Kawate, T., Michel, J. C., Birdsong, W. T., and Gouaux, E. (2009) Crystal structure of the ATP-gated P2X(4) ion channel in the closed state. *Nature 460*, 592–598.
(107) Hu, J., Xue, Y., Lee, S., and Ha, Y. (2011) The crystal structure of GXGD membrane protease FlaK. *Nature 475*, 528–531.
(108) Cao, Y., Jin, X., Huang, H., Derebe, M. G., Levin, E. J., Kabaleeswaran, V., Pan, Y., Punta, M., Love, J., Weng, J., Quick, M., Ye, S., Kloss, B., Bruni, R., Martinez-Hackert, E., Hendrickson, W. A., Rost, B., Javitch, J. A., Rajashankar, K. R., Jiang, Y., and Zhou, M. (2011) Crystal structure of a potassium ion transporter, TrkH. *Nature 471*, 336–340.
(109) Chang, G., Spencer, R. H., Lee, A. T., Barclay, M. T., and Rees, D. C. (1998) Structure of the MscL homolog from Mycobacterium tuberculosis: a gated mechanosensitive ion channel. *Science 282*, 2220–2226.
(110) Drew, D. E., Heijne, G., Nordlund, P., and Gier, J. W. (2001) Green

fluorescent protein as an indicator to monitor membrane protein overexpression in Escherichia coli. *FEBS letters 507*, 220–224.
(111) Drew, D., Slotboom, D., Friso, G., Reda, T., Genevaux, P., Rapp, M., Meindl-Beinker, N. M., Lambert, W., Lerch, M., Daley, D. O., Wijk, K., Hirst, J., Kunji, E., and Gier, J. (2005) A scalable, GFP-based pipeline for membrane protein overexpression screening and purification. *Protein science 14*, 2011–2017.
(112) Kawate, T., and Gouaux, E. (2006) Fluorescence-detection size-exclusion chromatography for precrystallization screening of integral membrane proteins. *Structure 14*, 673–681.
(113) Drew, D., Newstead, S., Sonoda, Y., Kim, H., Heijne, G., and Iwata, S. (2008) GFP-based optimization scheme for the overexpression and purification of eukaryotic membrane proteins in Saccharomyces cerevisiae. *Nature protocols 3*, 784–798.
(114) Solcan, N., Kwok, J., Fowler, P. W., Cameron, A. D., Drew, D., Iwata, S., and Newstead, S. (2012) Alternating access mechanism in the POT family of oligopeptide transporters. *The EMBO Journal 31*, 3411–3421.
(115) Hu, N., Iwata, S., Cameron, A. D., and Drew, D. (2011) Crystal structure of a bacterial homologue of the bile acid sodium symporter ASBT. *Nature 478*, 408–411.
(116) Newstead, S., Drew, D., Cameron, A. D., Postis, V. L., Xia, X., Fowler, P. W., Ingram, J. C., Carpenter, E. P., Sansom, M. S., McPherson, M. J., Baldwin, S. A., and Iwata, S. (2011) Crystal structure of a prokaryotic homologue of the mammalian oligopeptide-proton symporters, PepT1 and PepT2. *The EMBO journal 30*, 417–426.
(117) Li, Z., and Vance, D. E. (2008) Phosphatidylcholine and choline homeostasis. *Journal of Lipid Research 49*, 1187–1194.
(118) Jacobs, R. L., Zhao, Y., Koonen, D. P., Sletten, T., Su, B., Lingrell, S., Cao, G., Peake, D. A., Kuo, M., Proctor, S. D., Kennedy, B. P., Dyck, J. R., and Vance, D. E. (2010) Impaired de novo choline synthesis explains why phosphatidylethanolamine N-methyltransferase-deficient mice are protected from diet-induced obesity. *The Journal of Biological Chemistry 285*, 22403–22413.
(119) Cole, L. K., Dolinsky, V. W., Dyck, J. R., and Vance, D. E. (2011) Impaired phosphatidylcholine biosynthesis reduces atherosclerosis and prevents lipotoxic cardiac dysfunction in ApoE$^{-/-}$ Mice. *Circulation research 108*, 686–694.
(120) Shields, D. J., Lehner, R., Agellon, L. B., and Vance, D. E. (2003) Membrane topography of human phosphatidylethanolamine N-methyltransferase. *The Journal of Biological Chemistry 278*, 2956–2962.
(121) Vance, D. (2013) Physiological roles of phosphatidylethanolamine N-methyltransferase. *Biochimica et biophysica acta 1831*, 626–632.
(122) Li, Z., Agellon, L. B., and Vance, D. E. (2005) Phosphatidylcholine homeostasis and liver failure. *The Journal of Biological Chemistry 280*, 37798–37802.
(123) Lemieux, M. J., Song, J., Kim, M. J., Huang, Y., Villa, A., Auer, M., Li, X., and

Wang, D. (2003) Three-dimensional crystallization of the *Escherichia coli* glycerol-3-phosphate transporter: a member of the major facilitator superfamily. *Protein Science 12*, 2748–2756.
(124) Cornvik, T., Dahlroth, S., Magnusdottir, A., Herman, M. D., Knaust, R., Ekberg, M., and Nordlund, P. (2005) Colony filtration blot: a new screening method for soluble protein expression in *Escherichia coli*. *Nature methods 2*, 507–509.
(125) Clare, J. J., Rayment, F. B., Ballantine, S. P., Sreekrishna, K., and Romanos, M. A. (1991) High-level expression of tetanus toxin fragment C in Pichia pastoris strains containing multiple tandem integrations of the gene. *Biotechnology 9*, 455–460.
(126) Hohenblum, H., Gasser, B., Maurer, M., Borth, N., and Mattanovich, D. (2004) Effects of gene dosage, promoters, and substrates on unfolded protein stress of recombinant *Pichia pastoris*. *Biotechnology and Bioengineering 85*, 367–375.
(127) McQuibban, G. A., Saurya, S., and Freeman, M. (2003) Mitochondrial membrane remodelling regulated by a conserved rhomboid protease. *Nature 423*, 537–541.
(128) Pellegrini, L., Passer, B. J., Canelles, M., Lefterov, I., Ganjei, J. K., Fowlkes, B. J., Koonin, E. V., and D'Adamio, L. (2001) PAMP and PARL, two novel putative metalloproteases interacting with the COOH-terminus of Presenilin-1 and -2. *Journal of Alzheimer's disease 3*, 181–190.
(129) Lemberg, M. K., and Freeman, M. (2007) Functional and evolutionary implications of enhanced genomic analysis of rhomboid intramembrane proteases. *Genome research 17*, 1634–1646.
(130) Heinitz, S., Klein, C., and Djarmati, A. (2011) The p.S77N presenilin-associated rhomboid-like protein mutation is not a frequent cause of early-onset Parkinson's disease. *Movement Disorders 26*, 2441–2442.
(131) Jeyaraju, D. V., McBride, H. M., Hill, R. B., and Pellegrini, L. (2011) Structural and mechanistic basis of Parl activity and regulation. *Cell Death and Differentiation 18*, 1531–1539.
(132) Jeyaraju, D. V., Xu, L., Letellier, M., Bandaru, S., Zunino, R., Berg, E. A., McBride, H. M., and Pellegrini, L. (2006) Phosphorylation and cleavage of presenilin-associated rhomboid-like protein (PARL) promotes changes in mitochondrial morphology. *Proceedings of the National Academy of Sciences of the United States of America 103*, 18562–18567.
(133) Sík, A., Passer, B. J., Koonin, E. V., and Pellegrini, L. (2004) Self-regulated cleavage of the mitochondrial intramembrane-cleaving protease PARL yields Pbeta, a nuclear-targeted peptide. *The Journal of Biological Chemistry 279*, 15323–15329.
(134) McQuibban, G. A., and Bulman, D. E. (2011) The PARLance of Parkinson disease. *Autophagy 7*, 790–792.
(135) Shi, G., Lee, J., Grimes, D., Racacho, L., Ye, D., Yang, H., Ross, O., Farrer, M., McQuibban, G., and Bulman, D. (2011) Functional alteration of PARL contributes to mitochondrial dysregulation in Parkinson's disease. *Human Molecular Genetics 20*, 1966–1974.

(136) Cipolat, S., Rudka, T., Hartmann, D., Costa, V., Serneels, L., Craessaerts, K., Metzger, K., Frezza, C., Annaert, W., D'Adamio, L., Derks, C., Dejaegere, T., Pellegrini, L., D'Hooge, R., Scorrano, L., and Strooper, B. (2006) Mitochondrial rhomboid PARL regulates cytochrome c release during apoptosis via OPA1-dependent cristae remodeling. *Cell 126*, 163–175.
(137) Costa, A. C., Loh, S. H., and Martins, L. M. (2013) Drosophila Trap1 protects against mitochondrial dysfunction in a PINK1/parkin model of Parkinson's disease. *Cell Death & Disease 4*, e467.
(138) Szklarz, L. K., and Scorrano, L. (2012) The antiapoptotic OPA1/Parl couple participates in mitochondrial adaptation to heat shock. *Biochimica et Biophysica Acta 1817*, 1886–1893.
(139) Chao, J., Parganas, E., Boyd, K., Hong, C. Y., Opferman, J. T., and Ihle, J. N. (2008) Hax1-mediated processing of HtrA2 by Parl allows survival of lymphocytes and neurons. *Nature 452*, 98–102.
(140) Narendra, D. P., Jin, S. M., Tanaka, A., Suen, D., Gautier, C. A., Shen, J., Cookson, M. R., and Youle, R. J. (2010) PINK1 is selectively stabilized on impaired mitochondria to activate Parkin. *PLoS biology 8*, e1000298.
(141) Clark, K. M., Fedoriw, N., Robinson, K., Connelly, S. M., Randles, J., Malkowski, M. G., DeTitta, G. T., and Dumont, M. E. (2010) Purification of transmembrane proteins from *Saccharomyces cerevisiae* for X-ray crystallography. *Protein Expression and Purification 71*, 207–223.
(142) Privé, G. G. (2007) Detergents for the stabilization and crystallization of membrane proteins. *Methods 41*, 388–397.
(143) Deacon, S. E., Roach, P. C., Postis, V. L., Wright, G. S., Xia, X., Phillips, S. E., Knox, J. P., Henderson, P. J., McPherson, M. J., and Baldwin, S. A. (2008) Reliable scale-up of membrane protein over-expression by bacterial auto-induction: from microwell plates to pilot scale fermentations. *Molecular Membrane Biology 25*, 588–598.
(144) Veesler, D., Blangy, S., Siponen, M., Vincentelli, R., Cambillau, C., and Sciara, G. (2009) Production and biophysical characterization of the CorA transporter from *Methanosarcina mazei*. *Analytical Biochemistry 388*, 115–121.
(145) Youle, R. J., van der Bliek, A. M. (2012) Mitochondrial fission, fusion and stress. *Science 337,* 1062-1065.
(146) Kawajiir, S., Saiki, S., Sato S., and Hattori, N. (2010) Genetic mutations and functions of PINK1. *Trends in Pharmcological Sciences 32*, 573-580.